DISSERTATION

Postsynaptic plasticity of cholinergic synapses underlying learning in *Drosophila*

Postsynaptische Plastizität cholinerger Synapsen, die dem Lernen in *Drosophila* zugrunde liegen

zur Erlangung des akademischen Grades
Medical Doctor - Doctor of Philosophy (MD/PhD)

vorgelegt der Medizinischen Fakultät
Charité – Universitätsmedizin Berlin

von

Carlotta Pribbenow

Erstbetreuung: Prof. Dr. David Owald

Datum der Promotion: 28.02.2025

Table of Contents

List of Figures

List of Graphics

List of Abbreviations

AC – Ca2+/CaM-responsive adenylyl cyclase

ACh – Acetylcholine

AUC – Area under curve

AMPAR – α-amino-3-hydroxy-5-methyl-4-isoxazolepropionic acid receptor

DA – Dopamine

DAN – Dopaminergic neuron

Dlg – Discs large

GFP – Green fluorescent protein

ISI - Interstimulus interval

KC – Kenyon cell

LTD – Long term depression

LTM – Long term memory

LTP – Long term potentiation

MB – Mushroom body

MCH – 4-MethylcyclohexanolMBON – Mushroom body output neuron

MTM – Middle term memory

nAChR – Nicotinic acetylcholine receptor

NMDAR – N-methyl-D-aspartate receptor

OCT – Octanol

PDE – cAMP Phosphodiesterase

SEM – Standard error of mean

Shi – Shibire

STM – Short term memory

Zusammenfassung in Deutsch

Lernen findet bei Wirbeltieren häufig an glutamatergen Prä- und Postsynapsen statt. Im Gegensatz dazu wurde bei *Drosophila* bisher ausschließlich gezeigt, dass präsynaptische Plastizität cholinerger Synapsen am Lernen beteiligt ist. In meiner Dissertation liefere ich erste Beweise für postsynaptische Plastizität an der Synapse zwischen den intrinsischen Zellen (Kenyon Cells) des *Drosophila* Lernzentrums (Mushroom Body), und den extrinsischen M4/M6-Neuronen (M4/M6-Mushroom Body Output Neuronen). Ein bedeutsames Ergebnis war, dass wir postsynaptische Plastizität in M4/M6 Neuronen unter Umgehung der Präsynapse induzieren können. Auf Ebene der nikotinischen Acetylcholin Rezeptoren sehe ich, dass α5-Untereinheiten sowohl für die Bildung eines positiven Kurzzeitgedächtnisses als auch für das eines mittelfristigen Gedächtnisses in M4/M6- Neuronen benötigt wird. Die α2-Untereinheit und das scaffolding protein Discs large (Dlg), das Homolog von PSD-95 bei Säugetieren, werden dagegen nur für die Bildung eines mittelfristigen Gedächtnisses benötigt. Interessanterweise scheinen die Plastizitätsmechanismen an unterschiedlichen Synapsen unterschiedlich zu sein. Während diese Untereinheiten für die aversive Gedächtnisbildung in den M4/M6-MBONs entbehrlich sind, sind die α5-Untereinheit und Dlg für das aversive Lernen in anderen extrinsischen Neuronen, den MVP2-Neuronen erforderlich. Interessanterweise haben die α5- Untereinheit und Dlg wahrscheinlich einen Effekt auf die α2-Untereinheit. Darüber hinaus konnten wir in vivo zeigen, dass es an diesen Postsynapsen zu einer Mobilität der α2-Untereinheiten bei Duftpräsentation und bei Habituation in α'3 and M4 Neuronen kommt. Mit dieser Doktorarbeit unterstütze ich die Theorie, dass sich *Drosophila* als Modellorganismus für synaptische Plastizität eignet.

Abstract in English

Learning involves glutamatergic postsynaptic plasticity in vertebrate brains; in *Drosophila*, however, presynaptic plasticity of cholinergic synapses is believed to be involved in memory formation. Here, I document the first evidence of postsynaptic plasticity in *Drosophila* by establishing that postsynaptic associative plasticity can be induced after bypassing the presynapse at synapses of the fly learning and memory centre, the mushroom bodies (MBs). I demonstrate that: 1) the α5 nicotinic acetylcholine receptor (nAChR) subunit is necessary within the M4/M6 mushroom body output neurons (MBONs), the postsynaptic neurons downstream of the presynaptic intrinsic Kenyon cells, to induce appetitive memory; 2) the α2 subunit is required for later phases of appetitive memory; and 3) the α2 subunit plausibly acts downstream of the α5 subunit as well as the scaffolding protein Discs large (Dlg), a homologue of the mammalian protein PSD-95. Though these subunits are dispensable for aversive memory formation in the M4/M6 MBONs, I demonstrate that both the α5 subunit and Dlg are required for aversive memory formation in MVP2 MBONs, thus indicating a different plasticity mechanism at the Kenyon cell - MVP2 neuron synapse. Moreover, this work shows *in vivo* that α2 subunit rearrangements occur in non-associative (familiarity) memory formation and after odour presentation in α'3 and M4 MBONs. Notably, the work herein supports the theory that mechanisms of postsynaptic plasticity follow similar design principles across phyla despite utilization of different neurotransmitters.

1. Introduction

For a very long time it has been of great interest to understand how the brain mediates learning and memory. While the brain of vertebrates, especially of humans, is very complex and therefore considerably hard to understand, the relatively small number of cells of the *Drosophila* brain and its ability to remember learned information for over a 24 hour period, coupled with an unparalleled genetic toolbox with which single neurons can be targeted, make the *Drosophila* brain an ideal model for understanding the fundamental mechanics of learning and memory.

1.1. Learning and Memory

The ability to learn and subsequently adapt behaviour is a core component for an animal's survival. In *Drosophila* it was found that the mushroom body (MB), a bilateral structure centrally located within the brain, is the main storage site for associative memories (1). Associative learning was first demonstrated in *Drosophila* through olfactory conditioning by Quinn et al. (2) and subsequently modified to fit a Pavlovian conditioning paradigm by Tully and Quinn (3). More recently, Hattori (4) has described familiarity learning in *Drosophila* wherein flies react to a novel stimulus. If this stimulus is applied a couple times, it becomes no longer familiar, and the original reaction is adjourned (4).

On a molecular level, we now understand that learning does in fact take place at neuronal synapses. How synaptic plasticity on a molecular level is conducted has however been subject to numerous investigations. For instance, identifiable long-lasting changes in neurons in mammals can be achieved either by 1) rearranging or exchanging specific synaptic molecules (e.g., 5), 2) induction of the formation of larger connections between the pre- and the postsynapse (6), or 3) modulation of the physical amount of a neurotransmitter released (7). Moreover, in mammals it has been widely demonstrated that the changes occur at both the postsynapse (e.g. 5) and the presynapse (e.g. 6, 7). In contrast, it has been widely believed that in *Drosophila* only presynaptic plasticity is involved in learning and memory (e.g. 8, 9).

In further cladistic contrast, mammals mostly use glutamate as their hippocampal neurotransmitter (7, 10) while *Drosophila* uses acetylcholine (ACh) as the main excitatory neurotransmitter in the MB (11). In mammals, the ionotropic α-amino-3-hydroxy-5-methyl-4-isoxazolepropionic acid receptor (AMPAR) is known to be necessary for normal

synaptic transmission, while the N-methyl-D-aspartate receptor (NMDAR) acts as a fundamental protein necessary in LTP (long term potentiation) for the induction of synaptic plasticity and stability (10). During learning, the synapse is strengthened or weakened by AMPAR incorporation through lateral diffusion, exocytosis, or removal (10). Altogether, AMPAR dynamics play a crucial role in LTP and depend on NMDAR.

1.2.   The insect learning and memory centre: the Mushroom Body

Heisenberg and colleagues (1) first demonstrated that in *Drosophila* the bilateral, centrally located MBs are the main storage sites for associative memory formation. While a MBs consists of ~2,000 Kenyon Cells (KCs; 12), KCs in turn relay information onto only approximately 35 MB output neurons (MBONs) (12, 13). Mechanistically, odour identity is represented by unique KC activity patterns (14), with only 6-20% of the KCs responding to each odour (15). Additionally, the MB is also innervated by dopaminergic neurons (DANs) (13). Together, DANs and MBONs partition the MB into 15 compartments on 5 lobes (13). The value of the odour is then assigned by the DANs (16, 17). In *Drosophila*, there are two categories of DANs that innervate the MBs: 1) PPL-1 neurons, innervating the α and α' lobes as well as the peduncle of the MB and contribute negative valance in learning (18) and 2) PAM neurons, mostly innervating the β, β' and γ lobes of the MB and providing positive reinforcement during learning (18).

Learning itself takes place at the KC – MBON synapse, and activation of the odour specific KC is required to simultaneously occur with DAN release of dopamine onto KC presynapses during associative learning (19). The odour drive from KC to their specific MBONs, however, can either be potentiated or depressed after learning (19, 20, 21, 22). MBONs that direct avoidance behaviour receive less input after reward learning and increased input after aversive learning. Contrastingly, aversive learning reduces the input to MBONs driving approach behaviour (23).

Blocking the output of MBONs can impair either appetitive or aversive memory depending on the output neuron. For instance, β'2mp/γ5β'2a (M4/M6, respectively) and γ1pedc>α/β (MVP2) MBONs are required both for appetitive and aversive memory (21, 22, 24), with MVP2 MBONs probably inhibiting M4/M6 neurons (22). Intriguingly, and in line with MVP2 neurons inhibiting M4/M6 neurons, Ca^{2+} responses to the CS+ (conditioned stimulus) compared to the CS- (unconditioned stimulus) odour are decreased in M4β' (β'2mp)

MBONs following appetitive learning while the Ca^{2+} responses to CS+ are increased following aversive conditioning (21). Previous studies have also shown that circuit mechanisms exist downstream of KCs that most likely involve MBONs, DANs and KCs (12, 24, 25), and that these feedback loops are necessary for learning (25). At the synaptic level, presynaptic plasticity through a change of ACh release in KCs has been described (9) as well as have plastic changes in presynaptic bouton numbers in other cells in the *Drosophila* brain (8). Additionally, mutations of two presynaptic proteins, the Ca^{2+}/CaM-responsive adenylyl cyclase (AC) (the rutabaga mutant) and cAMP Phosphodiesterase (PDE) (the dunce mutant), have been found to impair memory in α/β and γ KCs (17, 26). Interestingly, artificial training (via paired acetylcholine and dopamine application) increases rut-AC dependent cAMP in KCs at the level of the α lobe and is thought to function as a coincidence detector (16, 27). However, while learning on a circuitry level has been extensively studied within *Drosophila*, little is known about learning at the postsynaptic level.

1.3. Nicotinic Acetylcholine Receptors

Synaptic connections between the KCs and the MBONs are cholinergic (11). Furthermore, subunits of the ACh nicotinic receptor (nAChR) are located in postsynapses of MBONs, and knockdown of the subunits alters odour-driven behaviour (11). nAChR subunits are conserved between vertebrates and *Drosophila*, and to date seven α (Dα1-Dα7) subunits and three β (Dβ1- Dβ3) subunits have been identified in *Drosophila* (28). Approximately 33-50% of nAChR subunit sequences are similar between the *Drosophila* and vertebrates, and it is believed that the *Drosophila* receptors form a comparable structure to vertebrates receptors (29). AChR are pentamers (28, 30) and ligands can bind at an allosteric transmembrane site or at an extracellular site (30). They are permeable for Na^+, K^+, and Ca^{2+} (28). AChRs can either be formed from homomeric or heteromeric combinations of subunits (28). The subunit composition at the KC-MBON synapse meanwhile remains unknown. Therefore, the synaptic transmission at the KC-MBON synapse could in theory be altered through either an exchange of whole receptors or of single receptor subunits.

1.4. Discs large

Synapses contain numerous scaffolding proteins, including Discs large (Dlg)/ PSD-95 (31). PSD-95, involved in learning and memory cascades (10), has been associated with Alzheimer's disease (32), and is required for NMDAR surface expression (31). PSD-95 also binds AMPARs through Stargazin and enhances AMPAR expression at the synapse through trapping and transiently stabilizing diffusing AMPARs at the postsynaptic membrane (10, 31). PSD-95 influences postsynaptic spine size and density, and likely affects presynaptic neurotransmitter release and vesicle pool size (33). Furthermore, PSD-95 associates with nAChR subunits decreases α7 subunit mobility (34). In *Drosophila*, Dlg has also been found to be required for appetitive and aversive short term memory (STM) in KCs (35).

1.5. Hypothesis

1.5.1. Evidence for postsynaptic plasticity in MBONs

Although both pre- and postsynaptic plasticity occurs in vertebrates (5, 6, 7), in *Drosophila* only presynaptic plasticity had been shown (8, 9). Experiments showing negligible synaptic output of KCs during acquisition have largely been seen as supportive of the notion that postsynaptic plasticity in not utilized (17), though similar experiments have also documented memory impairments (25, 36). Moreover, protein synthesis in MBONs is required for LTM (long term memory) formation (37). These latter two observations align with expectations for the additional involvement of a postsynaptic component to learning and memory in *Drosophila*. Therefore, I hypothesized that postsynaptic plasticity occurs at the KC-MBON synapse in *Drosophila*.

1.5.2. nAChR Receptor subunits are necessary for memory formation

The KC-MBON synapse is cholinergic (11) and *Drosophila* has seven α (Dα1-Dα7) and three β (Dβ1- Dβ3) nAChR subunits (28). These subunits form either homomeric or heteromeric receptors (28). Knockdown of specific subunits alters naïve odour avoidance (11), suggesting roles in learning and memory. Which receptor compositions characterize MBONs or whether specific nAChR subunits are required for learning and memory however remains unknown. I hypothesized that targeted perturbation of the individual nAChR subunits in specific MBONS, like M4/M6 and MVP2 that are required for

associative appetitive and aversive learning and memory (21, 22), and α'3 MBONs utilized in non-associative familiarity learning (4), alters the learning and memory performance of *Drosophila* flies.

1.5.3. Receptor dynamics are required for learning and specific nAChRs might play similar roles to those played by NMDAR and AMPAR in mammals

In vertebrates, glutamatergic receptor dynamics are required for long term plasticity (10) while *Drosophila* utilizes ACh as their main neurotransmitter (11). Notably in *Drosophila,* Dα1, Dα4, Dα5, and Dα6 subunits are required for naïve odour avoidance at the KC-MBON synapse (11), and learning takes place at the KC-MBON synapse (19). I therefore have hypothesized that receptor dynamics of nAChR are required for learning and memory at the KC-MBON synapse.

1.5.4. Specific scaffolding proteins like Dlg are necessary for the formation of memory

Receptor dynamics frequently rely on scaffolding proteins such as Dlg/PSD-95 (31). PSD-95 is required for NMDAR (31) and AMPAR surface expression (33, 10, 31) at glutamatergic synapses, and it influences postsynaptic spine size and density (33). It is also required at cholinergic synapses where it associates with nAChR subunits (34). Reduction in PSD-95 increases α7 subunit mobility (34). Moreover, PSD-95 has been shown to be involved in a cascade involved in learning and memory (10), while in *Drosophila* Dlg is necessary in KCs for appetitive and aversive STM (35). Therefore, I hypothesized that Dlg will be required for normal memory performance in flies.

2. Methods

2.1. Fly genetics

For fly-breeding, standard food and laboratory settings (25°C, 65% humidity, 12-hour light and 12 hour dark phase) were utilized, except for Gal-80 flies raised at <20°C. Fly lines included: MB011B , MB461B, MB112C, MB027B, OK107-Gal4, R13F02-Gal4, VT1211-GAL4, R58E02-LexA , DlgS97-RNAi, UAS-Dlg^{GFP}, UAS-SynaptoPhluorin, tubP-GAL^{80ts}, 247-dsRed, LexAop-CsChrimson, UAS-GCaMP6f, UAS-Shi^{ts} and the Bloomington stock flies 28688, 27493, 27671, 31985, 25943, 27251 and 25835 as UAS-nAChR^{RNAi} flies (Methods modified from 38).

2.2. T-maze memory

For T-Maze behaviour, 3-9 day old mixed sex flies were used. Octanol (OCT, Aldrich) and 4-Methylcyclohexanol (MCH, Aldrich) were alternately utilized as odour A or B (1:100 for aversive and 1:1000 for appetitive training; diluted in mineral oil; absolute concentrations were adjusted to odour bias). For aversive learning, odour A together with an electric shock (12 individual shocks, each 1.5s long; 120 V; interstimulus interval 3.5s) were given for 1min in a T-Maze, followed by a 45s resting period in air, 1min of odour B and 30s rest. After consolidation time (0min- 3hr), the flies were presented a choice in the dark between the odour A (CS+) and the odour B (CS-) for 2min (Graphic 1; (3)). For appetitive training, flies were starved for 20-24hr. They were then subjected to odour A for 2min followed by 30s rest in air, 2min odour B paired with sugar (saturated sucrose solution dried on filter paper), and 30s rest. After consolidation time (0min-3hr), flies were tested again (Graphic 2; (17)). Performance indices (PI) were calculated taking the number of flies choosing the CS+ or CS- odour: $(CS^+-CS^-)/(CS^++CS^-)$ giving half PI and PI calculated as the mean of two T-Mazes. For experiments using Shibiri (Shi), 30min before the synaptic neurotransmission blockage, the temperature was raised to 32°C. Afterwards, flies were kept at room temperature for the rest of the experiment to allow neurotransmission. For experiments with Gal^{80ts}, flies grew up at 18-20°C to suppress RNAi knockdown during development. 3-5 days before the experiment, the flies were transferred to 32°C (controls at 18-20°C) to induce RNAi expression (Methods modified from 38).
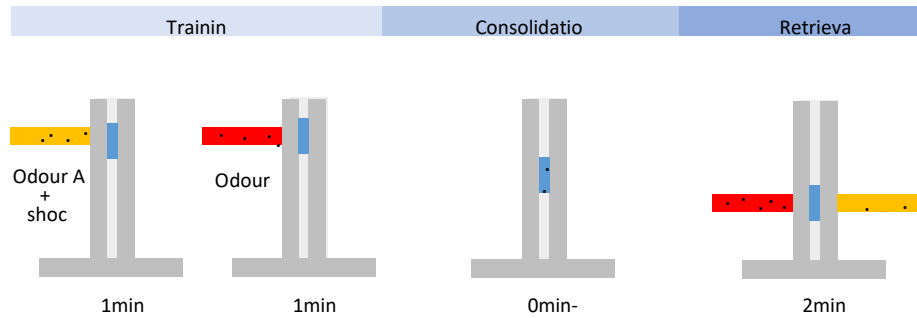
Graphic 1: Aversive T-Maze experiment
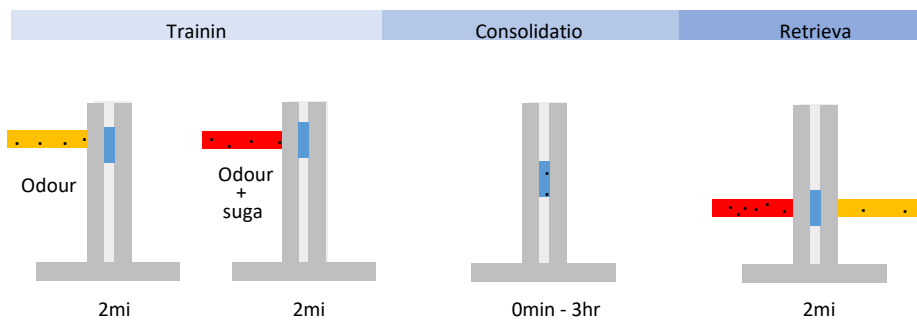
Graphic 2: Appetitive T-Maze experiment.

2.3. Receptor quantification in confocal single photon imaging

Brains from 2-8 day old females were fixed for 20min in 4% paraformaldehyde (Sigma) kept in PBST (0.1% Triton; 30min), washed twice in PBS (20min), mounted using Vectashield, and imaged on a confocal single photon inverse microscope (Leica SP5/STED) (64x oil objective)(Voxel size 123nmx 123nmx500nm). Laser power and gain were corrected for each brain; therefore normalisation to the neighbouring compartment or the whole MB was necessary. Analysis: ImageJ, ROIs were drawn manually. Each hemisphere was utilized separately as an *n* (Methods modified from 38).

2.4. Two photon calcium imaging

3-6 day old flies which were tethered under the multiphoton microscope (Femtonics) (21). Fluorescence signals were recorded (frame rate: 30Hz) with MESc software (Femtonics). Analysis: ROIs drawn manually, Savitzky-Golay filter, Matlab. R was used to calculate area under curve (AUC; first 3s after odour onset). To measure naïve odour responses in dendrites, flies were exposed to OCT and MCH five times each (1s; inter interstimulus interval (ISI): 30s). For paired training experiments, axonal arbours from starved flies were imaged while the flies were exposed to MCH (2x1s; averaged) before training (pre).

For training, MCH (5x1s; ISI: 6s) exposure was paired with feeding saturated sucrose solution (30s) from a feeding arm. After a 1min pause, flies were again exposed twice to MCH (2x1s; averaged) while imaging (post). For unpaired training experiments, flies were first fed with sucrose solution (30s). After a 45s break, MCH was presented (5x1s; ISI: 6s). AUCs for learning experiments were normalised to the mean of the pre-training per group (Methods modified from 38).

2.5. In vivo Fluorescence recovery after photobleaching (FRAP)

For fluorescence recovery after photobleaching (FRAP) *in vivo* experiments, 2-8 day old flies were tethered in a chamber using wax to immobilize the legs. The head capsule was removed in sugar-free HL3-like saline, afterwards sugar-free HL3-like saline with 30 units of Papain (Roche) was administered for 8min. A multi photon microscope (Nikon) (25× water-immersion objective; Nikon NIS Elements software) and a 6-channel delivery system (CON electronics) for MCH/OCT application (1:1000 in mineral oil) were used. Training paradigms consisted of bleaching (high intensity laser exposure focused ~1min) the GFP signal in the β'2 compartment followed by a baseline picture. Afterwards, training (10mM DA injection with a micropipette; odour presentation or paired DA application + odour presentation) was performed followed by fluorescence recovery measurement after 10 and 20mins. Analyses: FIJI; ROIs drawn manually. For inverse exponential decay, the fluorescence recovery [%] was inverted (1-percent), and then *log*-transformed. They were utilized in a linear mixed effects model without intercept. The interaction between training form and time was a fixed effect while time was a random effect (R-package lme4). Values were transformed back to the original scale for graphs. The regression coefficients were used to calculate if a recovery was significant, while for testing for significance between training types we used pairwise comparisons of estimated marginal means (R package emmeans). For correction for multiple comparisons, Tukey's method was used (Methods modified from 38).

2.6. Confocal single photon imaging in vivo

3-4 day old females were imaged under a SP5 single-photon confocal microscope (Leica microsystems; 3Hz). Flies were prepared as above. After bleaching (15-25s) the α'3 compartment a baseline image was taken. Flies were exposed to OCT (10x1s; ISI: 6s) (CON electronics; Leica acquisition software). At 0, 5, 10, 15, 20, 30, 60min post training,

the bleached brain plane was recorded for 10s (pixel size: 200nm). Analysis: ImageJ; ROIs drawn manually; Gaussian blur ($\sigma = 0.5$) (Methods modified from 38).

2.7. Explant brain widefield imaging

The head capsules and sheaths of 3-10 day old flies were recovered in carbogenated solution (103mM NaCl, 3mM KCl, 10mM trehalose, 5mM N-Tris, 10mM glucose, 7mM sucrose, 1mM NaH_2PO_4, 26mM $NaHCO_3$, 1.5mM $CaCl_2$, 4mM $MgCl_2$, 295 mOsm/kg, pH 7.3) (38). Thereafter, brains were perfused with carbogenated solution plus TTX (2µM; 20ml/10min). An Olympus MX51WI wide field microscope (40x Olympus LUMPLFLN objective; Olympus U25ND25 light filter) and an Andor iXON Ultra camera (controlled through Solis software) were used. ACh (0.1mM) injections to the M6 dendrites were performed using a P25-1-900 picospritzer (3-8psi). First, optogenetic responses were assessed:3 ACh pulses (15s), a 2-3min break, red light pulses (2s; ISI: 4s). Before and after training 3x ACh-evoked GCaMP6f responses were measured (pre and post). Training consisted of either 5 ACh injections, 5 red light pulses, or both paired. Responses were calculated relative to the baseline (baseline was set with polynomial interpolation function; NOSA) Analysis: NOSA; GraphPadPrism (Methods modified from 38).

2.8. Statistics

Normality testing was performed with the Shapiro-Wilkinson test. Normally distributed data were analysed by ANOVA followed by a post-hoc test or a (paired) t-test, while non-normally distributed data were analysed with a Kruskal Wallis test followed by a post-hoc test or a Wilcoxon matched-pairs signed rank test (Methods modified from 38) if not otherwise stated.

2.9. Activity measurements

Single 5-6 day old virgin female flies were placed in 65mm glass tubes (5mm diameter) which contained at one end fly food. The activity was measured with *Drosophila* Activity Monitors (DAM2; Trikinetics Inc. Waltham, MA) at 25°C with a 12hr light and 12 hr-dark phase. Every time the fly crosses the midline of the tube it counted as one activity. 4 days were analyzed, the first 36hr of the measurements were excluded since it was a new environment.

3. Results

3.1. Output of KCs is required for the acquisition of memory

To test whether the output of KCs or MBONs during the training phase was necessary, flies were trained to associate an odour (CS+) with sugar or shock (US) while blocking neurotransmission at 31°C using UAS-Shibire[TS] (Shi). After 30 minutes, the flies got the choice between this odour or a second odour (CS-) previously presented without an additional stimulus. Results show that blocking the output of KCs (R13F02-Gal4) during learning impaired appetitive, but not aversive, memory (Figure 1a,b). Meanwhile, blocking neurotransmission from M4/M6 (MB011B-Gal4) MBONs does not affect memory performance (Figure 1c). At permissive temperature (21°C), no memory impairment was observed (Figure 1d,e). It was concluded, therefore, that output of KCs is necessary during acquisition of olfactory appetitive learning.
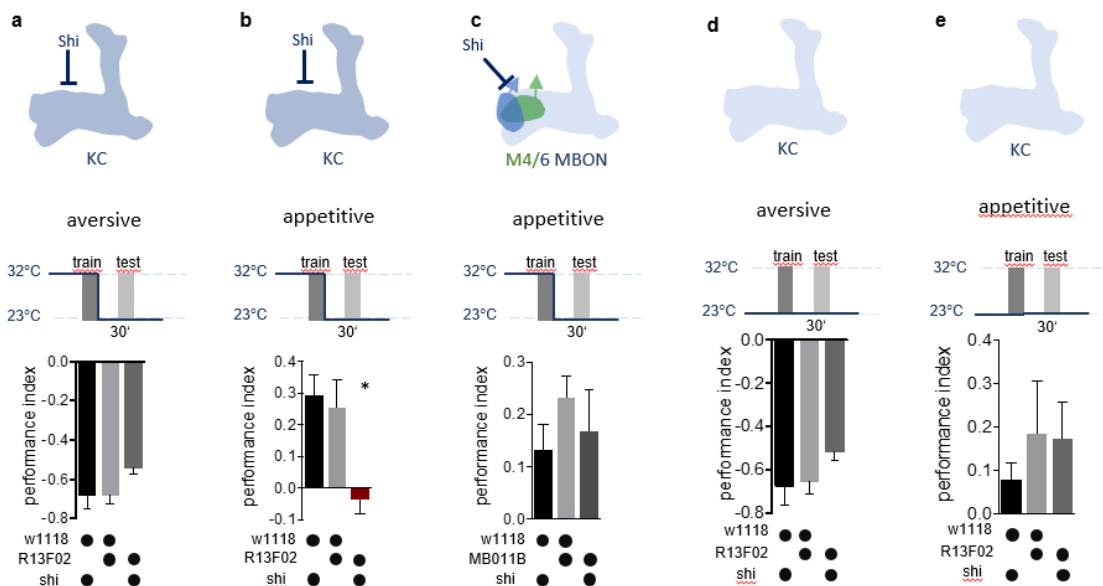

Figure 1: Output of KCs is required for the acquisition of memory

Figure and legend modified from Pribbenow et al., 2022 (38)

a-c) Flies expressing the temperature sensitive Shi in KCs or MBONs were trained while blocking the synaptic neurotransmitter release (32°C) and tested at 23°C (enabling synaptic output). Bar graphs: mean ± SEM. **a)** Inhibited synaptic transmission of KCs (R13F02-Gal4) during acquisition permits 30min aversive learning. n= 7 – 8; one-way ANOVA followed by Tukey's test (p > 0.05). **b)** Inhibited synaptic transmission of KCs during training abolishes 30min appetitive memory. n= 10 – 16; Kruskal-Wallis followed by Dunn's test (p < 0.05), * = p < 0.05. **c)** Inhibited synaptic transmission of M4/6 MBONs (MB011B-GAL4) during training permits 30min appetitive memory. n= 14 – 24; one-way ANOVA followed by Tuckey's test (p > 0.05). **d-e)** Temperature controls for Figure 1a and 1b: Flies stayed at 23°C (enables synaptic transmission) throughout the whole experiment. Box plots: mean ± SEM. **d)** 30min aversive memory was not significantly impaired at 23°C.; n= 7 – 9; Kruskal-Wallis followed by Dunn's test (p = 0.08). **e)** 30min appetitive memory was not significantly impaired at 23°C. n= 6 – 8; Kruskal-Wallis followed by Dunn's test (p = 0.7).

3.2. Knockdown of the α2 and α5 subunit in MBONs impair memory

Interestingly, previous studies showed that knockdown of the Dα1, Dα4, Dα5, and Dα6 subunits alters naïve odour avoidance in *Drosophila* (11). Since KCs are vital for appetitive memory (Figure 1b) and the KC-MBON synapse is cholinergic (11), the requirement of different nAChR subunits at the M4/M6 postsynapse for memory was tested. RNAi (RNA interference) directed to the nAChR subunits or the scaffolding protein Dlg were expressed in M4/M6 neurons (MB011B) and the flies were trained to associate an odour with sugar. Memory performance was tested, either immediately afterwards (short term memory; STM) or 3hr later (middle term memory; MTM), by giving the flies the choice between the previously associated odour with sugar (CS+) and another odour the flies had encountered before but without sugar (CS-). The number of *Drosophila* choosing the CS+ and CS- was used to calculate the performance index. Knockdown of the α5 subunit abolished appetitive STM, while knockdown of any other subunit had no effect on the expression of appetitive STM (Figure 2a). Meanwhile, for appetitive MTM expression more subunits and scaffolding proteins were required: Knockdown of α1, α2, α5 subunits and Dlg abolished appetitive MTM (Figure 2b). Importantly, in genetic controls appetitive STM and MTM performance were not affected (Figure 2c-d). Next, we wanted to exclude a developmental phenotype. Therefore, we suppressed the RNAi expression during development by using the temperature-sensitive Gal4 repressor tubP-GAL80ts at <20°C. We then induced the RNAi 3-5 days before the experiments by raising the temperature to 32°C. Importantly knockdown of α5 subunits still impaired appetitive STM and MTM, while knockdown of α2 subunits and Dlg impaired appetitive MTM (Figure 2 e-h). To control for the proficiency of the tubP-GAL80[ts], we again raised the flies at <20°C but this time kept them at this temperature throughout their lifespan. Importantly, in flies where the RNAi expression was suppressed continuously no memory impairment was measurable (Figure 2i-l).
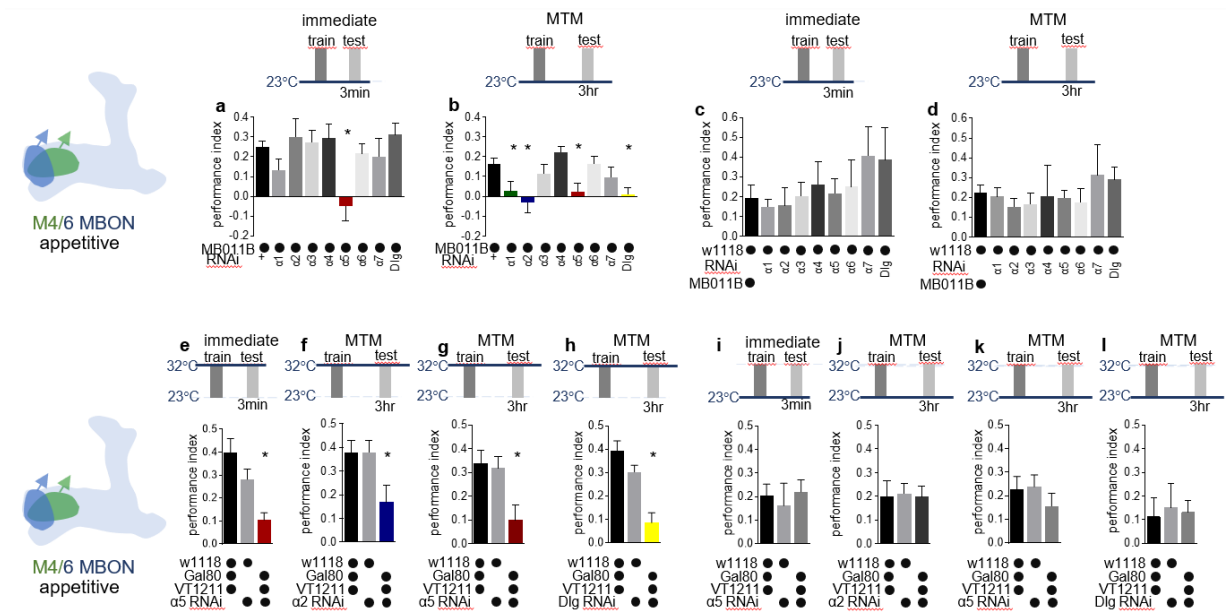
Figure 2: Knockdown of nAChR subunits impairs memory

Figure and legend modified from Pribbenow et al., 2022 (38)

a-y) Bar graphs: mean ± SEM **a)** Appetitive STM is abolished following knockdown of α5 subunits (UAS-RNAi) in M4/M6 neurons (MB011B-Gal4). n= 8 – 13, controls: n= 20; one-way ANOVA followed by Dunnett's test (p < 0.05), * = p < 0.05. **b)** Abolished appetitive MTM following knockdown of α1, α2, α5 nAChR subunits or Dlg (UAS-RNAi) in M4/6 MBONs (MB011B-Gal4). n= 12 – 26, controls: n= 38; Kruskal-Wallis followed by Dunn's test (p < 0.05), * = p < 0.05. **c)** Appetitive STM is not affected in genetic controls. n= 7 – 11, controls: n= 16, one-way ANOVA followed by Tukey's test (p > 0.05). **d)** Appetitive MTM is not affected in genetic controls. n= 7 – 33, controls: n= 41, one-way ANOVA followed by Tukey's test (p > 0.05) **e-h)** Supressed RNAi knockdown of nAChR subunits or Dlg during development (Gal80ts; <20°C) in M4/M6 MBONS (MB011B-Gal4). Induced RNAi expression 3-5 days before the experiments (32°C). **e)** RNAi knockdown of α5 subunits abolishes appetitive STM. n= 6 – 7; Kruskal-Wallis followed by Dunn's test (p < 0.05), * = p < 0.05. **f)** RNAi knockdown of α2 subunits abolishes appetitive MTM. n= 16 – 17; one-way ANOVA followed by Tukey's test (p < 0.05), * = p < 0.05. **g)** RNAi knockdown of α5 subunits abolishes appetitive MTM. n= 25 – 27; one-way ANOVA followed by Tukey's test (p < 0.05), * = p < 0.05. **h)** RNAi knockdown of Dlg abolishes appetitive MTM. n= 8 – 11; one-way ANOVA followed by Tukey's test (p < 0.05), * = p < 0.05. **i-l)** RNAi knockdown in M4/M6 neurons (MB011B-Gal4) of nAChR subunits or Dlg is during the whole lifetime suppressed using Gal80ts (<20°C). **i)** Without α5 subunit knockdown appetitive STM is intact. n= 9; one-way ANOVA followed by Tukey's test. **j)** Without α2 subunit knockdown appetitive MTM is intact. n= 9 – 11, one-way ANOVA followed by Tukey's test. **k)** Without α5 subunit knockdown appetitive MTM is intact. n= 10 – 11, one-way ANOVA followed by Tukey's test. **l)** Without Dlg knockdown appetitive MTM is intact. n=810, one-way ANOVA followed by Tukey's test.

Importantly, previous studies showed that, when the synaptic transmission from M6 neurons was blocked, appetitive STM and LTM were impaired but not abolished (21). Therefore, our next aim was to understand if α2 subunits were required in either one or both the M4 and M6 MBONs. We tested for the behavioural expression of memory performance after knocking down α2 subunits with an RNAi either in M4 or M6 MBONs using different driver lines as before. While the MB210B-Gal4 line labels both M4 and M6 MBONs, the 12C11-Gal4 line labels only M4 MBONs and the R66C08-Gal4 line labels only M6 MBONs. Flies were again trained in a T-maze to associate an odour with sugar. After 3hr the flies got to choose between this previously associated odour (CS+) or a different odour that they had encountered before but without the sugar reinforcement

(CS-). To first reinforce our previous results, we knocked down α2 subunits in M4/M6 MBONs. This led to an abolished appetitive MTM (Figure 3c). Importantly, knockdown of α2 subunits in either the M4 or M6 MBON abolished appetitive MTM performance completely (Figure 3a,b) .
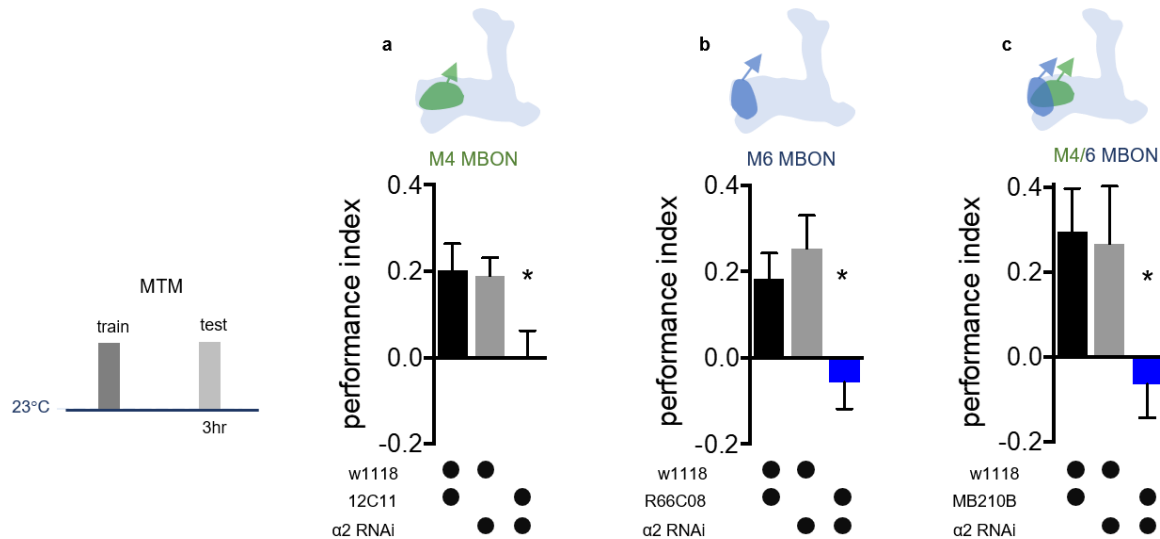

Figure 3: Knockdown of the α2 subunit in M4 and M6 MBONs impairs memory

a) Appetitive MTM is abolished following knockdown of α2 subunits (UAS-RNAi) in M4 neurons (12C11-Gal4). n= 21 – 25; Kruskal-Wallis followed by Dunn's test (p < 0.05), * = p < 0.05. b) Following the knockdown of α2 subunits in M6 neurons (R66C08-Gal4) appetitive MTM is abolished. n= 10 – 13; one-way ANOVA followed by Dunnett's test (p < 0.05), * = p < 0.05. c) Appetitive MTM is abolished following knockdown of the α2 subunit in M4/M6 neurons (MB210B-Gal4). n= 6 – 8; Kruskal-Wallis followed by Dunn's test (p < 0.05), * = p < 0.05.

Since different MBONs might utilize different mechanisms of memory formation, we also tested the MVP2 neuron (MB112C-Gal4), previously described as inhibiting the M4/M6 neurons and having an increased activity upon starvation (22). Additionally, the MVP2 MBONs are required for aversive memory (22). Interestingly, the same subunits and Dlg were required as in M4/M6 MBONs - although for different forms of learning. While α2 subunit knockdown impaired appetitive STM (Figure 4a), knockdown of α5 subunits or Dlg had no effect on appetitive STM (Figure 4b). Meanwhile, aversive memory was not impaired when any subunit was knocked down in M4/M6 MBONs (38): knockdown of α5 and Dlg in MVP2 neurons impaired aversive STM (Figure 4d), and knockdown of either α1 or α2 subunits again had no effect on aversive STM (Figure 4c).
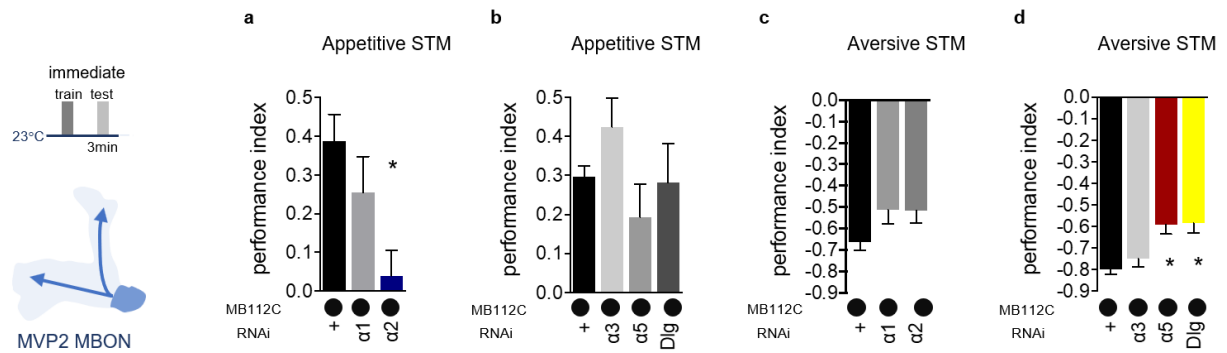
Figure 4: Knockdown of nAChR subunits in MVP2 neurons impairs appetitive and aversive memory

a) Knockdown of α2 subunits (UAS-RNAi) in MVP2 MBONs (MB112C-Gal4) abolishes appetitive STM. n= 15 – 17; one-way ANOVA followed by Tukey's test (p < 0.05), * = p < 0.05. **b)** Knockdown of α3, α5 subunits or Dlg in MVP2 MBONs does not impair appetitive STM. n= 5 – 7; Kruskal-Wallis followed by Dunn's test (p > 0.05). **c)** Knockdown of α1 or α2 subunits in MVP2 MBONs does not impair aversive STM. n= 14 – 18; Kruskal-Wallis followed by Dunn's test (p > 0.05). **d)** Knockdown of α5 subunits or Dlg in MVP2 MBONs abolishes aversive STM. n= 6 – 9; Kruskal-Wallis followed by Dunn's test (p < 0.05), * = p < 0.05.

These results show a requirement for learning of α2 and α5 subunits as well as Dlg in different MBONs. While α5 subunits are required for appetitive STM and MTM in M4/M6 MBONs together, there is a requirement for α2 subunits for appetitive MTM in both M4 and M6 MBONs separately. Dlg is additionally required for appetitive MTM in M4/M6 MBONs. Interestingly in the MVP2 neurons the same subunits are required for learning and memory, however for different learning forms as α2 is required for appetitive STM in MVP2 MBONs and α5 subunits as well as Dlg for aversive STM.

3.3.   Evidence for postsynaptic plasticity in MBONs

While vertebrates utilize both pre- and postsynaptic plasticity (e.g. 5-7), in *Drosophila* only presynaptic plasticity has so far been observed (e.g. 8, 9). However, certain findings have indicated that postsynaptic plasticity might exist in *Drosophila.* For instance, memory performance was impaired when synaptic transmission from KCs was blocked (25, 36, Figure 1b) and protein synthesis in MBONs is required for LTM formation (37). To further investigate postsynaptic contributions to plasticity, the KC-presynapse in explant brain preparations was experimentally bypassed. While feedback signalling was suppressed using TTX, the output of KCs was artificially mimicked by focal ACh application (measuring Ca^{2+} responses in M6 (MB011B-Gal4) MBON dendrites using GCaMP6f (UAS-GCaMP6f)). Involvement of dopaminergic neurons was tested by activating PAM neurons (R58E02-LexA) with the red light-activatable channelrhodopsin CsChrimson

(lexAop-CsChrimsontdTomato) (Figure 5a). ACh evoked Ca^{2+} responses of MBONs before and after training were compared (Figure 5b). Three different training protocols were utilized: 1) ACh application; 2) activation of PAM neurons; and 3) activation of PAM neurons paired with ACh application. We detected no changes in the Ca^{2+} responses pre and post ACh or DA training (Figure 5c,d). Notably, significantly elevated Ca^{2+} responses following paired training were observed (Figure 5e). Next, we wanted to know if α2 subunits play a role in the postsynaptic weight changes after training. Since α2 subunits are required for appetitive MTM (Figure 2b), but not for appetitive STM (Figure 2a), α2 subunits were a likely candidate to influence postsynaptic plasticity. To test this, we knocked down α2 subunits in M4/M6 MBONs (MB011BGal4>UAS-nAChR RNAi). Strikingly, no synaptic weight changes could be observed following paired training in α2 knockdown flies (Figure 5f).

Taken together these experiments demonstrate that, evidence for postsynaptic plasticity exists independent of the presynapse. This postsynaptic plasticity takes place when ACh activates the postsynaptic MBONs while reinforcement by DA release from DANs occurs. Consistent with the demonstrated behavioural experiments, postsynaptic plasticity requires α2 subunits.
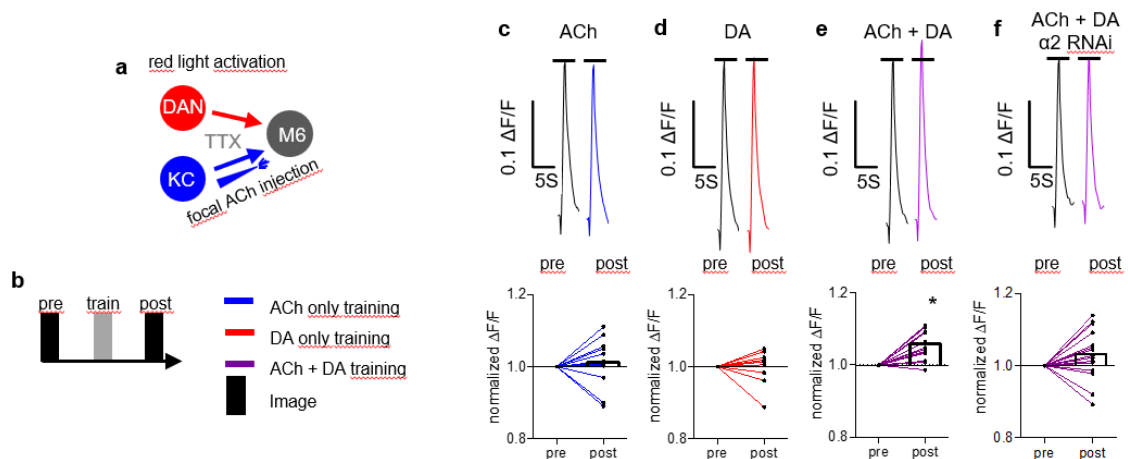
Figure 5: Evidence for postsynaptic plasticity

Figure and legend modified from Pribbenow et al., 2022 (38)

a) Red light initiates Dopamine exocytosis from DANs (R58E02-LexA>lexAop-CsChrimsontdTomato). KC neurotransmitter release is mimicked by focal acetylcholine injections. In M6 neurons postsynaptic Ca^{2+} responses were measured with GCaMP6f (MB011B-GAL4>UAS-GCaMP6f). Feedback signalling and network activity is blocked with TTX. **b)** Before and after training ACh-evoked GCaMP6f responses were measured (pre and post). Training consisted of either ACh application ('ACh only'); red light ('DA only') or both paired ('ACh+DA'). **c-f)** Above: dendritic M6 calcium response trace to ACh application pre (black traces) and post (coloured traces) training. Below:

quantification of peak responses. Before-after plots and bar graphs (mean). **c)** No significant changes in Ca^{2+} transients to ACh application pre-and post 'ACh only' training. n= 13, ratio paired t-test. **d)** No significant changes in Ca^{2+} transients pre- and post 'DA only' training. n= 10, ratio paired t-test. **e)** facilitation in ACh-evoked calcium transients following paired training. n= 18, ratio paired t-test, * = p < 0.05. **f)** facilitation in ACh-evoked calcium transients following paired training is impaired when α2 was knocked down in M4/M6 neurons (MB011B-Gal4>UAS-RNAi). n= 15, ratio paired t-test.

3.4. α5 subunits and Dlg work upstream of α2 subunits

It is known that the KC-MBON synapse is cholinergic (11), and in *Drosophila* seven α (Dα1-Dα7) and three β (Dβ1- Dβ3) nAChR subunits (28) are known. These nAChR subunits can form either homomeric or heteromeric receptors (28). We demonstrated that α5 subunits are required for appetitive STM and MTM and that α2 subunits, as well as the scaffolding protein Dlg, are mandatory for appetitive MTM (Figure 2a,b) in M4/M6 MBONs. We therefore wanted to know which receptor compositions characterize MBONs. Assays of expression established that GFP-tagged endogenous nAChR α-subunits and Dlg are non-uniformly distributed throughout the different compartments of the MB. While Dlg and both α2 and α5 subunits are ample within the γ lobe, they are slightly less abundant in the β2, β'2 or γ1 compartments (Figure 6a). Strikingly, within the γ lobe α4 subunit concentration was the highest (Figure 6a).

To further localize the fluorescence signals of α2 and α5 subunits, RNAi knockdown experiments driving the nAChR-RNAi in M4/M6 neurons (VT1211-Gal4) were performed. The relative fluorescence in the γ5 and β'2 compartments, in which the M4/M6 MBONs originate, was calculated and compared to adjoining unmanipulated compartments (Figure 6b–e). As expected, knockdown of α2 subunits significantly decreased the amount of α2 subunits within the γ5 and β'2 compartment (Figure 6d,e). The same applied to α5 subunits: α5 subunit knockdown in M4/M6 MBONs significantly diminished the relative fluorescence of α5 subunits within the γ5 and β'2 compartment (Figure 6b,c). These results indicate a dendritic location of the subunits in M4/M6 neurons. Intriguingly, knockdown of α5 subunits in the M4/M6 neurons additionally significantly decreased the amount of α2 subunits in the β'2 compartment (Figure 6e) and partly diminished it in the γ5 compartment (Figure 6d). Moreover, a significant reduction of α2 subunits could be observed in the γ5 and β'2 compartment following Dlg knockdown (Figure 6d,e). Conversely, Dlg and α2 knockdowns had no effect on α5 subunit fluorescence (Figure 6b,c).

In previous experiments, we showed that knockdown of α2 and α5 subunits impairs memory performance in MVP2 neurons as well (Figure 4a,d). However, the subunits are required for different forms of learning then in M4/M6 MBONs. We therefore wanted to know if the same influence of α5 subunits on α2 subunits would exist in these neurons. As expected, knocking down α2 subunits in MVP2 MBONs decreased the relative fluorescence of α2^{GFP} in the γ1 compartment compared to the unmanipulated γ4 compartment. However, no effect of knockdown of α5 subunits on the α2 fluorescence signal was detectable (Figure 6f).

Overall, we demonstrate that nAChR subunits are distributed non-uniformly throughout the MB compartments and that the fluorescence signal likely derives from MBONs. Importantly, we see an effect of α5 subunit and Dlg on α2^{GFP} fluorescence levels indicating that α5 subunits and Dlg might function upstream of α2 subunits.
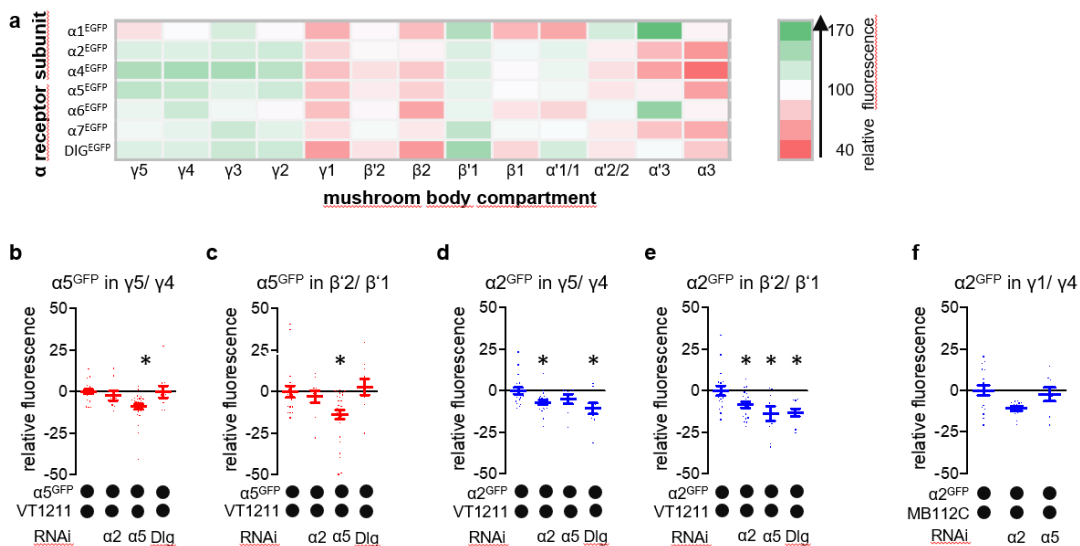
Figure 6: Distribution of nAChR subunits

Figure and legend modified from Pribbenow et al., 2022 (38). 4g was newly added.

a) Fluorescence quantification of GFP-tagged a-subunits (except for α3 subunit). Fluorescence of each compartment is displayed relatively to the mean fluorescence of the whole MB. n= 7 – 18. **b-f)** Bar graph and individual data: normalized mean ± SEM; GFP fluorescence in γ5 compartment relative to unmanipulated γ4 compartment; β'2 compartment relative to unmanipulated β'1 compartment and γ1 compartment relative to unmanipulated γ4 compartment. **b)** Significant decrease of α5^{GFP} in the γ5 compartment following knockdown of α5 (UAS-RNAi) in M4/M6 neurons (VT1211-Gal4). n= 9 – 28; Kruskal-Wallis followed by Dunn's test (p < 0.05), * = p < 0.05. **c)** Significant reduction of α5^{GFP} in the following knockdown of α5 in M4/6 neurons. n= 10 – 28; Kruskal-Wallis followed by Dunn's test (p < 0.05), * = p < 0.05. **d)** Significant decrease of α2^{GFP} in the γ5 compartment following knockdown of Dlg or α2 in M4/M6 neurons. n= 8 – 20; Kruskal-Wallis followed by Dunn's test (p < 0.05), * = p < 0.05. **e)** Significant reduction of α2^{GFP} in the β'2 compartment following knockdown of α2 or α5 subunits or Dlg in M4/M6 neurons. n= 9 – 20; one-way ANOVA followed by Dunnett's test (p < 0.05), * = p < 0.05. **f)** Significant reduction of α2^{GFP} in the γ1 compartment following knockdown of α2 subunits in MVP2 neurons (MB112C). n= 8 – 17; Kruskal-Wallis followed by Dunn's test (p > 0.05), * = p < 0.05.

3.5. Activity of GFP-tagged α nAChR collection flies is normal

Next, we performed a control experiment to exclude a behavioural phenotype and evaluate the functional integrity of the newly generated GFP-tagged α-nAChR collection flies which we use to evaluate nAChR subunit contribution to postsynaptic plasticity. Since neurotransmission from MB neurons is required for normal rhythmic locomotor activity (40), we assessed the activity profiles of these flies with activity monitors. Herein, flies are separated into glass tubes and every time they cross the midline it is counted as one activity bout. As expected, flies were more active during the day when the light was turned on then during the night without light (Figure 7a-c). In GFP-tagged α2 and α5-nAChR flies, no significant differences in activity patterns compared to control flies were observed in the overall amount of activity, the activity during the day, or the amount of activity during the night (Figure 7a-d). We therefore conclude that the GFP-tagged α2 and α5-nAChR flies can be used for future research and that tagging does not interfere with receptor functionality.
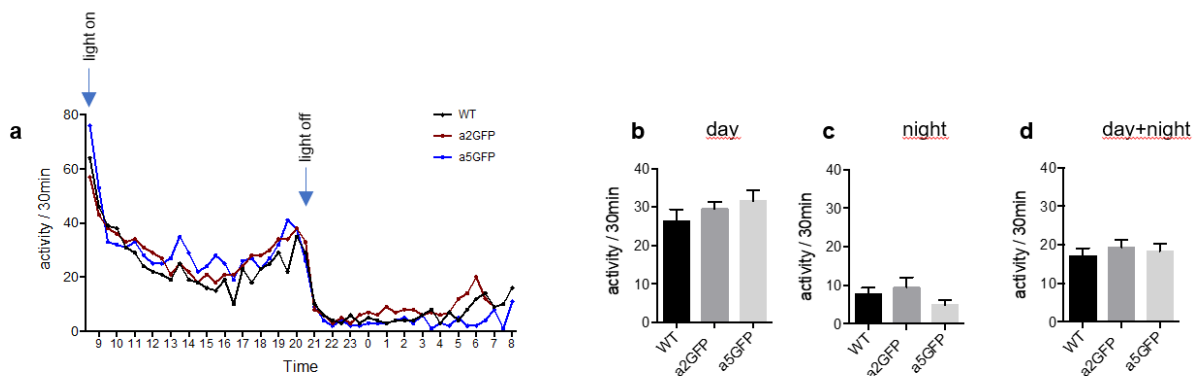
Figure 7: GFP-tagged flies activity is normal

a) Activity traces of Wildtype flies and α2 and a5^{GFP}-tagged nAChR subunit flies. Line diagram: mean; n= 9 – 12. **b-d)** Bar graph: normalized mean ± SEM. **b)** Activity of Wildtype flies and α2 and α5 subunit GFP-tagged flies is comparable; n= 9 – 12; one-way ANOVA followed by Dunnett's test (p > 0.05). **c)** Activity during the night of Wildtype and α2 and α5 subunit GFP-tagged flies is comparable. n= 9 – 12; Kruskal-Wallis followed by Dunn's test (p > 0.05). **d)** Activity during the day of Wildtype and α2 and α5 subunit GFP-tagged flies is comparable. n= 9 – 20; Kruskal-Wallis followed by Dunn's test (p > 0.05).

3.6. Physiological roles of α2 subunits

We demonstrated that α2 and α5 subunits are required for appetitive memory performance (Figure 2a,b), and that without α2 subunits physiological plasticity after training is impaired (Figure 5f). To evaluate the further roles of α2 and α5 subunits in postsynaptic plasticity, we first evaluated odour evoked Ca^{2+} responses in M4 dendrites. Flies, in which either the α2 or α5 subunits had been knocked down in M4/M6 neurons (VT1211-Gal4), were exposed to 10 alternating odour puffs (MCH and OCT) (Figure 8a). Initial odour-evoked GCaMP6f responses in M4 dendrites at the level of the β'2 compartment were significantly elevated in α5 knockdown flies compared to controls (Figure 8b). No changes in initial GCaMP6f responses were observed in α2 knockdown flies. No changes in the GCMP6f responses were observed in control flies over multiple odour exposures (Figure 8c). Interestingly, responses decreased following multiple odour exposures in α5 knockdown flies (Figure 8e). This indicates a possible pre-potentiation of the postsynapse. Meanwhile, knockdown of α2 subunits did not change Ca^{2+} responses to multiple odours (Figure 8d). Previous studies showed that M4/M6 MBONs can be modified bidirectionally following learning (21), and therefore postsynaptic effects following appetitive training in α2 knockdown animals were examined. Flies were trained under the microscope by exposing them to MCH together with sugar (paired training) or exposing them first to sugar and then to MCH (unpaired training). Odour evoked GCaMP6f responses in M4 axons were measured and compared before and after training (Figure 8f,g). As expected, neither in control flies nor in α2 knockdown flies, significant Ca^{2+} changes were observed following unpaired training (Figure 8j,k). Following paired training, a significant depression in responses was measured in control flies (Figure 8h). Strikingly, this synaptic depression was no longer present following α2 subunit knockdown (Figure 8i).In vertebrates the synapse is strengthened or weakened by AMPAR incorporation or removal during learning (10). To further test the hypothesis that receptor movements are required for postsynaptic plasticity in *Drosophila*, in vivo fluorescence recovery after photobleaching (FRAP) experiments using the GFP-tagged α2 nAChR subunits were performed. The recovery of the α2 GFP fluorescence was used as a proxy for receptor incorporation. (Please note that removal of receptors cannot be observed with this method.) Initially, an image of the β'2 compartment was taken followed by fluorescence bleaching of the β'2 compartment. Pictures were taken prior to, and then

10 and 20 minutes after, the training. Training consisted either of dopamine application, odour exposure, or odour exposure paired with dopamine application. One training protocol was performed per fly and OCT was used as the odour (Figure 8l). Odour exposure induced an increase in the fluorescence recovery after 10 and 20 minutes, indicating an increasing amount of $\alpha 2^{GFP}$ in the $\beta'2$ compartment (Figure 8m). Notably, dopamine application did not induce any fluorescence recovery (Figure 8m). Notably, dopamine application together with odour exposure prevented the previously seen recovery following odour application alone (Figure 8m). Air alone did not cause any fluorescence recovery, further indicating that the odour application induces the fluorescence recovery (Figure 8n).

Taken together, we see indication for a pre-potentiation of the synapse when $\alpha 5$ subunits are down-regulated. Additionally, $\alpha 2$ subunits seem to be required for appetitive training, and odour application alone facilitates $\alpha 2$ subunit movements.
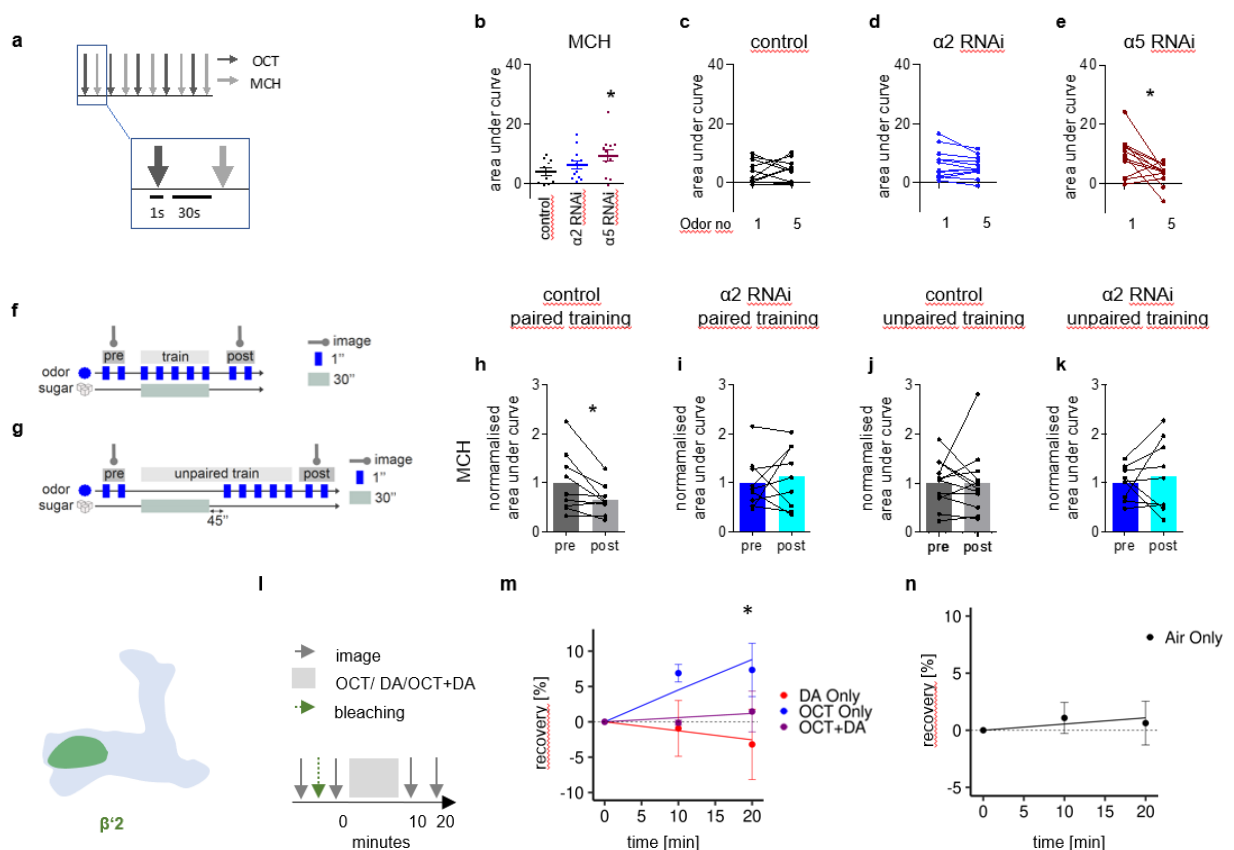

Figure 8: α2 subunit movements are required for learning

Figure and legend modified from Pribbenow et al., 2022 (38)

a) Flies were 10x exposed to OCT and MCH, alternating (1s; ISI: 30s). GCaMP6f responses in M4 dendrites were measured. **b)** α5 knockdown (UAS-RNAi) in M4/6 neurons (VT1211-Gal4) significantly increases MCH AUC responses. Mean ± SEM; one-way ANOVA followed by Dunnett's test ($p < 0.08$), * = $p < 0.05$; n= 10 – 12. **c-e)** Before-after plots. **c)** There is a similar response to the first and the fifth MCH application in control flies. n= 10; paired t-test. **d)** There is a similar response to the first and the fifth MCH application in flies were α2 (UAS-RNAi) is knocked down in M4/M6 neurons. n= 12; paired t- test. **e)** A significant decrease in GCaMP6f responses to the fifth MCH exposure was seen when α5 is knocked down in M4/M6 neurons. n= 12; Wilcoxon matched-pairs signed rank test; * = $p < 0.05$. **f)** paired training under the microscope. Imaging of the Axonal area. **g)** unpaired training under microscope. Imaging of the Axonal area. **h-k)** Analysis of the AUC, Before-after plots and bar graphs (mean). **h)** Following paired training control flies show significantly reduced MCH-evoked GCaMP6f responses in M4 neurons. n= 9; paired t-test; * = $p < 0.05$. **i)** Following paired training α2 knockdown flies show no alteration in GCaMP6f signals to MCH. n= 9; paired t-test. **j)** Following unpaired training the control flies show no alteration in MCH-evoked GCaMP6f responses in M4/M6 neurons. n= 12; Wilcoxon matched-pairs signed rank test. **k)** Following unpaired training, α2 knockdown flies show no alteration in MCH-evoked GCaMP6f signals. n= 9; paired t-test. **l)** experimental protocol. First the β'2 compartment was bleached. Before, plus 10 and 20 minutes after the training the α2^{GFP} fluorescence was measured. Training consisted of DA injection; OCT presentation or paired DA application + OCT presentation. **m)** Inverse exponential decay fit of FRAP following training. **n)** Control experiments. Training consisted of air only. inverse exponential decay fit regression coefficient. n= 9, t-test, Satterthwaite's method for approximating a degree of freedom. Regression coefficient differs not significantly from 0.

3.7. α2 subunits play a role in postsynaptic plasticity for non-associative learning

There are different learning forms in *Drosophila*. In M4/M6 MBONs, required for associative memory, we see a requirement and movement of α2 subunits for postsynaptic plasticity (Figures 2b; 3a,b,c; 5f; 8i,m). To investigate the roles of α2 and α5 subunits in α'3 MBONs required for non-associative familiarity learning (4), nAChR subunit movements were investigated in the α'3 compartment (Figure 9). It had previously been shown that odour induces α2 dynamics in the M4 MBONs (Figure 8m). FRAP experiments were therefore again turned to using GFP-tagged α2 and α5 subunits as well as Dlg. First, an image was taken before the bleaching. This was followed by 10 MCH puffs. Fluorescence signal was measured immediately thereafter and after 5, 10, 15, 20, 30 and 60 minutes (Figure 9a). The recovery of the α2^{GFP} fluorescence was significantly increased following MCH odour exposure after 15, 20 and 30 minutes (Figure 9c). No increases in the amount of α5 subunits or Dlg were observed (Figure 9d,e). To verify that the recovery of the α2^{GFP} signal was due to receptors located to the MBON dendrites, α2 subunits expressing UAS-α2RNAi were knocked down in α'3 MBONs (MB027B-Gal4). The previously observed recovery of the α2^{GFP} fluorescence following MCH exposure was abolished in these flies (Figure 9b). Additionally, to test the hypothesis that α5 subunits were acting upstream of α2 subunits, α5 subunits in the α'3 MBONs (MB027B Split-Gal4 >UAS-α2RNAi) were knocked down. Again, the α2^{GFP} fluorescence signal recovery was abolished following the α5 knockdown (Figure 9b).

Overall, in non-associative memory, an increase in α2 subunits can be seen. This increase is abolished after knockdown of either α2 or α5 subunits. Further indicating that α5 subunits act upstream of α2 subunits.
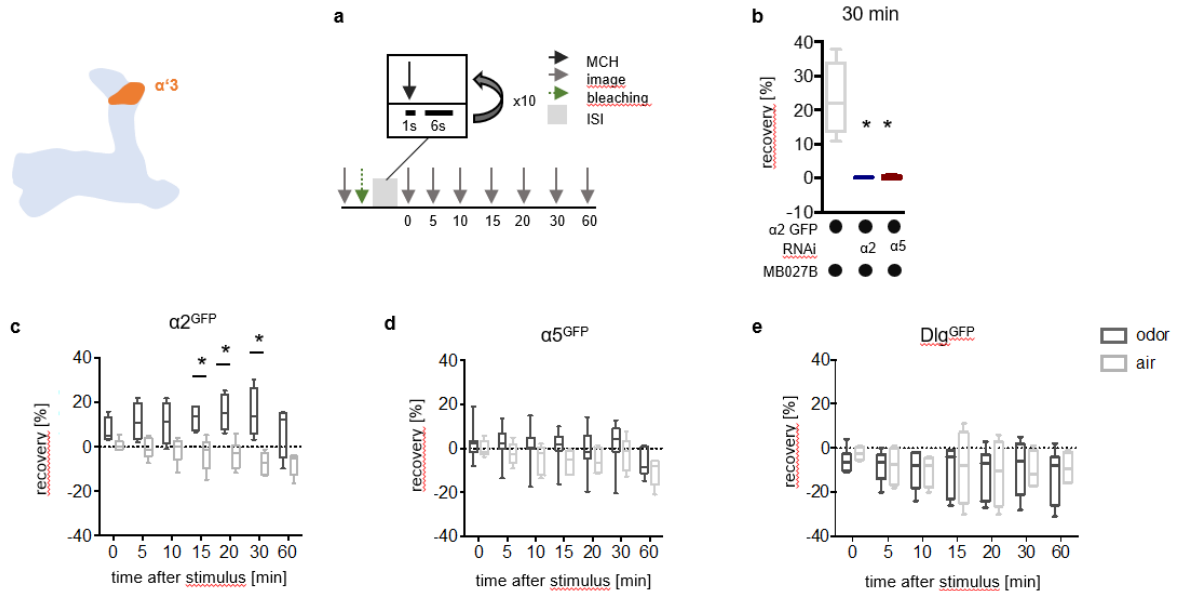
Figure 9: α2 subunit movements are required for learning in α'3 MBONs

Figure and legend modified from Pribbenow et al., 2022 (38)

a) Training scheme for FRAP experiments in the α'3 compartment. 10x MCH exposure (1s; ISI: 6s). Images were taken 0, 5, 10, 15, 20, 30 and 60 minutes afterwards. **b-e)** Recovery normalized to baseline recording. Box plots: median and 75 % quartiles. **b)** 30 minutes after odour exposure and knockdown of α2 or α5 in α'3 MBONs (MB027B - GAL4>UAS-RNAi) α2^{GFP} recovery was impaired. n= 4 – 5; Kruskal-Wallis followed by Dunn's test (p < 0.05), * = p < 0.05. **c)** α2^{GFP} recovery is significantly increased following odour training compared to controls. n= 4 – 6; multiple t - tests with Sidak-Bonferroni correction, * = p < 0.05. **d)** No α5^{GFP} recovery following odour training. n= 5 – 7, multiple t - tests with Sidak-Bonferroni correction. **e)** No Dlg^{GFP} recovery following odour training. n= 5 - 7; multiple t-tests with Sidak-Bonferroni correction

3.8.   Model for postsynaptic plasticity.

Based on the shown results, I created a model for postsynaptic plasticity at the KC-MBON synapse. Naïve odour exposure induces a Ca^{2+} response in M4 neurons (Figure 8b,d). On a subunit level, α2 subunit recovery after photobleaching is increased following odour exposure (Figure 8m). This could likely represent receptor exocytosis or lateral diffusion. On the behavioural level, an avoidance of the odour can be observed (21). When flies are trained to associate an odour with sugar they will afterwards approach of the odour (Figure 1). Meanwhile the Ca^{2+} response in M4 neurons is depressed and receptor incorporation is abundant (Figure 8h,m). Noteworthily, α5 subunits are required for appetitive STM (Figure 2a) and α5 subunits and Dlg seem to influence α2 subunit level (Figures 6d,e, 9b).

The data presented here implicate a model in which α5 subunits are required for inducing postsynaptic plasticity, potentially through calcium influx (though not addressed in this study). Additionally, they implicate that α5 subunits and Dlg are acting upstream of α2 subunits and potentially as inducing α2 receptor dynamics.
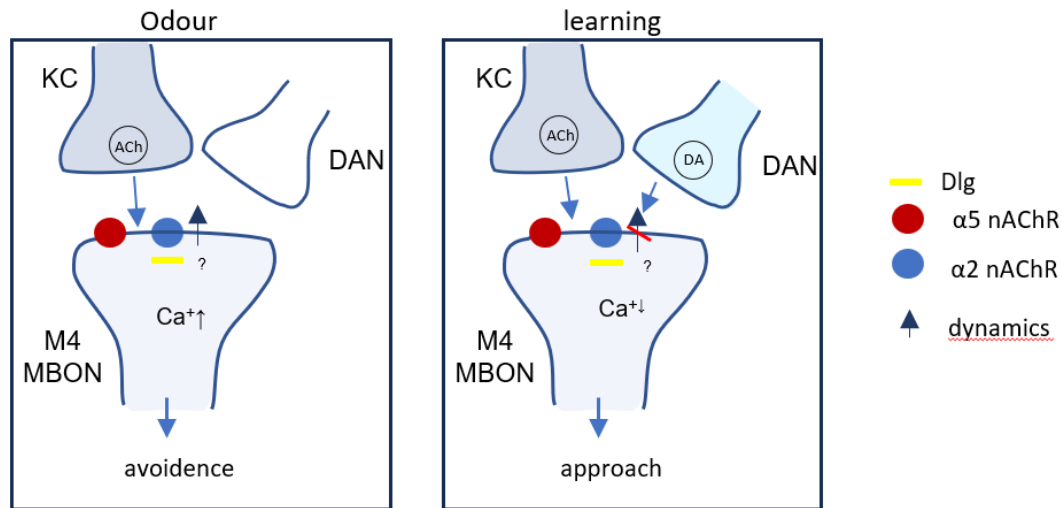

Figure 10: Model for postsynaptic plasticity

Model modified from Pribbenow et al., 2022 (38)

When flies smell an odour ACh is released. This induces a facilitation of Ca^{2+} responses in M4 MBONs as well as α2 subunit incorporation. In contrast when the flies learn appetitively Ca^{2++} responses are decreased in M4 MBONs and no α2 subunit dynamics are visible.

4. Discussion

4.1. Evidence for postsynaptic plasticity in MBONs

I hypothesized that postsynaptic plasticity at the KC-MBON synapse occurs in *Drosophila*. To isolate potential presynaptic from postsynaptic activity, I first revisited experiments blocking presynaptic neurotransmitter release from KCs during acquisition (17, 25, 36) and found that this impaired appetitive but not aversive STM (Figure 1). This slightly contrasted similar experimental results obtained by Schwaertzel et al. (17) who used a different driver line (MB247-Gal4) (which acts less strongly in α'/β' KCs). Neurotransmitter release from M4/M6 neurons is known to be required for appetitive memory expression (21, 24), and in line with previous experiments (24) I subsequently demonstrated that it was dispensable for acquisition (Figure 1). . However, as this did not preclude the possibility of postsynaptic plasticity, we performed proof-of-principle experiments by inducing postsynaptic plasticity circumventing the presynapse. To address this, we first demonstrated that local ACh injection to M6 neuron dendrites, paired with DA release from DANs, induces a facilitation of Ca^{2+} responses in M6 neurons (Figure 5). These experiments were performed in TTX in order to suppress network activity. In theory, ACh injection to axonal terminals can induce Ca^{2+} transients in dopaminergic terminals (39). However, a coincidental carbon monoxide signal is also necessary to induce dopamine release from presynaptic terminals (27) and control experiments in the *absence* of CsChrimson expression (thereby limiting dopamine release) showed no influence of DANs on ACh injection responses in M6 MBONs (38). Together, this indicted that incidental activation of DANs during pre-training is not likely. Although our artificial training of the postsynapse through ACh application does not mirror exact physiological conditions, these experiments establish that, by bypassing the presynapse, postsynaptic plasticity at the KC-MBON synapse can occur. Of note, the observed small amplitude of potentiation agrees with *in vivo* experiments (21).

4.2. nAChR Receptor subunits are necessary for memory formation

Through my proof-of-principle experimentations I had shown that postsynaptic plasticity in MBONs exists, thus raising the question: how could it work mechanistically? Addressing this question required gaining greater understanding of roles played by nAChRs subunits. I had hypothesized that by experimentally perturbing individual nAChR subunits in MBONs I could alter the learning or memory performance of *Drosophila* flies.

First, I assayed nAChR subunit distribution throughout the MB and found topographic non-uniformity (Figure 6). Most subunits were abundant in the γ lobe but less so in the β2 compartment. α5 subunits were particularly enriched in the γ lobe, while α2 subunits were comparably enhanced in the β2 and β'2 compartments (Figure 6). Additionally, it could be shown that the subunit^{GFP} signal derives from MBONs by knocking down the subunits in the M4/M6 neurons (Figure 6). The subunit^{GFP} fluorescence was afterwards significantly decreased. As nAChR subunits can form homomeric or heteromeric channels (28), this differential distribution of nAChR subunits implies a considerable heterogeneity in the nAChR assemblies — albeit it remains impossible to draw conclusions on specific receptor composition.

Knockdown of α1, α4, α5, and α6 subunits in M4/M6 MBONs reduces peak Ca^{2+} responses to MCH (α2 subunits had not been examined; (11)). Seemingly in contrast to these results, we found that naïve odour responses were significantly increased after knockdown of α5 subunit in M4 neurons (Figure 8) but were unaltered following ACh application in M6 neurons (38). These differences can be explained, firstly by the different stimulation methods (ACh vs. odour) and secondly by differences in measurement location (on the M4/M6 presynaptic boutons by Bernstadt et al. 2016 (11), whileat the dendritic side here). Indeed, while odours activate only a sparse number of KCs (15), ACh application likely mimics a broader activation.

Previous experiments had revealed that some nAChR subunits (Dα1, Dα4, Dα5, and Dα6) are required for naïve odour avoidance (11). To further investigate possible requirements for learning, individual nAChR subunits in MBONs were knocked down. These experiments established that α5 subunits are mandatory for appetitive STM and MTM in M4/M6 MBONs, while α1 and α2 subunits are only essential for appetitive MTM (Figures 2,3). Notably, a developmental phenotype was ruled out using the temperature sensitive repressor of Gal4, Gal80^{ts}, during development (Figure 2). The MVP2 MBON was additionally investigated as this neuron inhibits the M4/M6 MBONs and activity is state dependent (22). Therefore, the plasticity roles at this neuron plausibly could have been different. Indeed, knock down of α2 subunits impaired appetitive STM, yet knocking down α5 subunits impaired aversive STM (Figure 4). Blocking the synaptic output of MVP2 neurons inhibits both appetitive and aversive memory. Additionally, odour-evoked activity in MVP2 neurons is increased in hungry flies, and this increase in activity promotes appetitive memory expression. Interestingly, activation of the MVP2 neurons

even enables appetitive memory formation in fed flies (22). Thus, these results indicate different plasticity rules for different kinds of MBONs.

Theoretically, if nAChR subunits are vital for learning they should impair learning dependent postsynaptic Ca^{2+} facilitation or depression. And, in fact, knockdown of α2 subunits in M4/M6 neurons impairs learning dependent Ca^{2+} facilitation in M6 neurons (Figure 5) as well as the learning dependent Ca^{2+} transient depression in M4 MBONs (Figure 8). This depression in the dendritic odour-evoked responses following learning has previously been described (21).

M4 and M6 neurons have separate, distinct roles in memory formation and extinction (20). Therefore, it is not surprising that both neurons show opposite learning induced Ca^{2+} responses and yet both of the learning-induced Ca^{2+} responses are abolished by knocking down α2 subunits in the neurons.

4.3. Receptor dynamics are required for learning and specific nAChRs might play similar roles to those played by NMDAR and AMPAR in mammals

I had hypothesised that receptor dynamics of nAChR are required for learning and memory at the KC-MBON synapse. Although mammals and *Drosophila* utilize different neurotransmitters in learning (7, 10, 11), and *Drosophila* synapses additionally lack anatomical spines (38), the operational mechanics of learning at the receptor level conceivably follow similar principles. Within the relevant mammalian neurons upon activation of NMDAR, and the consequent Ca^{2+} influx, either increased incorporation or removal of AMPAR occurs, which is mandatory for LTP or LTD (10). In *Drosophila*, we herein showed that nAChR subunits are vital for learning (Figures 2,3,4,5,8). Intriguingly, in different MBONs, multiple odour exposures enhance the α2[GFP] signal - indicating enhanced receptor dynamics - while α5 subunits do not show any such dynamics (Figures 8,9). This resembles the dynamics of mammalian AMPAR and NMDAR movements following learning.

Among our experimental observations is a depression in Ca^{2+} transients in M4 neurons following paired training (Figure 8). Strikingly, dopamine application does not induce GFP-tagged receptor dynamics in FRAP experiments and even prevents dynamics if it is paired with an odour (Figure 8). Notably, in this experimental design the α2[GFP] signal is bleached before training and therefore immobilisation or removal of receptors cannot be

detected. Indeed, in mammals, LTD depends on AMPAR internalisation through endocytosis (10).

Importantly, I ruled out activity dependent phenotypes in GFP-tagged subunit flies through the performance of control experiments (Figure 7). Overall, these experiments demonstrated that learning in *Drosophila* depends on specific nAChR subunits both at the behavioural and the synaptic level.

AMPAR dynamics are dependent on NMDAR at glutamatergic synapses (10). Similarly, I also observed a dependence in the expression of α2 subunits on α5 subunits (Figures 6, 9) while, to the contrary, knocking down α2 subunits does not affect the level of α5 subunit expression (Figure 6). I therefore conclude: 1) that *Drosophila* α2 and α5 subunits plausibly follow similar mechanistic principles to those followed by mammalian AMPAR and NMDAR; and 2) that α2 subunit dynamics reveal a previously unknown postsynaptic receptor plasticity in *Drosophila*.

4.4. Specific scaffolding proteins like Dlg are necessary for the formation of memory

For effective receptor dynamics, scaffolding proteins like the *Drosophila* Dlg (a homologue of mammalian PSD-95 (31)) are required. PSD-95 traps and briefly stabilizes diffusing AMPARs at the postsynapse (10), is required for NMDAR surface expression (31), associates with nAChR subunits, and its reduction increases α7 subunit mobility (34). Furthermore, it controls postsynaptic spine size and density (33) and is involved in learning and memory (10). Knockdown of Dlg in M4/M6 neurons, moreover, abolishes appetitive MTM (Figure 2), showing that Dlg is required for learning and memory. Likewise, knockdown of Dlg in MVP2 MBONs abolishes aversive STM (Figure 4). Since MVP2 neurons inhibit M4/M6 neurons and are state dependent (22), it is possible that these neurons follow different principles for learning. Additionally, I found that knockdown of Dlg in M4/M6 MBONs decreased the amount of α2 subunits in the γ5 and β'2 compartment compared to its unmanipulated compartments (Figure 6). This suggests a role of Dlg upstream of α2 subunits and a role in postsynaptic plasticity. Indeed, knockdown of PSD-95 increases α7 subunit mobility (34). Interestingly in mammals, PSD-95 interacts with the protein stargazin to bind to AMPAR and localize them to the membrane (31). Taken together, a requirement of Dlg for learning and memory in MBONs, with Dlg potentially acting upstream of α2 subunits, can be observed.

4.5.   Error analysis

Herein, with proof-of-principle experiments I show evidence for postsynaptic plasticity while bypassing the presynapse. Replacing the presynaptic KC signal through ACh application, this experiment does not precisely mirror physiological conditions since odour normally activates only 6-20% of the KCs (15). The relatively small but significant increase in the Ca^{2+} response following training nevertheless correspondents with previous *in vivo* observations (21). Therefore, these artificial training experiments nonetheless demonstrate postsynaptic plasticity in *Drosophila*.

My thesis also shows that nAChRs are required for learning in different MBONs. The experiments were performed at the KC-MBON synapse. But there are different synapses in the *Drosophila* brain not all using ACh as their neurotransmitter, and therefore one cannot conclude that every synapse uses the same principles. Even within different MBONs, the same subunits were mandatory (though for different functions).

Additionally, FRAP experiments showed a recovery of the subunit-GFP-signal following odour exposure. With the resolution utilized, we nonetheless cannot say if the additional subunit-GFP-signal delineated from lateral diffusion of the subunits or rather from exocytosis. Additionally, after paired training, GFP-signal recovery is abundant. Bleaching the GFP-signal stable receptors or removal of receptors through endocytosis or lateral diffusion cannot be observed.

While the technical resolution of my assays permits me to determine distribution of nAChR subunits in the MBONs, it is incapable of delineating how individual receptors are therein assembled. Moreover, I see evidence that α5 subunits and Dlg might act upstream of α2 subunits. But it has not been shown on a molecular level and cannot be generalized for every MBON (i.e., while there is evidence in M4/M6 and α'3 MBONs it is still unknown for the MVP2 neuron especially under the premise that α2 subunits are vital for appetitive STM).

Taken together, I show evidence for postsynaptic plasticity in *Drosophila* that involves nAChR subunits.

4.6.   Future research

There are many different lanes of possible future research. On the one hand, there are receptor subunits for which the role in memory formation is unclear. Additionally, we see different requirements for subunits in MVP2 neurons compared to M4/M6 MBONs. This

potentially could be state (e.g., starvation state) dependent, since MVP2 neurons are hunger gating (22) and state dependency of plasticity should be investigated. Additionally, molecular mechanisms behind postsynaptic plasticity should be further researched, including addressing other molecular substrates. For instance, one can ask: How do dynamics of *Drosophila* nAChR mechanistically work? And, as mentioned above, do they involve lateral diffusion, endocytosis, and/or exocytosis? Additional fundamental questions remain, including: What role does Dlg play in the regulation of nAChR mobility? Which other molecular substrates are required, and in which way for postsynaptic plasticity? These, and many other questions, will further improve our comprehension of the physical mechanisms of learning and memory. Since plasticity rules at glutamatergic synapses in vertebrates and cholinergic synapses in *Drosophila* are comparable, this information and this model can afterwards be used to understand medical conditions associated with learning deficits.

4.7.   Conclusions

In my thesis, I show that the nAChR subunit α5 is vital for appetitive STM, and that α2, α5 subunits and Dlg are necessary for appetitive MTM. Additionally, in a proof-of-principle experiment, we were able to show that postsynaptic plasticity can be induced separately of the presynapse. I show evidence that α5 subunits and Dlg act upstream of α2 subunits, that altered α2 dynamics reveals postsynaptic receptor plasticity, and conclude that α2 and α5 subunits could follow similar principles as AMPAR and NMDAR. Based on these findings, I propose a model in which receptor trafficking is increased following odour application in M4 neurons in parallel with a brief facilitation in Ca^{2+} transients. Meanwhile a synaptic depression takes place after appetitive conditioning potentially induced by receptor removal. On the contrary, familiarity learning induced by multiple odour exposures again causes a synaptic depression and increases α2 subunit receptor dynamics.

Literature

1. Heisenberg M, Borst A, Wagner S, Byers D. *Drosophila* Mushroom Body Mutants are Deficient in Olfactory Learning: Research Papers. Journal of Neurogenetics. 1985; 2(1):1-30. doi:10.3109/01677068509100140

2. Quinn WG, Harris WA, Benzer S. Conditioned Behavior in *Drosophila* melanogaster. Proc Natl Acad Sci USA. 1974; 71(3):708-712. doi:10.1073/pnas.71.3.708

3. Tully T, Quinn WG. Classical conditioning and retention in normal and mutant *Drosophila* melanogaster. J Comp Physiol A. 1985; 157(2):263-277. doi:10.1007/BF01350033

4. Hattori D, Aso Y, Swartz KJ, Rubin GM, Abbott LF, Axel R.. Representations of novelty and familiarity in a mushroom body compartment. Cell. 2017; 169(5):956-969.e17. doi: 10.1016/j.cell.2017.04.028

5. Durand GM, Kovalchuk Y, Konnerth A. Long-term potentiation and functional synapse induction in developing hippocampus. Nature. 1996; 381(6577):71-75. doi:10.1038/381071a0

6. Bosch M, Castro J, Saneyoshi T, Matsuno H, Sur M, Hayashi Y. Structural and Molecular Remodeling of Dendritic Spine Substructures during Long-Term Potentiation. Neuron. 2014; 82(2):444-459. doi:10.1016/j.neuron.2014.03.021

7. Dolphin AC, Errington ML, Bliss TVP. Long-term potentiation of the perforant path in vivo is associated with increased glutamate release. Nature. 1982; 297(5866):496-497. doi:10.1038/297496a0

8. Elkahlah NA, Rogow JA, Ahmed M, Clowney EJ. Presynaptic developmental plasticity allows robust sparse wiring of the *Drosophila* mushroom body. eLife. 2020; 9:e52278. doi:10.7554/eLife.52278

9. Stahl A, Noyes NC, Boto T, Botero V, Broyles CN, Jing M, Zeng J, King LB, Li Y, Davis RL, Tomchik SM. Associative learning drives longitudinally graded presynaptic plasticity of neurotransmitter release along axonal compartments. eLife. 2022; 11:e76712. doi:10.7554/eLife.76712

10. Chater TE, Goda Y. The shaping of AMPA receptor surface distribution by neuronal activity. Frontiers in Synaptic Neuroscience. 2022; 14. doi: 10.3389/fnsyn.2022.833782

11. Barnstedt O, Owald D, Felsenberg J, Brain R, Moszynski JP, Talbot CB, Perrat PN, Waddell S. Memory-Relevant Mushroom Body Output Synapses Are Cholinergic. Neuron. 2016; 89(6):1237-1247. doi:10.1016/j.neuron.2016.02.015

12. Li F, Lindsey JW, Marin EC, Otto N, Dreher M, Dempsey G, Stark I, Bates AS, Pleijzier MW, Schlegel P, Nern A, Takemura SY, Eckstein N, Yang T, Francis A, Braun A, Parekh R, Costa M, Scheffer LK, Aso Y, Jefferis GSXE, Abbott LF, Litwin-Kumar A, Waddell S, Rubin GM. The connectome of the adult *Drosophila* mushroom body provides insights into function. eLife. 2020; 9:e62576. doi:10.7554/eLife.62576

13. Aso Y, Hattori D, Yu Y, Johnston RM, Iyer NA, Ngo TT, Dionne H, Abbott LF, Axel R, Tanimoto H, Rubin GM. The neuronal architecture of the mushroom body provides a logic for associative learning. eLife. 2014; 3:e04577. doi:10.7554/eLife.04577

14. Wang Y, Guo HF, Pologruto TA, Hannan F, Hakker I, Svoboda K, Zhong Y. Stereotyped Odor-Evoked Activity in the Mushroom Body of *Drosophila* Revealed by Green Fluorescent Protein-Based Ca $^{2+}$ Imaging. J Neurosci. 2004; 24(29):6507-6514. doi:10.1523/JNEUROSCI.3727-03.2004

15. Turner GC, Bazhenov M, Laurent G. Olfactory Representations by *Drosophila* Mushroom Body Neurons. Journal of Neurophysiology. 2008; 99(2):734-746. doi:10.1152/jn.01283.2007

16. Tomchik SM, Davis RL. Dynamics of Learning-Related cAMP Signaling and Stimulus Integration in the *Drosophila* Olfactory Pathway. Neuron. 2009;64(4):510-521. doi:10.1016/j.neuron.2009.09.029

17. Schwaerzel M, Monastirioti M, Scholz H, Friggi-Grelin F, Birman S, Heisenberg M. Dopamine and Octopamine Differentiate between Aversive and Appetitive Olfactory Memories in Drosophila. J Neurosci. 2003; 23(33):10495-10502. doi:10.1523/JNEUROSCI.23-33-10495.2003

18. Waddell, S. Reinforcement signalling in drosophila; dopamine does it all after all. Current Opinion in Neurobiology. 2013; 23(3): 324–329. doi: 10.1016/j.conb.2013.01.005

19. Handler A, Graham TGW, Cohn R, Morantte I, Siliciano AF, Zeng J, Li Y, Ruta V. Distinct Dopamine Receptor Pathways Underlie the Temporal Sensitivity of Associative Learning. Cell. 2019; 178(1):60-75.e19. doi:10.1016/j.cell.2019.05.040

20. Bouzaiane E, Trannoy S, Scheunemann L, Plaçais PY, Preat T. Two Independent Mushroom Body Output Circuits Retrieve the Six Discrete Components of *Drosophila* Aversive Memory. Cell Reports. 2015; 11(8):1280-1292. doi:10.1016/j.celrep.2015.04.044

21. Owald D, Felsenberg J, Talbot CB, Das G, Perisse E, Huetteroth W, Waddell S. Activity of Defined Mushroom Body Output Neurons Underlies Learned Olfactory Behavior in Drosophila. Neuron. 2015; 86(2):417-427. doi:10.1016/j.neuron.2015.03.025

22. Perisse E, Owald D, Barnstedt O, Talbot CB, Huetteroth W, Waddell S. Aversive Learning and Appetitive Motivation Toggle Feed-Forward Inhibition in the *Drosophila* Mushroom Body. Neuron. 2016; 90(5):1086-1099. doi:10.1016/j.neuron.2016.04.034

23. Owald D, Waddell S. Olfactory learning skews mushroom body output pathways to steer behavioral choice in Drosophila. Current Opinion in Neurobiology. 2015; 35:178-184. doi:10.1016/j.conb.2015.10.002

24. Ichinose T, Kanno M, Wu H, Yamagata N, Sun H, Abe A, Tanimoto H. Mushroom body output differentiates memory processes and distinct memory-guided behaviors. Current Biology. 2021; 31(6):1294-1302.e4. doi:10.1016/j.cub.2020.12.032

25. Ichinose T, Aso Y, Yamagata N, Abe A, Rubin GM, Tanimoto H. Reward signal in a recurrent circuit drives appetitive long-term memory formation. eLife. 2015; 4:e10719. doi:10.7554/eLife.10719

26. Scheunemann L, Jost E, Richlitzki A, Day JP, Sebastian S, Thum AS, Efetova M, Davies SA, Schwärzel M. Consolidated and Labile Odor Memory Are Separately Encoded within the *Drosophila* Brain. J Neurosci. 2012; 32(48):17163-17171. doi:10.1523/JNEUROSCI.3286-12.2012

27. Ueno K, Morstein J, Ofusa K, Naganos S, Suzuki-Sawano E, Minegishi S, Rezgui S P, Kitagishi H, Michel BW, Chang CJ, Horiuchi J, Saitoe M. Carbon Monoxide, a Retrograde Messenger Generated in Postsynaptic Mushroom Body Neurons, Evokes Noncanonical Dopamine Release. J Neurosci. 2020; 40(18):3533-3548. doi:10.1523/JNEUROSCI.2378-19.2020

28. Dupuis J, Louis T, Gauthier M, Raymond V.. Insights from honeybee (Apis mellifera) and fly (*Drosophila* melanogaster) Nicotinic acetylcholine receptors: From genes to behavioral functions. Neuroscience & Biobehavioral Reviews. 2012; 36(6): 1553–1564. doi: 10.1016/j.neubiorev.2012.04.003

29. Gundelfinger ED, Hess N. Nicotinic acetylcholine receptors of the central nervous system of Drosophila. Biochim Biophys Acta. 1992; 1137(3):299-308. doi:10.1016/0167-4889(92)90150-a

30. Lansdell SJ, Collins T, Goodchild J, Millar NS. The *Drosophila* nicotinic acetylcholine receptor subunits Dα5 and Dα7 form functional homomeric and heteromeric ion channels. BMC Neurosci. 2012; 13(1):73. doi:10.1186/1471-2202-13-73

31. Zheng C, Seabold GK, Hořák M, Petralia RS. MAGUKs, Synaptic Development, and Synaptic Plasticity. The Neuroscientist. 2011; 17(5): 493–512. doi: 10.1177/1073858410386384

32. Shao CY, Mirra SS, Sait HBR, Sacktor TC, Sigurdsson EM. Postsynaptic degeneration as revealed by PSD-95 reduction occurs after advanced Aβ and tau pathology in transgenic mouse models of Alzheimer s disease. Acta Neuropathol. 2011; 122(3):285-292. doi:10.1007/s00401-011-0843-x

33. El-Husseini AED, Schnell E, Chetkovich DM, Nicoll RA, Bredt DS. PSD-95 Involvement in Maturation of Excitatory Synapses. Science. 2000; 290(5495):1364-1368. doi:10.1126/science.290.5495.1364

34. Gómez-Varela D, Schmidt M, Schoellerman J, Peters EC, Berg DK. PMCA2 via PSD-95 Controls Calcium Signaling by α7-Containing Nicotinic Acetylcholine Receptors on Aspiny Interneurons. J Neurosci. 2012; 32(20):6894-6905. doi:10.1523/JNEUROSCI.5972-11.2012

35. Bertin F, Moya-Alvarado G, Quiroz-Manríquez E, Ibacache A, Köhler-Solis A, Oliva C, Sierralta J. Dlg Is Required for Short-Term Memory and Interacts with NMDAR in the *Drosophila* Brain. IJMS. 2022; 23(16):9187. doi:10.3390/ijms23169187

36. Krashes MJ, Keene AC, Leung B, Armstrong JD, Waddell S. Sequential Use of Mushroom Body Neuron Subsets during *Drosophila* Odor Memory Processing. Neuron. 2007; 53(1):103-115. doi:10.1016/j.neuron.2006.11.021

37. Wu JK, Tai CY, Feng KL, Chen SL, Chen CC, Chiang AS. Long-term memory requires sequential protein synthesis in three subsets of mushroom body output neurons in Drosophila. Sci Rep. 2017; 7(1):7112. doi:10.1038/s41598-017-07600-2

38. Pribbenow C, Chen YC, Heim MM, Laber D, Reubold S, Reynolds E, Balles I, Fernández-d V Alquicira T, Suárez-Grimalt R, Scheunemann L, Rauch C, Matkovic T, Rösner J, Lichtner G, Jagannathan SR, Owald D. Postsynaptic plasticity of cholinergic synapses underlies the induction and expression of appetitive and familiarity memories in Drosophila. eLife. 2022; 11:e80445. doi:10.7554/eLife.80445

39. Cervantes-Sandoval I, Phan A, Chakraborty M, Davis RL. Reciprocal synapses between mushroom body and dopamine neurons form a positive feedback loop required for learning. eLife. 2017; 6:e23789. doi:10.7554/eLife.23789

40. Mabuchi I, Shimada N, Sato S, Ienaga K, Inami S, Sakai T. Mushroom body signaling is required for locomotor activity rhythms in drosophila. Neuroscience Research. 2016; 111: 25–33. doi: 10.1016/j.neures.2016.04.005

Eidesstattliche Versicherung

„Ich, Carlotta Pribbenow, versichere an Eides statt durch meine eigenhändige Unterschrift, dass ich die vorgelegte Dissertation mit dem Thema: „Postsynaptic plasticity of cholinergic synapses underlying learning in *Drosophila* Postsynaptische Plastizität cholinerger Synapsen, die dem Lernen in *Drosophila* zugrunde liegen" selbstständig und ohne nicht offengelegte Hilfe Dritter verfasst und keine anderen als die angegebenen Quellen und Hilfsmittel genutzt habe.

Alle Stellen, die wörtlich oder dem Sinne nach auf Publikationen oder Vorträgen anderer Autoren/innen beruhen, sind als solche in korrekter Zitierung kenntlich gemacht. Die Abschnitte zu Methodik (insbesondere praktische Arbeiten, Laborbestimmungen, statistische Aufarbeitung) und Resultaten (insbesondere Abbildungen, Graphiken und Tabellen) werden von mir verantwortet.

Ich versichere ferner, dass ich die in Zusammenarbeit mit anderen Personen generierten Daten, Datenauswertungen und Schlussfolgerungen korrekt gekennzeichnet und meinen eigenen Beitrag sowie die Beiträge anderer Personen korrekt kenntlich gemacht habe (siehe Anteilserklärung). Texte oder Textteile, die gemeinsam mit anderen erstellt oder verwendet wurden, habe ich korrekt kenntlich gemacht.

Meine Anteile an etwaigen Publikationen zu dieser Dissertation entsprechen denen, die in der untenstehenden gemeinsamen Erklärung mit dem/der Erstbetreuer/in, angegeben sind. Für sämtliche im Rahmen der Dissertation entstandenen Publikationen wurden die Richtlinien des ICMJE (International Committee of Medical Journal Editors; www.icmje.og) zur Autorenschaft eingehalten. Ich erkläre ferner, dass ich mich zur Einhaltung der Satzung der Charité – Universitätsmedizin Berlin zur Sicherung Guter Wissenschaftlicher Praxis verpflichte.

Weiterhin versichere ich, dass ich diese Dissertation weder in gleicher noch in ähnlicher Form bereits an einer anderen Fakultät eingereicht habe.

Die Bedeutung dieser eidesstattlichen Versicherung und die strafrechtlichen Folgen einer unwahren eidesstattlichen Versicherung (§§156, 161 des Strafgesetzbuches) sind mir bekannt und bewusst."

Datum   Unterschrift

Anteilserklärung an den erfolgten Publikationen

Carlotta Pribbenow hatte folgenden Anteil an den folgenden Publikationen:

Publikation 1: **Carlotta Pribbenow**, Yi-chun Chen, M-Marcel Heim, Desiree Laber, Silas Reubold, Eric Reynolds, Isabella Balles, Tania Fernández-d V Alquicira, Raquel Suárez-Grimalt, Lisa Scheunemann, Carolin Rauch, Tanja Matkovic, Jörg Rösner, Gregor Lichtner, Sridhar R Jagannathan, David Owald, Postsynaptic plasticity of cholinergic synapses underlies the induction and expression of appetitive and familiarity memories in Drosophila, eLIFE, 2022

Beitrag im Einzelnen

- I established the behaviour experiments in our lab.
- I planned the experiments for Figure 1-8 and all the additional figures from the "Manteltext"
- I executed experiments for Figure 1,2,4 and all the additional figures from the "Manteltext"
- Figures 1-5, 7,8 from the Paper and all the additional figures from the "Manteltext" were created on the basis of my statistical evaluation
- I designed the figures 1-8 and all the additional figures from the "Manteltext"
- I was involved in creating the model for Figure 9.
- Writing of the Manuscript and reply to the reviewers
- Presentation of the Project on scientific conferences

_____

Unterschrift, Datum und Stempel des/der erstbetreuenden Hochschullehrers/in

_____

Unterschrift des Doktoranden/der Doktorandin

Druckexemplar der Publikation

Postsynaptic plasticity of cholinergic synapses underlies the induction and expression of appetitive and familiarity memories in *Drosophila*

Carlotta Pribbenow[1], Yi-chun Chen[1†], M-Marcel Heim[1†], Desiree Laber[1†], Silas Reubold[1†], Eric Reynolds[1†], Isabella Balles[1], Tania Fernández-d V Alquicira[1], Raquel Suárez-Grimalt[1,2], Lisa Scheunemann[1,3,4], Carolin Rauch[1], Tanja Matkovic[4], Jörg Rösner[5], Gregor Lichtner[1,6], Sridhar R Jagannathan[1], David Owald[1,2,3]*

[1]Institute of Neurophysiology, Charité – Universitätsmedizin Berlin, corporate member of Freie Universität Berlin and Humboldt-Universität zu Berlin, and Berlin Institute of Health, Berlin, Germany; [2]Einstein Center for Neurosciences Berlin, Berlin, Germany; [3]NeuroCure, Charité – Universitätsmedizin Berlin, corporate member of Freie Universität Berlin and Humboldt-Universität zu Berlin, and Berlin Institute of Health, Berlin, Germany; [4]Institut für Biologie, Freie Universität Berlin, Berlin, Germany; [5]NWFZ, Charité – Universitätsmedizin Berlin, corporate member of Freie Universität Berlin and Humboldt-Universität zu Berlin, and Berlin Institute of Health, Greifswald, Germany; [6]Universitätsmedizin Greifswald, Department of Anesthesia, Critical Care, Emergency and Pain Medicine, Greifswald, Germany

*For correspondence:
david.owald@charite.de

†These authors contributed
equally to this work

Abstract In vertebrates, several forms of memory-relevant synaptic plasticity involve postsynaptic rearrangements of glutamate receptors. In contrast, previous work indicates that *Drosophila* and other invertebrates store memories using presynaptic plasticity of cholinergic synapses. Here, we provide evidence for postsynaptic plasticity at cholinergic output synapses from the *Drosophila* mushroom bodies (MBs). We find that the nicotinic acetylcholine receptor (nAChR) subunit α5 is required within specific MB output neurons for appetitive memory induction but is dispensable for aversive memories. In addition, nAChR α2 subunits mediate memory expression and likely function downstream of α5 and the postsynaptic scaffold protein discs large (Dlg). We show that postsynaptic plasticity traces can be induced independently of the presynapse, and that in vivo dynamics of α2 nAChR subunits are changed both in the context of associative and non-associative (familiarity) memory formation, underlying different plasticity rules. Therefore, regardless of neurotransmitter identity, key principles of postsynaptic plasticity support memory storage across phyla.

Editor's evaluation

Learning-dependent plasticity is thought to take place predominantly presynaptically in Drosophila. This paper by the Owald group adds important evidence for postsynaptic plasticity mechanisms, including that appetitive memory is impaired when nAChR subunits (α2, α5) and scaffold protein Dlg are downregulated in specific mushroom body output neurons. In a tour-de-force, they combine physiology, *Drosophila* genetics, and behaviour and the work also emphasises the similarities in learning and memory mechanisms between vertebrates and invertebrates.

Introduction

The efficacy of synaptic transmission, also referred to as synaptic weight, can be increased or decreased following changes in neural activity profiles or concurrent action of neuromodulators, such as dopamine. Resulting changes to how synapses relay information underlie synaptic plasticity, which is widely believed to be the basis of memory storage (Glanzman, 2010; Korte and Schmitz, 2016; Nicoll, 2017). While, it is generally accepted that synaptic plasticity can serve as memory substrate from flies to humans, it is unclear to what degree neurophysiological and molecular principles underlying synaptic plasticity are evolutionarily conserved. One main difference between vertebrates and invertebrates is that memory-storing synapses in vertebrates use glutamate as their primary transmitter, while those in invertebrates (at least for Drosophila melanogaster and Sepia officinalis) use acetylcholine (Barnstedt et al., 2016; Owald and Waddell, 2015; Shomrat et al., 2011). Furthermore, it is widely established that invertebrate nervous systems utilize presynaptic plasticity (with plasticity referring to changes leading to either strengthening (potentiation) or weakening (depression) of synaptic transmission and the rearrangement or exchange of synaptic molecules underlying changed transmission) for storing memories, while the degree to which postsynaptic plasticity can be used is less clear. In contrast, it is well established (Glanzman, 2010; Korte and Schmitz, 2016; Nicoll, 2017) that storing information in vertebrates can depend on both pre- and postsynaptic mechanisms, including postsynaptic rearrangements of neurotransmitter receptors.

Detailed knowledge of the anatomical wiring and functional signaling logic of the Drosophila learning and memory centers, the mushroom bodies (MBs; third ['higher']-order brain center; learning takes place three synapses downstream of sensory neurons; Owald and Waddell, 2015; Owald et al., 2015; Aso et al., 2019; Aso et al., 2014b; Aso et al., 2014a; Bouzaiane et al., 2015; Cohn et al., 2015; Felsenberg et al., 2018; Felsenberg et al., 2017; Hattori et al., 2017; Ichinose et al., 2015; Lewis et al., 2015; Pai et al., 2013; Perisse et al., 2016; Séjourné et al., 2011; Plaçais et al., 2013) allow one to address to what extent synaptic mechanisms underlying memory storage are comparable across evolution, despite the use of different neurotransmitter systems. The weights of Kenyon cells (KCs) to MB output neuron (MBON) synapses are modulated by dopaminergic neurons (DANs), which anatomically divide the MBs into at least 15 functional compartments. At the level of these compartments, information is stored on appetitive and aversive (odor) associations, in addition to non-associative information, such as the relative familiarity of an odor (Owald and Waddell, 2015; Owald et al., 2015; Aso et al., 2019; Aso et al., 2014b; Aso et al., 2014a; Bouzaiane et al., 2015; Cohn et al., 2015; Hattori et al., 2017; Hige et al., 2015; Takemura et al., 2017), a distinct form of habituation. Summed up (Owald and Waddell, 2015), output from the individual MB compartments will give rise to specific behaviors, weighing up appetitive and aversive associations as well as, for instance, the familiarity of a stimulus.

Studies so far have identified several traits pointing toward presynaptic storage mechanisms within the KCs during memory formation (Bilz et al., 2020; Boto et al., 2014; Handler et al., 2019; Ehmann et al., 2018). Indeed, some studies that have blocked neurotransmitter release from KCs during learning Dubnau et al., 2001; McGuire et al., 2001; Schwaerzel et al., 2002 have brought postsynaptic contributions to synaptic plasticity into question.

In vertebrates, typically, postsynaptic long-term changes (Korte and Schmitz, 2016; Kandel et al., 2014; Lüscher and Malenka, 2011) are mediated via NMDA-sensitive glutamate receptors (NMDAR) that induce ('induction'; Nicoll, 2017) an expression phase ('expression'; Nicoll, 2017) through changed glutamatergic AMPA receptor (AMPAR) dynamics in dependence of postsynaptic scaffolds like PSD-95 (Won et al., 2017). Invertebrate nAChRs in principle could take over similar functions to their glutamatergic counterparts in vertebrates, despite their differing molecular characteristics (Thompson et al., 2010). Indeed, nAChRs are pentamers that can be composed of homomeric assemblies of α subunits or heteromeric combinations of different α and β subunits. The composition of subunits determines the physiological properties of the nAChRs (Thompson et al., 2010; Dent, 2010; Ihara et al., 2020; Lansdell et al., 2012), and synaptic weights could, in theory, be adjusted through the exchange of receptor subunits or entire complexes.

Here, we capitalize on the genetic accessibility to individual output neurons of the MBs to directly test whether postsynaptic receptors play a role in memory storage. Derived from combined neurophysiological, behavioral, light microscopic, and molecular approaches, our data are supportive of a sequential role for nAChR subunits in appetitive memory storage at the level of MBONs. Using

artificial training protocols, we demonstrate that postsynaptic calcium transients can change in response to concurrent activation of DANs and application of acetylcholine, circumventing KC output. Blocking KC output during appetitive, but not aversive, learning abolishes memory performance. Moreover, specific knockdown of the α5 nAChR subunit, but none of the other six α subunits, in the M4/6 MBONs (also known as MBON-γ5β'2a, MBON-β'2mp, MBON- β2β'2a, and MBON-β'2mp bilateral) – an output junction involved in coding appetitive and aversive memories (*Owald et al., 2015*; *Bouzaiane et al., 2015*; *Lewis et al., 2015*) – impairs immediate appetitive memories. Knockdown of α2 or α5, however, interferes with 3-hr appetitive memories, as does knockdown of the scaffold discs large (Dlg). We report differential distribution of α subunits throughout the MB and demonstrate that signal recovery of GFP (green fluorescent protein)-tagged subunits (as measured through fluorescence signal recovered after photobleaching) is changed through plasticity protocols. In addition, postsynaptically expressed non-associative familiarity learning that is encoded at the level of the α'3 neurons of the MBs also depends on α5 and α2 signaling as well as α2 dynamics. We propose a temporal receptor model and speculate that, in *Drosophila*, nAChR subunits α5 and α2 take roles similar to NMDAR and AMPAR in vertebrates for memory induction and expression, indicating that the general principle for postsynaptic plasticity independent of the neurotransmitter system used could be conserved throughout evolution.

Results

Neurotransmitter release from KCs is required for appetitive learning

If the postsynapse need not see the neurotransmitter during training, it would likely be dispensable for memory induction. One key argument in favor of exclusively presynaptic memory storage mechanisms in *Drosophila* is based on experiments suggesting that blocking KC or KC subset output selectively during (olfactory) learning leads to unaltered or mildly changed memory performance (*Dubnau et al., 2001*; *Krashes et al., 2007*; *McGuire et al., 2001*; *Schwaerzel et al., 2002*). However, other studies have reported memory impairments following KC subset or downstream circuit element block during training (*Krashes et al., 2007*; *Yamazaki et al., 2018*; *Ichinose et al., 2021*). Moreover, protein synthesis was shown to be required at the level of MBONs for long-term memory formation (*Pai et al., 2013*; *Widmer et al., 2018*; *Wu et al., 2017*). To corroborate that the postsynapse or downstream circuits would need to 'see' the neurotransmitter for memory storage, we first revisited experiments blocking KC output selectively during T-maze training, exposing the animals either to sugar-odor or shock-odor pairings (*Figure 1a–b*, *Figure 1—figure supplement 1a-b*).

We expressed the temperature-sensitive *dynamin* mutant UAS-*Shibire*ᵗˢ (Shi) at the level of KCs (R13F02-Gal4), trained animals at the restrictive temperature (32°C), and tested for memory performance at permissive temperature (23°C) 30 min later. These manipulations allowed us to interfere with the synaptic vesicle exo-endocycle specifically during conditioning, while reinstating neurotransmission afterward: by choosing the 30-min time point, we made sure to restore functional Dynamin and not to interfere with any process underlying memory retrieval. Consistent with previous reports (*Dubnau et al., 2001*; *McGuire et al., 2001*; *Schwaerzel et al., 2002*), a slight drop in aversive memory performance (*Figure 1a*) was not statistically different from their genetic controls, and also observable in the permissive temperature controls (23°C; see *Figure 1—figure supplement 1a*). In contrast, memories were completely abolished following block of KC output during appetitive training (*Figure 1b*, *Figure 1—figure supplement 1b*).

While it remained unclear as to how far postsynaptic plasticity at the KC to MBON synapse could be involved in memory storage, several lines of evidence have implicated circuit mechanisms downstream of KCs to be involved in memory formation (*Pai et al., 2013*; *Ichinose et al., 2021*; *Widmer et al., 2018*; *Wu et al., 2017*). We next asked whether the requirement for neurotransmission during appetitive learning was specific to the KC output synapse. To do so, we took an analogous approach, this time blocking neurotransmission from downstream M4/6 (MBON-γ5β'2a, MBON-β'2mp, MBON-β2β'2a, and MBON-β'2mp bilateral) MBONs (MB011B Split-Gal4) during appetitive training. We focused on the M4/6 set of MBONs as blocking these during memory retrieval crucially interferes with appetitive memory expression, while, on a physiological level, memory-related plasticity is observable (*Owald and Waddell, 2015*; *Owald et al., 2015*; *Felsenberg et al., 2018*). When blocking M4/6 during appetitive training, but not retrieval, memory scores were similar to those of control groups
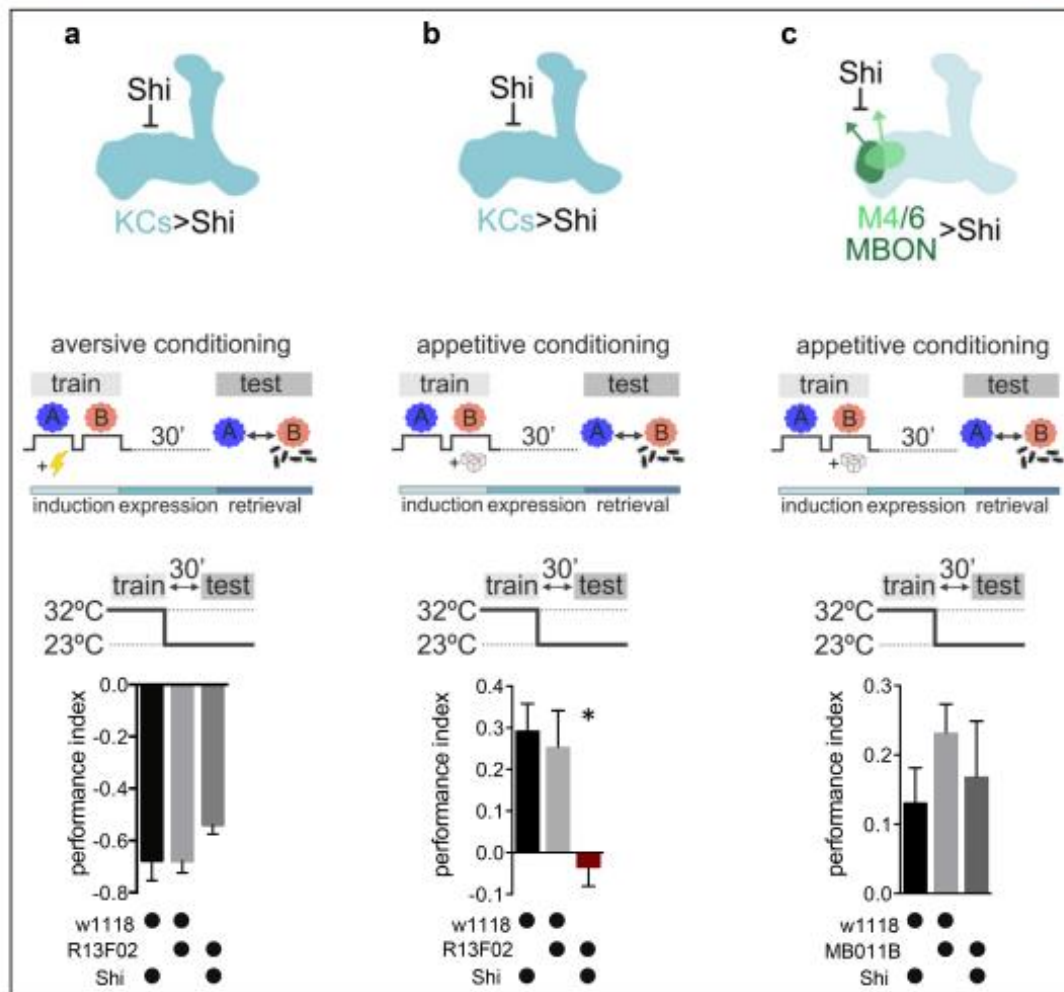
Figure 1. Kenyon cell (KC) neurotransmitter release is required for the acquisition of appetitive memories. (a–c) Flies expressing temperature-sensitive Shibire (Shi) within KCs or mushroom bodies output neurons (MBONs) are trained at restrictive temperature (32°C), and subsequently placed at permissive temperature (23°C) throughout the consolidation and retrieval phase. Memory performance was tested 30 min after training at permissive temperature. Shi blocks neurotransmitter release at 32°C. (a) Block of neurotransmitter release from KCs (driver line R13F02-Gal4) during training does not impact 30-min aversive memory performance. Bar graphs: mean ± SEM; n=7–8; one-way ANOVA followed by Tukey's test (p>0.05). (b) Block of neurotransmitter release from KCs (driver line R13F02-Gal4) during training impairs 30-min appetitive memory performance. Bar graphs: mean ± SEM; n=10–16; Kruskal-Wallis followed by Dunn's test (p<0.05), *p<0.05. (c) Block of neurotransmitter release from M4/6 MBONs (driver line MB011B [Split-GAL4]) during training does not impact 30-min appetitive memory performance. Bar graphs: mean ± SEM; n=14–24; one-way ANOVA followed by Tukey's test (p>0.05). Also see *Figure 1—figure supplement 1* for further information.

The online version of this article includes the following figure supplement(s) for figure 1:

Figure supplement 1. Permissive temperature controls accompanying *Figure 1*.

(*Figure 1c*), suggesting that the sites of plasticity are likely to be the KC to MBON synapse in general, with one major site specifically being the connections between KCs and M4/6 MBONs.

Thus, our experiments suggest that neurotransmitter release from KCs during training is required for the formation of appetitive memories but is less crucial for the formation of aversive memories.

The α5 nAChR subunit is required for induction and α2 for expression of appetitive memories

Requirement for presynaptic neurotransmitter release alone does not necessarily mean that postsynaptic plasticity is involved in appetitive memory formation. To address a putative postsynaptic role in memory formation, we next interfered with the postsynaptic receptor composition. Given that KCs are cholinergic, we screened for memory requirement of all nicotinic α subunits at the level of the M4/6 MBONs (MB011B Split-Gal4; *Figure 2*) using previously published (*Barnstedt et al., 2016; Cervantes-Sandoval et al., 2017*) genetically targeted RNAi (UAS-nAChR[RNAi], please see Methods for detailed lines). We concentrated on the nAChR α subunits, as they are crucial components for all possible heteromeric or homomeric receptor pentamers (*Dent, 2010*).

When flies were tested for immediate appetitive memory, only knockdown of the α5 subunit produced performance that was statistically different from the controls (*Figure 2a, Figure 2—figure supplement 1a, Figure 2—figure supplement 2e*). Testing 3-hr appetitive memory performance revealed a significant memory impairment in flies with α1, α2, and α5 knockdown (*Figure 2b, Figure 2—figure supplement 1b, Figure 2—figure supplement 2f-h*). While α5 subunits can form homomeric channels (*Lansdell et al., 2012*), α1 and α2 can partake in heteromeric channels together (*Ihara et al., 2020*). We therefore concentrated on the α5 and α2 nAChR subunits in subsequent analyses.

To exclude developmental contributions to the observed memory defects, we repeated the immediate and 3-hr appetitive memory experiments for α5 as well as the 3-hr appetitive memory experiments for α2 knockdown animals, while suppressing RNAi expression (VT1211-Gal4>UAS-nAChR[RNAi]) using the temperature-sensitive Gal4 repressor Gal80[ts] (tubP-GAL80[ts]) during development (<20°C), up until 3–5 days (32°C) before memory testing. Memory impairments were confirmed in all cases (*Figure 2e-g*; 32°C) but not detected in temperature controls where the RNAi expression was suppressed throughout (<20°C; *Figure 2—figure supplement 2a-c*).

We also tested aversive immediate and 3-hr memory using the same genetic settings (*Figure 2c and d, Figure 2—figure supplement 1c,d*). None of the knockdowns differed significantly from controls, with the exception of α7 at the 3-hr time point. As, comparable to vertebrate systems, α7 also plays a significant role at presynaptic neurites (*Eadaim et al., 2020*), we did not follow up on this observation in this study.

As M4/6 output is also required for appropriate aversive memory expression (*Owald et al., 2015; Bouzaiane et al., 2015*), α2 and α5 knockdown not impacting aversive memory performance suggested that the observed appetitive memory impairments were not simply a consequence of lost postsynaptic responsiveness to acetylcholine. To further corroborate this, we turned to a brain explant preparation and applied acetylcholine focally to the dendrites of M4/6 neurons (VT1211-Gal4) that expressed the calcium indicator UAS-GCaMP6f, for both control and knockdown settings, in the presence of the blocker of voltage-gated sodium channels TTX (*Barnstedt et al., 2016; Raccuglia et al., 2019*). Dendritic calcium transients were comparable between all groups (*Figure 3—figure supplement 1e*). We also observed presynaptic calcium transients in all genotypes (*not shown*) after applying acetylcholine to the presynaptic MBON boutons, making presynaptic deficits following α2 or α5 knockdown unlikely.

Therefore, we conclude that, at the level of M4/6 neurons, immediate and 3-hour appetitive memories are affected by knockdown of the α5 subunit, whereas 3-hr memories also require the presence of α1- and α2-bearing receptors in addition. The observed temporal profile of requirement for memory of α1- and α2-bearing receptors relative to those incorporating the α5 subunit could potentially point to a temporal sequence of receptor function during initial memory formation and subsequent memory expression.

The postsynaptic scaffold Dlg is required for 3-hr appetitive memory

At mammalian glutamatergic synapses, postsynaptic receptor-mediated changes in synaptic weight (the efficacy of neurotransmitter-mediated signal propagation) rely on receptor stabilization or destabilization that can be mediated via scaffolding molecules. One such scaffold, PSD-95, that is mostly involved in AMPAR motility, is conserved at *Drosophila* synapses. The ortholog Dlg (*Bachmann et al., 2004; Soukup et al., 2013*) is expressed throughout the brain, with MB compartment-specific enrichment noted previously (*Crittenden et al., 1998*; also compare Figure 4a,b). We investigated

Figure 2. Specific nicotinic acetylcholine receptor (nAChR) α subunits are needed for specific memories in M4/6 neurons. Training and testing protocols indicated schematically. A and B indicate different odors. (a) Immediate appetitive memories are impaired following RNAi knockdown of the α5 nAChR subunit in M4/6 mushroom bodies output neurons (MBONs; driver line MB011B [Split-GAL4]). Bar graphs: mean ± SEM; n=8–13, for controls: n=20; one-way ANOVA followed by Dunnett's test (p<0.05), *p<0.05. Note: data depicted correspond to initial screen, please see *Figure 2—figure supplement*

Figure 2 continued on next page

eLife Research article

Figure 2 continued

2e for alternate display including all genetic controls. (**b**) RNAi knockdown of the α1, α2, α5 nAChR subunits or discs large (Dlg) in M4/6 MBONs (driver line MB011B [Split-GAL4]) impairs 3-hr appetitive memories. Bar graphs: mean ± SEM; n=12–26, for controls: n=38; Kruskal-Wallis followed by Dunn's test (p<0.05), *p<0.05. Note: data depicted correspond to initial screen, please see *Figure 2—figure supplement 2* f–i for alternate display including all genetic controls. (**c**) Immediate aversive learning is not impaired by RNAi knockdown of any subunit in M4/6 MBONs (driver line MB011B [Split-GAL4]). Bar graphs: mean ± SEM; n=6–8, for controls: n=12; Kruskal-Wallis followed by Dunn's test (p>0.05). (**d**) 3-hr aversive memory is not affected by knockdown of α subunits with the exception of α7 (driver line MB011B [Split-GAL4]). Bar graphs: mean ± SEM; n=21–32, for controls: n=61. Kruskal-Wallis followed by Dunn's test (p<0.05), *p<0.05. (**e**) RNAi knockdown of the α5 subunit in M4/6 MBONs (driver line VT1211-Gal4) is suppressed during development using Gal80^{ts}. 3–5 days before the experiment RNAi knockdown was induced. Immediate memory is significantly impaired. Bar graphs: mean ± SEM; n=6–7; Kruskal-Wallis followed by Dunn's test (p<0.05), *p<0.05. (**f**) RNAi knockdown of the α2 subunit in M4/6 MBONs (driver line VT1211-Gal4) is suppressed during development using Gal80^{ts}. 3–5 days before the experiment RNAi knockdown was induced. 3-hr memories are significantly impaired. Bar graphs: mean ± SEM; n=16–17; one-way ANOVA followed by Tukey's test (p<0.05), *p<0.05. (**g**) RNAi knockdown of the α5 subunit in M4/6 MBONs (driver line VT1211-Gal4) is suppressed during development using Gal80^{ts}. 3–5 days before the experiment RNAi knockdown was induced. 3-hr memories are significantly impaired. Bar graphs: mean ± SEM; n=25–27; one-way ANOVA followed by Tukey's test (p<0.05), *p<0.05. (**h**) RNAi knockdown of Dlg in M4/6 MBONs (driver line VT1211-Gal4) is suppressed during development using Gal80^{ts}. 3–5 days before the experiment RNAi knockdown was induced. 3-hr memories are significantly impaired. Bar graphs: mean ± SEM; n=8–11; one-way ANOVA followed by Tukey's test (p<0.05), *p<0.05. Also see *Figure 2—figure supplements 1 and 2* for further information.

The online version of this article includes the following figure supplement(s) for figure 2:

Figure supplement 1. Genetic controls and alternate data display of data presented in *Figure 2*.

Figure supplement 2. Genetic controls and alternate data display of data presented in *Figure 2*.

appetitive and aversive memory performance following M4/6-specific knockdown of Dlg (*Figure 2, Figure 2—figure supplement 1a-d*; MB011B Split Gal4 >UAS-Dlg^{RNAi}). Performance scores comparable to controls were found for both immediate appetitive and aversive memories (*Figure 2a,c and d, Figure 2—figure supplement 1a,c and d*). Dlg knockdown (VT1211-Gal4>UAS-Dlg^{RNAi}), however, specifically abolished 3-hr appetitive memory performance (*Figure 2b, Figure 2—figure supplements 1b and 2i*), while Gal80^{ts} experiments excluded a developmental defect (*Figure 2h, Figure 2—figure supplement 2d*). The temporal profile of Dlg requirement therefore closely matched that of α2 nAChR subunits.

Bypassing the presynapse: induction of persistent associative plasticity in the postsynaptic compartment

Recent ultrastructural data has revealed direct synaptic connections between DANs and MBONs (*Takemura et al., 2017*; *Eichler et al., 2017*), giving rise to a motif that could allow for postsynaptic plasticity induction (reflected by the lasting change of synaptic weights; see schematic in *Figure 3a*). In order to directly test whether postsynaptic plasticity could take place at the level of MBONs, we next conducted neurophysiological proof-of-principle experiments.

To minimize potential non-associative effects on synaptic properties induced by acute sensory experiences or general network activity, we used an explant brain preparation bathed in TTX from flies expressing the red light-activatable channelrhodopsin CsChrimson (lexAop-CsChrimson^{tdTomato}) in a subset of DANs (PAM neurons; R58E02-LexA) and the calcium indicator GCaMP6f (UAS-GCaMP6f) in M4/6 MBONs (MB011B Split Gal4).

While dopamine release was controlled by red light flashes, neurotransmitter release from KCs was mimicked by focal pressure ejection of acetylcholine to the dendrites of the M6 (MBON-γ5β'2a) MBON (M6 was chosen for technical reasons, as these neurons are most accessible for the used imaging technique). We verified that KC presynapses do not respond to acetylcholine application (*Barnstedt et al., 2016*), using both calcium imaging and imaging of synaptic vesicle exocytosis at the level of KC axons (*Figure 3c* and *Figure 3—figure supplement 1f,g*). The observed absence of KC activation, with acetylcholine being applied from an external source (*Figure 3a*), minimized noise attributable to possible presynaptic contributions.

Our protocols consisted of training phases where we differentiated between temporal pairing of acetylcholine and optogenetic activation of DANs ('paired', *Figure 3b and h*), dopamine only ('red-light only', *Figure 3b, e and g*), or 'acetylcholine only' (*Figure 3b, d and f*). Acetylcholine application preceded (pre) and followed each training step (post) to assess potential synaptic weight changes following training ('testing'). We found that test responses were significantly elevated following the
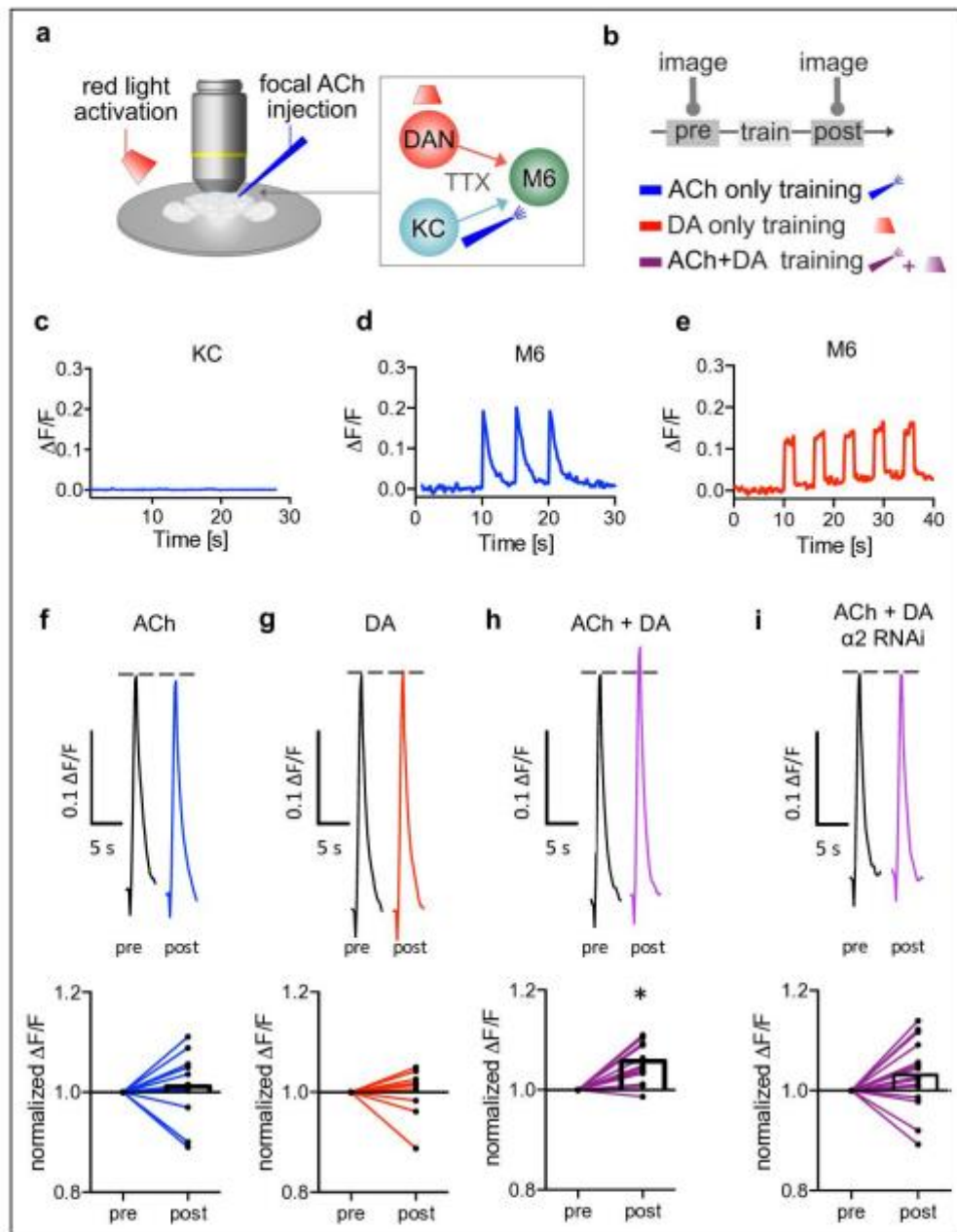
Figure 3. Induction of postsynaptic plasticity bypassing the presynapses. (a) Left: explant brain experimental configuration. Right: connectivity scheme of mushroom bodies (MB) output synapses. Cholinergic Kenyon cells (KCs) and dopaminergic neurons are presynaptic to M6 MB output neurons (MBONs). Only connections relevant for this protocol are shown for simplicity. Red light pulses trigger release of dopamine (DA) from dopaminergic neurons (R58E02-LexA>lexAop-CsChrimson[tdTomato]), while KC input is circumvented and mimicked by focal acetylcholine (ACh; 0.1 mM) injections to

Figure 3 continued on next page

Figure 3 continued

M6 dendrites in an explant brain preparation. Postsynaptic responses at the level of M6 are measured using GCaMP6f (MB011B [Split-GAL4] >UAS-GCaMP6f). TTX (tetrodotoxine) in the bath suppresses feedback signaling and overall network activity within the circuit. (**b**) Training scheme (top). Baseline responses to ACh application were initially established (pre). Subsequent training protocols consist of either pairing ACh application with simultaneous activation of dopaminergic neurons (purple connection lines), activation of dopaminergic neurons (red light only, red connection lines), or ACh only (blue, connection lines). This is followed by a test trial (post) through ACh application. (**c**) Averaged traces of axonal KC calcium changes induced by focal ACh injections. No apparent transients are observable; n=7. Line is mean ± SEM. (**d**) Sample trace of dendritic M6 calcium changes induced by focal ACh injections. (**e**) Sample trace of dendritic M6 calcium changes induced by red-light pulses. (**f-i**) Above: sample calcium traces in response to ACh injections recorded from M6 dendrites pre (black traces) and post (colored traces) training. Below: peak quantification. (**f**) Changes in ACh-evoked calcium transients; comparison of mean peaks pre- and post-'ACh only' training. Before-after plots and bar graphs (mean); n=13, ratio paired t-test. (**g**) Changes in ACh-evoked calcium transients; comparison of mean peaks pre- and post 'red light only' training. Before-after plots and bar graphs (mean); n=10, ratio paired t-test. (**h**) Changes in ACh-evoked calcium transients; comparison of mean peaks pre- and post 'paired' training. Before-after plots and bar graphs (mean); n=18, ratio paired t-test, *p<0.05. (**i**) Changes in ACh-evoked calcium transients following RNAi knockdown of the α2 subunit in M4/6 MBONs; comparison of mean peaks pre- and post 'paired' training. Before-after plots and bar graphs (mean); n=15, ratio paired t-test. Also see **Figure 3—figure supplement 1** for further information.

The online version of this article includes the following figure supplement(s) for figure 3:

Figure supplement 1. Control experiments and non-normalized data display for **Figure 3**.

---

paired condition (acetylcholine application and red light; *Figure 3h*). This plasticity was not observed when testing after acetylcholine only or dopamine only training (*Figure 3f and g*). Importantly, we also did not observe any changes when pairing acetylcholine application with red light in non-CsChrimson-expressing controls (*Figure 3—figure supplement 1c,d*).

Because we are using global acetylcholine application instead of sparse activation of single synapses, these experiments likely do not reflect in vivo physiological settings (*Owald et al., 2015*). However, our proof of principle experiments demonstrate that postsynaptic plasticity at the level of MBONs can take place independently of the presynapses of the KCs. Intriguingly, we did not observe changes in calcium transient magnitudes when knocking-down α2 (UAS-nAChR[RNAi]) in M4/6 (MB011B-Split Gal4; *Figure 3i*), which is consistent with postsynaptic plasticity being linked to the requirement of nicotinic receptors in memory storage.

Non-uniform distribution of nAChR α-subunits throughout MB compartments

Our data so far are suggestive of α2-containing nicotinic receptors being involved in appetitive memory storage. To test whether receptor levels were interdependent, we made use of a newly established CRISPR (clustered regularly interspaced short palindromic repeats)-based genomic collection of GFP-tagged endogenous nAChR subunits (for details see Methods) covering all α subunits (with the exception of α3) under control of their endogenous promoter, allowing for analyses of receptor distribution and dynamics in a dense neuropile in situ.

We first characterized receptor subunit signals throughout the 15 MB compartments, several of which have been shown to be involved in the encoding of specific memories. We found a non-uniform distribution (*Figure 4a and b, Figure 4—figure supplement 1*) that was unique for each subunit, indicating considerable heterogeneity of receptor composition. α5, which is required for immediate and 3-hr appetitive memories, was abundant throughout the γ lobe, including γ5 (innervated by M6) and slightly less at the level of β′2 (innervated by M4 and in parts by M6). α2 subunits, required for 3-hr appetitive memories, showed similarly high relative abundance in β′2 and γ5 (*Figure 4a and b*). Of note, these subunits were also detected in other MB output compartments, such as α′3, which harbors MBONs involved in non-associative familiarity learning (*Hattori et al., 2017*).

We next evaluated whether the fluorescent signals of the α2 and α5 subunits (with α5 potentially functioning upstream of α2, *Figure 2*) observed in the β′2 and γ5 compartments were derived from receptors within the dendritic processes of M4/6. To do so, we performed cell-specific knockdown experiments using VT1211-Gal4 to drive subunit-specific RNAi (UAS-nAChR[RNAi]) and quantified the relative fluorescent signal of the knockdown compartment relative to the neighboring unmanipulated compartments (*Figure 4c–f*).
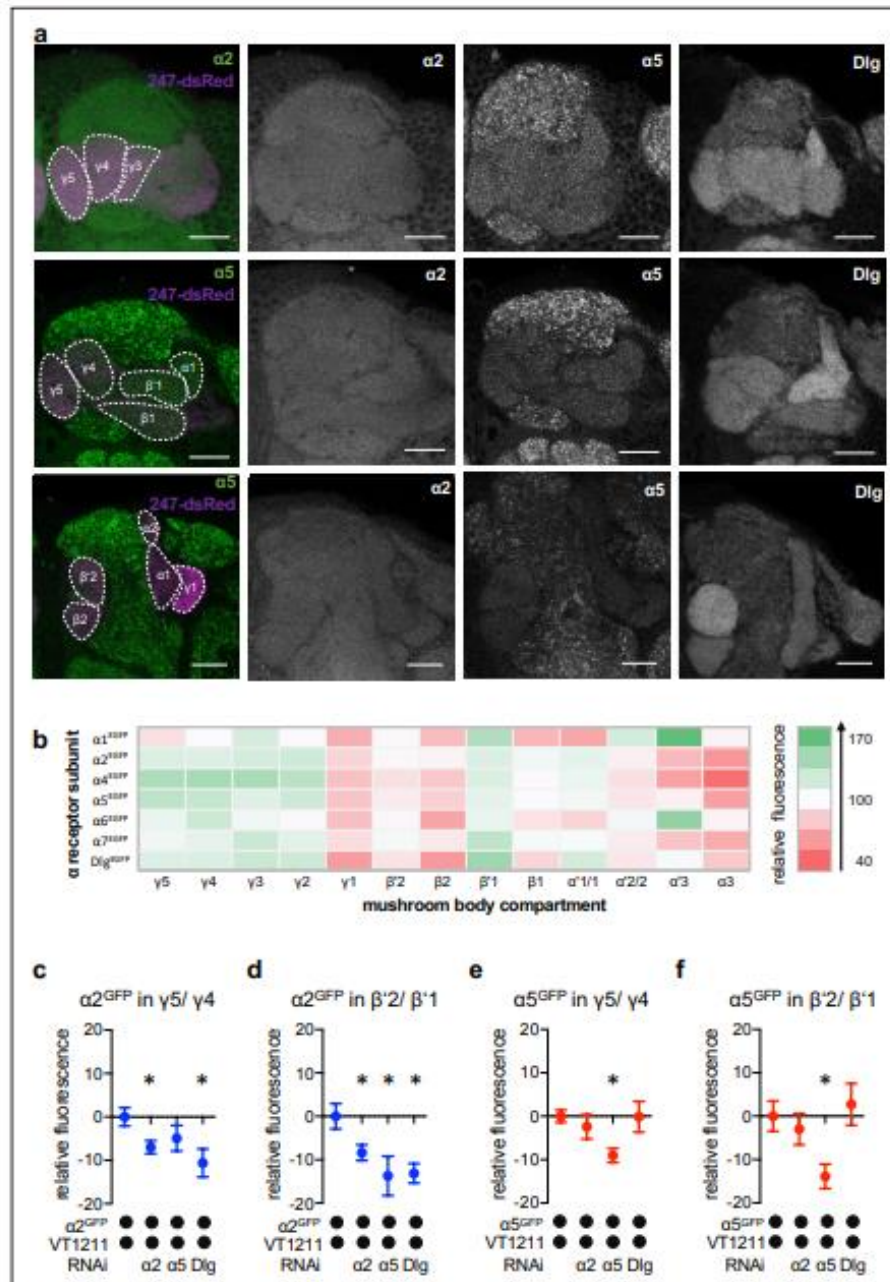
Figure 4. Nicotinic acetylcholine receptor (nAChR) α subunit localization throughout the mushroom bodies (MB): MB output neuron (MBON)-specific RNAi alters subunit distribution. (**a**) Representative images of the GFP-tagged nAChR subunits α2 and α5 as well as discs large (Dlg). Individual images displayed here are taken from different animals. For other subunits, see *Figure 4—figure supplement 1*. Scale bar: 20 μm. Left: merge of α subunit signal (green) with MB compartments marked with 247-dsRed (magenta). Compartments are indicated by dashed lines. Top row: γ compartments;

Figure 4 continued on next page

Knockdown of the α5 nAChR subunit reduced the relative α5^{GFP} signal specifically and significantly in γ5 and β'2 (*Figure 4e and f*). α5 abundance was, however, unaltered when knocking down α2 or Dlg, which is in line with α5 functioning as a possible trigger for plasticity processes.

Likewise, confirming that the observed signal was derived from M4/6 MBON dendrites, α2 knockdown reduced relative α2^{GFP} levels significantly throughout the β'2 and γ5 compartments (*Figure 4c and d*). Strikingly, we also observed reduced α2 nAChR subunit levels following α5 subunit knockdown in the β'2 compartment or Dlg knockdown in the β'2 and γ5 compartments (*Figure 4c and d*), which would be in line with a Dlg-dependent sequential requirement of receptor subunits during memory formation (also compare behavioral data in *Figure 2*).

Our data therefore are consistent with a role of α5 nAChR subunits and Dlg functioning upstream of α2 subunit-positive receptors, at least within the β'2 compartment.

nAChR subunits shape synaptic MB output properties

We next focused on implications of α2 subunit knockdown on postsynaptic function of M4/6 MBONs. Axonal calcium transients had previously been shown to be decreased following knockdown of α subunits (*Barnstedt et al., 2016*). However, depending on the overall topology of dendritic input sites, both increased or decreased postsynaptic drive could lead to changed dendritic integration properties or potential interference of synaptic inputs, resulting in reduced signal propagation (*Stuart and Spruston, 2015*).

To directly test dendritic responses, we expressed UAS-GCaMP6f in M4/6 MBONs (VT1211-Gal4) (*Figure 5a*) and exposed the flies repeatedly to alternating puffs of the odors octanol (OCT) and methylcyclohexanol (MCH) (*Figure 5b*). We focused our experiments on the β'2 compartment (*Figure 5*), as this is innervated by M4 MBONs that show input-specific plasticity following appetitive learning (*Owald et al., 2015*). Initial dendritic odor responses were not different between α2 subunit knockdown (VT1211-Gal4>UAS-α2^{RNAi}) and controls (*Figure 5c and d*), while initial odor-evoked dendritic calcium transients were elevated following knockdown of α5 (*Figure 5c, d* and *Figure 5—figure supplement 1b, c*). Neither control animals nor α2 knockdown animals (VT1211-Gal4>UAS-α2^{RNAi}) showed significant changes in odor-specific calcium transients after several exposures to MCH (*Figure 5e and f*). Odor responses following α5 knockdown (VT1211-Gal4>UAS-α5^{RNAi}), however, clearly depressed after multiple odor exposures (*Figure 5g*), indicating that loss of α5, in comparison to the controls, can actually lead to synapses being potentiated (synaptic weights are already high) from the start, even prior to the application of odors. On the contrary, compared to controls, α2 nAChR subunit knockdown interfered with odor-evoked transmission to a lesser extent. We did not observe any changes in calcium signals at the level of the corresponding KC axons, further supporting that the observed plasticity was of postsynaptic origin (*Figure 5—figure supplement 1g,h*).

The α2 nAChR subunit is required for the formation of appetitive memory traces in vivo

Of note, we observed a facilitation in M4/6 of controls when using repeated application of OCT, indicating that some parameters underlying the observed responses are odor-dependent (*Figure 5—figure supplement 1d*). However, the only slight effects on MCH-induced responses observed for α2
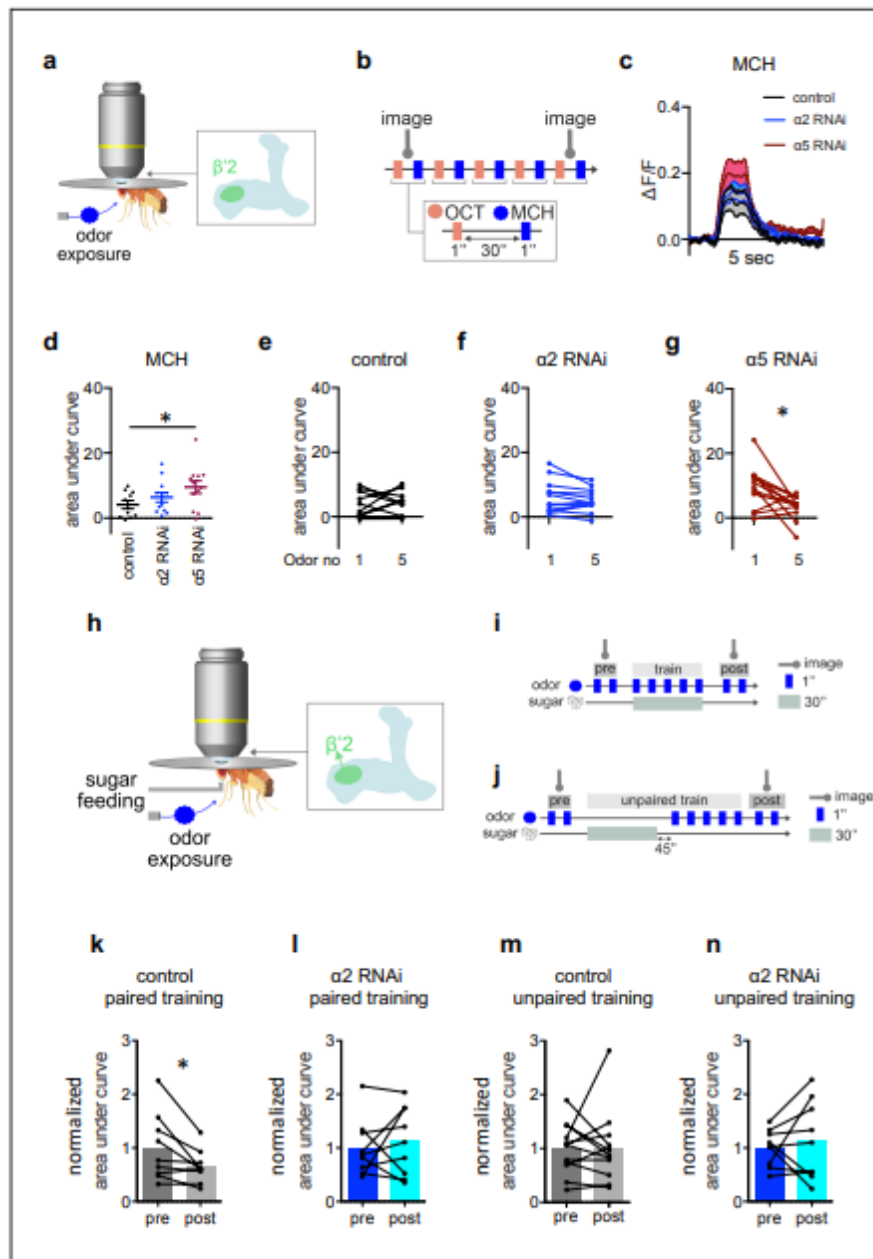
Figure 5. α2 is required for learning-associated plasticity in vivo. (**a**) Scheme indicating the dendritic imaging area (**c–g**) at the level of the β'2 compartment. (**b**) Odor exposure protocol. Five octanol (OCT) stimuli were alternatingly administered with five methylcyclohexanol (MCH) stimuli. 1-s odor puffs were separated by 30 s breaks. (**c**) Averaged traces of GCaMP6f (calcium) responses to MCH from control (black), α2 (blue), and α5 RNAi (red; driven in M4/6, respectively, driver line VT1211-Gal4) flies. Solid traces are mean, shaded areas SEM; n=10–12. (**d**) Area under curve (AUC) quantification

Figure 5 continued on next page

Figure 5 continued

of averaged initial odor responses to MCH following α5 knockdown in M4/6 neurons (driver line VT1211-Gal4). Mean ± SEM; one-way ANOVA followed by Dunnett's test; *p<0.05; n=10–12. (**e**) Control flies show no significant increase between the first and the fifth response to MCH. n=10; paired t-test. (**f**) α2 RNAi flies show no difference between the first and fifth odor response to MCH. Nicotinic acetylcholine receptor (nAChR) subunit RNAi is driven in M4/6 neurons (driver line VT1211-Gal4). n=12; paired t- test. (**g**) α5 RNAi flies show a significant decrease in calcium transients over the course of consecutive odor exposures. nAChR subunit RNAi is driven in M4/6 neurons (driver line VT1211-Gal4). n=12; Wilcoxon matched-pairs signed rank test; *p<0.05. (**h**) Arrow in scheme for absolute training indicates the axonal imaging area of M4 (**k–n**). (**i**) Scheme for absolute paired training under the microscope: flies are exposed to two brief stimuli of the odor (MCH) before training while recording GCaMP6f signals (preresponse). Immediately after, flies are presented with a sugar solution for 30 s accompanied by 5 pulses of odor stimuli. 1 min after training, flies are exposed to two brief odor stimuli again while recording GCaMP6f signals (postresponse). Axonal imaging area indicated by arrow. (**j**) Scheme for absolute unpaired training under the microscope: as in (i) except flies are exposed to 5 pulses of odor stimuli 45 s after presenting the sugar solution for 30 s. 1 min after training, the flies are exposed to two brief odor stimuli again while recording GCaMP6f signals (postresponse). Axonal imaging area indicated by arrow. (**k**) Control flies show a significant decrease in odor-evoked GCaMP6f signals. AUC of response to MCH (trained odor) following paired training (driver line VT1211-Gal4, axonal imaging). Before-after plots and bar graphs (mean); n=9; paired t-test; *p<0.05. (**l**) α2 RNAi flies show no significant decrease in odor-evoked GCaMP6f signals. AUC of response to MCH (trained odor) following paired training (driver line VT1211-Gal4, axonal imaging). Before-after plots and bar graphs (mean); n=9; paired t-test. (**m**) Control flies show no significant decrease in odor-evoked GCaMP6f signals. AUC of response to MCH (trained odor) following unpaired training (driver line VT1211-Gal4, axonal imaging). Before-after plots and bar graphs (mean); n=12; Wilcoxon matched-pairs signed rank test. (**n**) α2 RNAi flies show no significant decrease in odor-evoked GCaMP6f signals. AUC of response to MCH (trained odor) following unpaired training (driver line VT1211-Gal4, axonal imaging). Before-after plots and bar graphs (mean); n=9; paired t-test. Also see *Figure 5—figure supplement 1* for further information.

The online version of this article includes the following figure supplement(s) for figure 5:

Figure supplement 1. Additional data and display of non-normalized data accompanying *Figure 5*.

knockdown animals, allowed us to next investigate the role of α2 during in vivo associative appetitive learning.

We performed in vivo training under the microscope experiments using an absolute paradigm, pairing odor (MCH) exposure with sugar feeding during training, this time imaging from the axonal compartment to assess the integrated signal originating from the dendritic input. Comparing odor responses at the level of M4 (VT1211-Gal4>UAS-GCaMP6f) before and after training revealed a significant depression for control animals in line with previous observations (*Owald et al., 2015*; *Lewis et al., 2015*; *Figure 5k, Figure 5—figure supplement 1l*). Importantly, this training-induced depression was neither observed in controls, where odor and sugar were administered unpaired (*Figure 5m, Figure 5—figure supplement 1n*), nor after MBON-specific knockdown of α2 (VT1211-Gal4>UAS-GCaMP6f, UAS-α2^{RNAi}; *Figure 5l and n, Figure 5—figure supplement 1m,o*).

Together, our data point toward a mechanism, where nicotinic receptor subunits shape synaptic properties (*Figure 5*), with α2 as a postsynaptic substrate underlying appetitive training-induced plasticity processes.

In vivo imaging of postsynaptic receptor plasticity reveals altered α2 dynamics

Structural changes at the level of the receptor composition are hallmarks of postsynaptic plasticity expression in vertebrates. Typically, rearrangements can be measured by altered dynamics (or motility) of receptors that can reflect incorporation or removal of receptor complexes. We next sought to test whether dynamic receptor behavior could serve as a structural correlate of cholinergic postsynaptic memory trace expression. To do so, we turned to in vivo imaging experiments of the endogenously tagged α2 subunit (α2^{GFP}; *Figure 4, Figure 6, Figure 6—figure supplement 1*). Following artificial appetitive training protocols (*Figure 6a–c*, focal dopamine only, odor only, or odor paired with focal dopamine, consecutively, see methods), in situ receptor dynamics were estimated at the level of the β'2 compartment of the MB by measuring fluorescence recovery after photobleaching (FRAP; *Figure 6a–c*).

Exposing the fly to MCH induced significantly increased fluorescence recovery when compared to dopamine injections only or odor paired with dopamine (*Figure 6d and e*). Dopamine, therefore, does not induce plasticity on its own, and furthermore, it suppresses odor-induced recovery when applied simultaneously with an odor. To control for recovery either depending on the type of odor used or the order of conditions applied, we next conducted similar experiments using OCT this time with each condition applied in separate flies. We only observed significant recovery in the odor only condition,
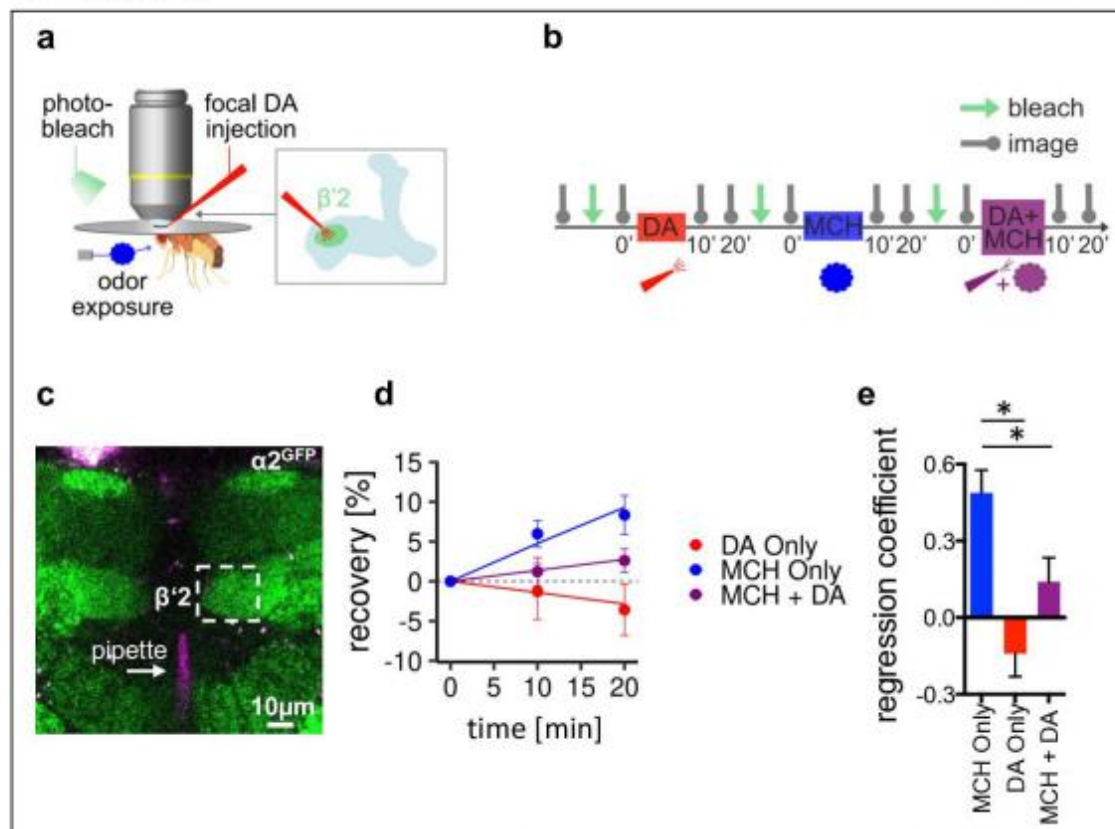
Figure 6. α2 nicotinic acetylcholine receptor (nAChR) subunits dynamically rearrange. (**a**) In vivo imaging configuration and scheme of site of dopamine (DA) injection during fluorescence recovery after photobleaching (FRAP) experiments at the level of the Kenyon cell to mushroom body output neuron synapses of the β'2 compartment. (**b**) FRAP experimental protocol. After bleaching, the baseline picture was taken followed by DA injection, odor presentation, and odor presentation simultaneously with DA injection in the same fly. Fluorescence recovery was monitored at the 10- and 20-min time points. (**c**) Example image of α2^{GFP} expression; white dashed box shows the β'2 output zone; DA injection pipette (with Texas red) is labeled in magenta. Scale bar: 10 μm. (**d**) Inverse exponential decay fit of FRAP following methylcyclohexanol (MCH) exposure (blue line), MCH exposure simultaneously with DA injection (purple line), and DA injection alone (red line). (**e**) Regression coefficient for the inverse exponential decay fit. Bar graphs: regression coefficients of recovery kinetics ± standard error of regression; n=9–10, linear mixed effects model followed by pairwise comparison from estimated marginal trends. *p < 0.05. Also see *Figure 6—figure supplement 1* for further experiments.

The online version of this article includes the following figure supplement(s) for figure 6:

Figure supplement 1. Receptor subunit recovery, accompanying *Figure 6*.

whereas dopamine and odor paired with dopamine induced no significant recovery (*Figure 6—figure supplement 1a–d*).

Thus, our data indicate that pairing odor presentation with dopamine application stalls α2^{GFP} dynamics, potentially by either stabilizing the already present amount of receptor or hindering new incorporation of α2-containing receptors. Interestingly the opposite, increased receptor dynamics, is observed after odor exposure without reinforcer. Note that the absence of acute stimuli (constant air stream only) did not induce signal recovery, demonstrating that it is the presence of the odor that changes baseline receptor behavior (*Figure 6—figure supplement 1e*). Thus, stalling α2 dynamics

can be correlated to depression of M4/6 MBON synapses *Owald et al., 2015*; *Felsenberg et al., 2018* following appetitive training (*Figure 5k*).

Familiarity learning alters postsynaptic receptor dynamics

Our data so far suggest that regulation of α2 subunits downstream of α5 is involved in postsynaptic plasticity mechanisms underlying appetitive but not aversive memory storage. Besides associative memories, non-associative memories, such as familiarity learning, a form of habituation, are also stored at the level of the *Drosophila* MBs. We next asked whether postsynaptic plasticity expressed through α5 and α2 subunit interplay, was exclusive to appetitive memory storage, or would represent a more generalizable mechanism that could underlie other forms of learning represented in the MBs. We turned to the α'3 compartment at the tip of the vertical MB lobe that has previously been shown to mediate odor familiarity learning. This form of learning allows the animal to adapt its behavioral responses to new odors and permits for assaying direct odor-related plasticity at the level of a higher-order integration center. Importantly, this compartment follows different plasticity rules, because the odor serves as both the conditioned (activating KCs) and unconditioned stimulus (activating corresponding DANs; *Hattori et al., 2017*). While allowing us to test whether the so far uncovered principles could also be relevant in a different context, it also provides a less complex test bed to further investigate whether α5 functions upstream of α2 dynamics.

Confirming previous observations (*Hattori et al., 2017*), a repeated odor application paradigm (*Figure 7a*) led to the depression of postsynaptic calcium transients at the level of the α'3 MBONs (MB027B Split-Gal4 >UAS-GCaMP6f; *Figure 7b*). We did not detect a corresponding depression on the presynaptic side when imaging arbors of a sparse α'β' KC driver line (MB369B Split-Gal4 >UAS-GCaMP6f) within α'3 (*Figure 7b*), further indicating that memories were predominantly stored postsynaptically in this compartment. We next performed in vivo FRAP experiments following familiarity learning paradigms. After odor training, we observed clear recovery rates of α2^{GFP} signals compared to the control group, however, not of α5^{GFP} or Dlg^{GFP} (*Figure 7c–f, Figure 7—figure supplement 1*). Therefore, increased α2 subunit dynamics are triggered through training events and, at the level of the α'3 compartment, accompany postsynaptic depression of the MBONs.

To invariantly test whether the observed recovery was attributable to α2 expressed in α'3 MBONs, we trained animals while knocking down α2 specifically in α'3 MBONs (α2^{GFP} and MB027B Split-Gal4 >UAS-α2^{RNAi}). In accordance with the observed signal recovery deriving from MBONs, no recovery was observed after α2 knockdown (*Figure 7g*). Importantly, we did not observe α2^{GFP} recovery when performing specific α5 knockdown in α'3 MBONs (α5^{GFP} + MB027B Split-Gal4 >UAS-α5^{RNAi}, *Figure 7g*), indicating a role of α5 upstream of α2 also in this compartment.

α5 subunits govern induction and α2 subunits expression of non-associative familiarity learning

Finally, we tested whether interfering with α5 and α2 nAChR subunits at the level of α'3 MBONs (MB027B Split-GAL4) would also impact familiarity learning behavior (*Figure 8*). Flies were covered in dust and subjected to repeated odor exposures (*Hattori et al., 2017*). As expected (*Hattori et al., 2017*), control flies readily groomed to remove the dust, however, typically stopped this action when detecting the novel odor (*Figure 8a–c*). Over subsequent trials, control flies learned that this odor was familiar and stopped reacting to the stimulus, continuing grooming (*Figure 8a–c, Figure 8—figure supplement 1*). Expressing RNAi to the α2 subunit (UAS-nAChR^{RNAi}) at the level of the α'3 MBONs (MB027B Split-Gal4) clearly impacted learning: flies learned with decreased efficacy and only after several trials (*Figure 8a–d*). Strikingly, α5 RNAi-expressing flies failed to stop grooming even to the first stimulus. Indeed, they acted as if they had already learned that an odor was familiar (*Figure 8a–d*).

Together, our data are in line with a model where α5 can induce memory formation, while lack of α5 leads to fully potentiated synapses. Subsequent expression of memory traces requires α2-containing receptors. Importantly, recovery accompanies synaptic depression at the level of the α'3 MBONs, while being suppressed by paired training in the β'2 compartment. Moreover, α2 appears to be involved in both depression and facilitation of synapses. Thus, synapses could bidirectionally utilize plasticity of the same receptor subunit for storing different types of information (*Figure 9*).
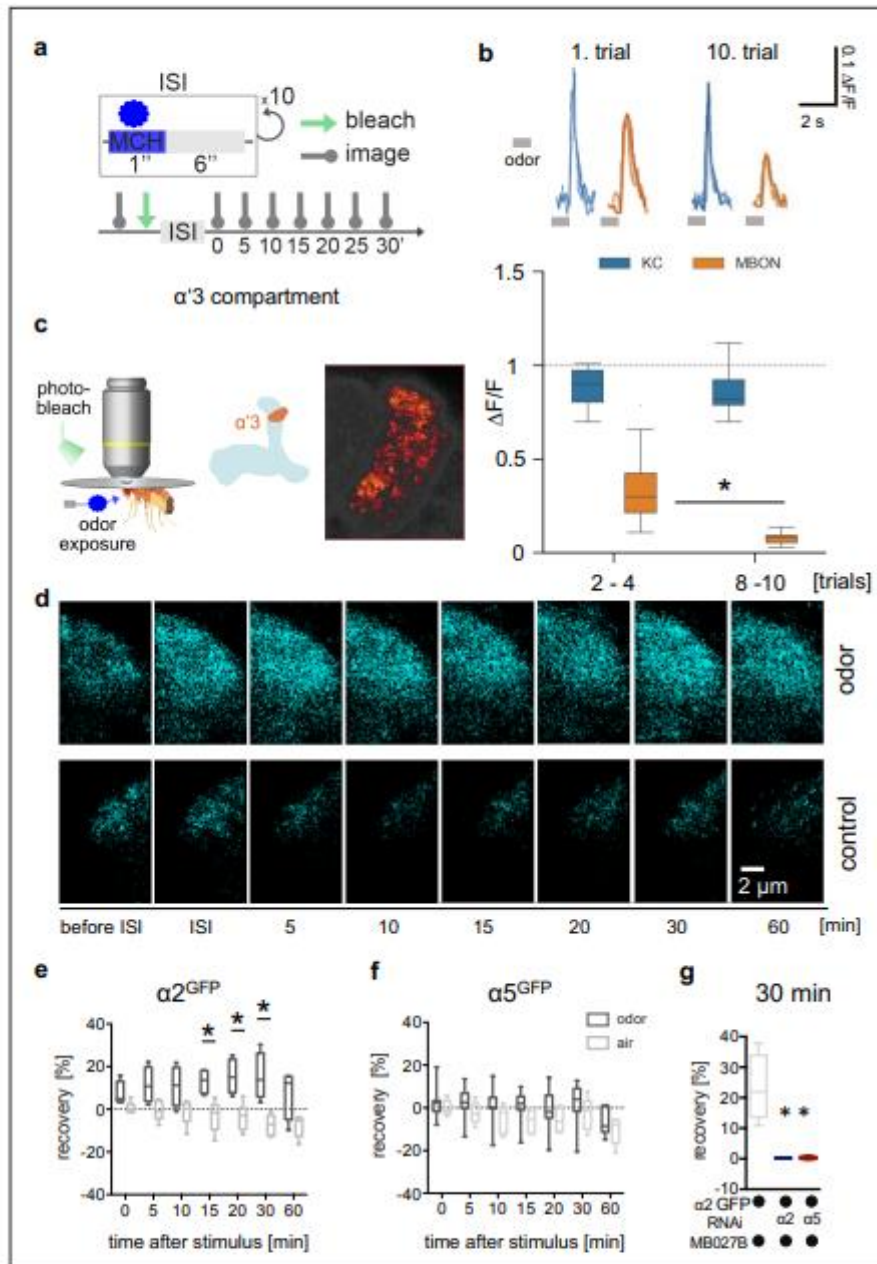
Figure 7. Non-associative plasticity alters postsynaptic α2 subunit receptor dynamics. (a) Training scheme indicating odor application, bleaching, and imaging time points. MCH was given 10 times for 1 s with a pause of 6 s in-between. Images were taken after training in absence of odor immediately afterward and 5, 10, 15, 20, 30, and 60 min later. (b) Top: Calcium peaks in response to odor stimuli of presynaptic Kenyon cells (KCs; MB369B as driver line) and adjacent postsynaptic mushroom body output neurons (MBONs; driver line: MB027B [Split-GAL4]). Individual calcium responses to trials

Figure 7 continued on next page

Figure 7 continued

1 and 10 for MBONs (orange lines) and KCs (blue lines). Bottom: Averaged calcium responses to odor stimuli of presynaptic KCs and postsynaptic MBONs of trials 2–4 and 8–10, respectively. Responses decrease at the level of MBONs but not at the level of KCs over 10 trials. Box plots are median and 75% quartiles; n=15; Kruskal-Wallis followed by Dunn's test (p<0.05), *p<0.05. (c) In vivo imaging configuration (left), scheme of α'3 compartment analyzed (right), and representative α5^{GFP} fluorescent image (smoothed). Scale bar: 10 µm. (d) Example images of α2^{GFP} fluorescence recovery after photobleaching (FRAP) experiment at the level of the α'3 compartment at specific time points before and after training. Top row: after training; bottom row: control settings. Scale bar: 2 µm. (e) FRAP of α2^{GFP} nicotinic acetylcholine receptor (nAChR) subunit in the α'3 compartment after odor presentation. α2^{GFP} shows significant recovery following odor training compared to the controls. Recovery rate is normalized to the baseline recorded after selective bleaching of the α'3 mushroom bodies (MB) compartment. Box plots are median and 75% quartiles; n=4–6; multiple t-tests with Sidak-Bonferroni correction, *p<0.05. (f) FRAP of α5^{GFP} subunit in the α'3 compartment after odor presentation. α5^{GFP} did not show significant recovery compared to the controls. Recovery rate is normalized to the baseline recorded after selective bleaching of α'3 MB compartment. Box plots are median and 75% quartiles; n=5–7, multiple t-tests with Sidak-Bonferroni correction. (g) FRAP of α2^{GFP} nAChR subunit in the α'3 compartment after odor presentation and knockdown of either the α2 or α5 subunit (RNAi) in the α'3 MBON (driver line MB027B [Split-GAL4]). α2^{GFP} shows no recovery 30 min after odor training in α2 or α5 knockdown animals compared to the controls. Recovery rate is normalized to the baseline recorded after selective bleaching of the α'3 MB compartment. Box plots are minimum value to maximum value; n=4–5; Kruskal-Wallis followed by Dunn's test (p<0.05), *p<0.05. Also see *Figure 7—figure supplement 1* for further information.

The online version of this article includes the following figure supplement(s) for figure 7:

Figure supplement 1. Discs large GFP (Dlg^{GFP}) fluorescence recovery after photobleaching (FRAP), accompanying *Figure 7*.

Discussion

Synaptic plasticity that manifests itself in synaptic weight changes is widely recognized as substrate for memory storage throughout the animal kingdom. How synapses adapt in order to change their efficacy during learning has been a focus of attention over the last decades. While it is undisputed that both pre- and postsynaptic mechanisms of memory storage exist in vertebrates, invertebrate memory-related synaptic plasticity has been largely localized to the presynaptic compartment (*Bilz et al., 2020; Boto et al., 2014; Handler et al., 2019; Ehmann et al., 2018; Tully et al., 1994*). However, the core of the debate boils down to a key question: do vertebrates and invertebrates use similar mechanisms to store memories or are there fundamental differences? A first clear difference appears to be the use of different neurotransmitter systems, glutamate and acetylcholine, respectively, in the vertebrate and *Drosophila* learning centers (*Barnstedt et al., 2016*).

Postsynaptic plasticity in associative memory storage

Here, we use the genetic tractability of the *Drosophila* system to directly address postsynaptic plasticity during olfactory memory storage in invertebrates. Large amounts of evidence from *Drosophila* so far suggest a presynaptic mode of memory storage (*Bilz et al., 2020; Boto et al., 2014; Handler et al., 2019; Ehmann et al., 2018; Tully et al., 1994*). Moreover, several studies indicated that block of KCs during learning does not interfere with memory performance (*Dubnau et al., 2001; McGuire et al., 2001; Schwaerzel et al., 2002*). However, other studies blocking KC subsets did find impairments (*Krashes et al., 2007; Yamazaki et al., 2018; Trannoy et al., 2011*) in the context of short-term appetitive memory, while downstream circuit elements have been implicated in appropriate memory formation (*Pai et al., 2013; Widmer et al., 2018; Wu et al., 2017*). Here, we revisited such experiments and found, in accordance with previous studies, only mild, if any, requirement for aversive memory storage. We, however, fully abolished appetitive memories (*Figure 1*) by blocking KC output during acquisition, providing the basis for a model of postsynaptic plasticity (*Figure 9*) that is induced and expressed through distinct nAChR subunits (*Figures 2–8*).

Our study hints toward different pre- and postsynaptic storage mechanisms underlying aversive and appetitive memories. It also argues against the assumption that appetitive and aversive memories will necessarily use the same molecular machinery to store information. Interestingly, arguing for a division of appetitive and aversive storage sites, subpopulations of KCs have been implicated in aversive and appetitive memory, respectively (*Perisse et al., 2013*). Moreover, postsynaptic contributions were previously ruled out for a synaptic junction required for storage of aversive but not appetitive memories, which is fully consistent with our findings (*Hige et al., 2015*). However, a recent study investigating postsynaptic calcium transients across MB compartments could be in line with postsynaptic modifications occurring following aversive training in some MB output compartments (*Hancock et al., 2022*). Additionally, the requirement of MBON signaling has been demonstrated, particularly
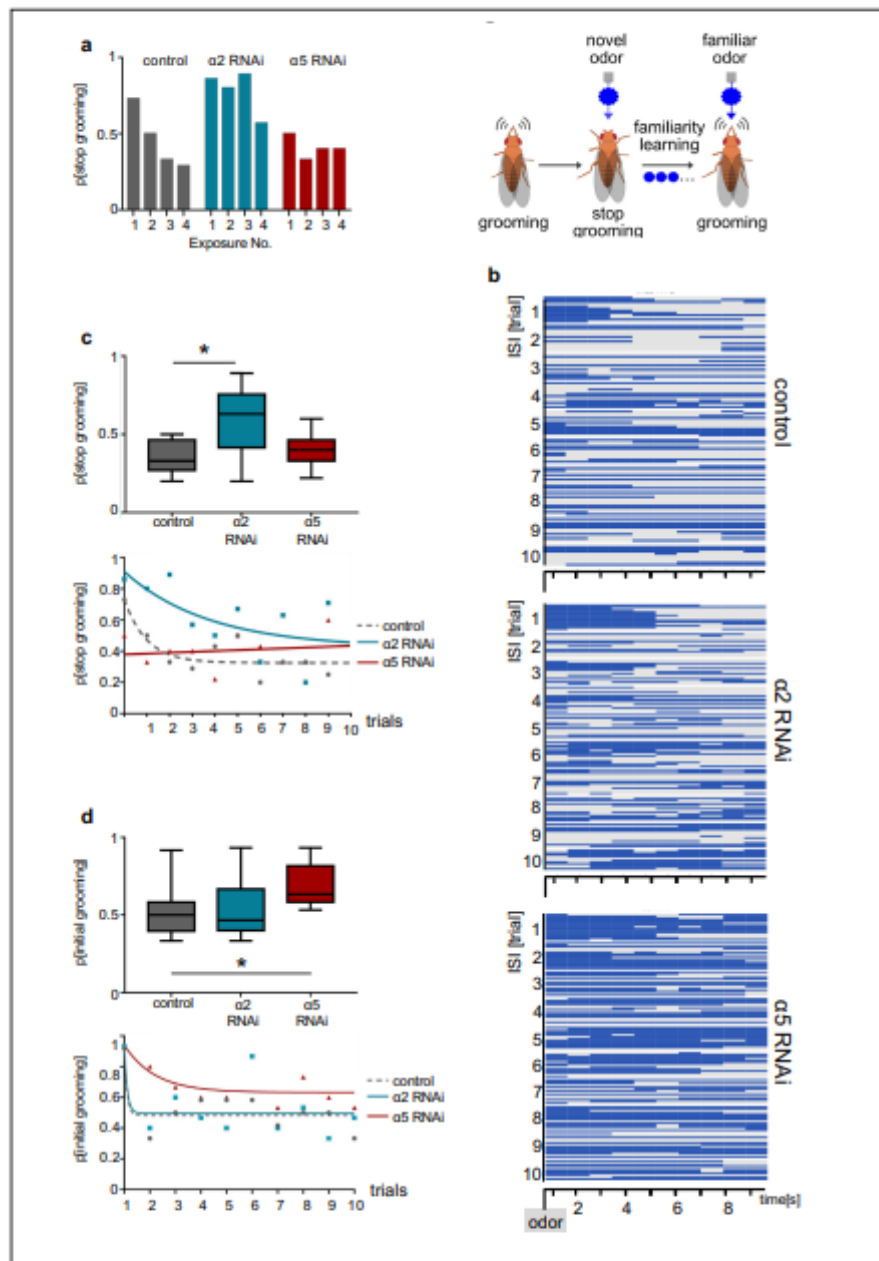
Figure 8. α2 and α5 nicotinic acetylcholine receptor (nAChR) subunits are required for non-associative familiarity learning at the level of α′3 mushroom body output neurons (MBONs). (a) Scheme of behavioral responses to novel and familiar odors (right). (Left): Knockdown of α nAChR subunits at the level of α′3 MBONs alters odor familiarity learning and the probability to stop grooming. α2 RNAi knockdown delays familiarity learning effects to novel odors. α5 RNAi knockdown flies do not show a novelty response at all. (b) Grooming behavior response of dusted flies following the repeated

Figure 8 continued on next page

eLife Research article

Figure 8 continued

presentations of a novel odor (MCH). Ethogram of grooming behavior (blue) during 10 intervals of odor exposures. Horizontal lines in each trial correspond to a single experimental fly within a trial group. Not grooming (gray) flies can further be categorized between pausing and wandering (see *Figure 8—figure supplement* 1). n=15. (**c**) Knockdown of α2 subunit in α'3 MBONs (driver line MB027B [Split-GAL4]) impairs odor familiarity learning significantly; animals show a higher probability to terminate grooming responses during the learning period. The learning period is defined as the odor exposure rounds following the first exposure. Bottom graph: Non-linear representation of grooming flies over 10 training trials. Note that α5 behavioral responses are best described by linear representation. Box plots are median and 75% quartiles; n=9, one-way ANOVA followed by Dunnett's test (p<0.05) *p<0.05. (**d**) Knockdown of α5 subunits in α'3 MBONs (driver line MB027B [Split-GAL4] leads to an increased probability to start grooming earlier. Bottom graph, non-linear representation of grooming flies over 10 training trials. Box plots are median and 75% quartiles; n=9, Kruskal-Wallis followed by Dunn's test (p<0.05), *p<0.05. Also see *Figure 8—figure supplement* 1 for further information.

The online version of this article includes the following figure supplement(s) for figure 8:

Figure supplement 1. Additional ethograms, accompanying *Figure 8*.

in the context of longer-term memory storage (*Pai et al., 2013*; *Ichinose et al., 2021*; *Widmer et al., 2018*; *Wu et al., 2017*). Thus, we do not wish to exclude a potential involvement of postsynaptic plasticity in aversive memory formation per se. On the contrary, it is conceivable that aversive memories also could have an appetitive component (release from punishment).

Postsynaptic plasticity at the KC to MBON synapse

Recent anatomical studies *Takemura et al., 2017*; *Eichler et al., 2017* have reported both dopaminergic innervation of presynaptic KC compartments and, somewhat unexpectedly, direct synapses between presynaptic dopaminergic terminals and MBONs. We devised an experiment where we substituted KC input to the postsynaptic MBON compartment through artificial acetylcholine injection, while rendering DANs switchable through optogenetics. A protocol that trained and subsequently tested the synaptic junction between KCs and MBONs, demonstrates that plasticity (represented by a change in calcium responses to acetylcholine injection) was inducible by pairing dopaminergic with postsynaptic MBON activation that lasted beyond the training stage and was observable by mere 'recall-like' activation of the system (*Figure 3*).

Our proof-of-principle experiments uncovered the ability to potentiate after pairing M6 MBON activation and stimulating a broad population of DANs that convey information on sugar, water, or the relative valence of aversive stimuli (*Owald and Waddell, 2015*), while we find postsynaptic plasticity to be required for appetitive memory performance (*Figure 3*). However, previous studies looking into 'natural' appetitive sugar conditioning uncovered a relative depression in M4 (another MBON of the M4/6 cluster) dendrites, when comparing the responses of the paired (CS+) and unpaired odor (CS−) 1 hr after appetitive conditioning (*Owald and Waddell, 2015*; *Owald et al., 2015*; *Felsenberg et al., 2018*). Moreover, we here show that in vivo appetitive absolute training depresses subsequent responses to the trained odor (*Figure 5*). It is important to note that, here (*Figure 3*), for our in vitro experiments, we perform global activation of the postsynaptic compartment and not the natural typical coverage of 5% of input synapses per odor (*Honegger et al., 2011*) (that allow for differential conditioning). Induced changes are therefore likely not comparable to the natural settings, where sparse sets of KCs and DANs are active within a tight temporal window. Moreover, we here abolish network contributions (by suppressing active signal propagation), to be able to concentrate on synaptic mechanisms during plasticity induction. Thus, our artificial training (*Figure 3*) through global dendritic activation likely does not mirror precise physiological conditions, allowing for plasticity of a sparse set of synapses to convey odor specificity to a memory. However, the relatively small amplitude of plasticity (here: potentiation) observed actually fits previous (*Owald et al., 2015*) in vivo observations. Moreover, similar protocols (*Zhao et al., 2018*) that involved broad activation of KCs (and thus did not circumvent the presynaptic compartment) have demonstrated comparable plasticity induction at this synaptic junction. It should also be noted that because we are using TTX and local training of KC to M6 synapses in our experiments, we are furthermore missing additional disinhibition that in vivo is mediated via the GABAergic MVP2 MBON (*Felsenberg et al., 2018*; *Perisse et al., 2016*). Of note, how difficult it can be to infer how dendrites compute and integrate all input channels is exemplified by the observation that high levels of odor-mediated dendritic activation after α5 knockdown (*Figure 5, Figure 5—figure supplement 1*) appear to be translated to reduced axonal calcium transients (*Barnstedt et al., 2016*), effectively leading to decreased signal transduction within the MBON.
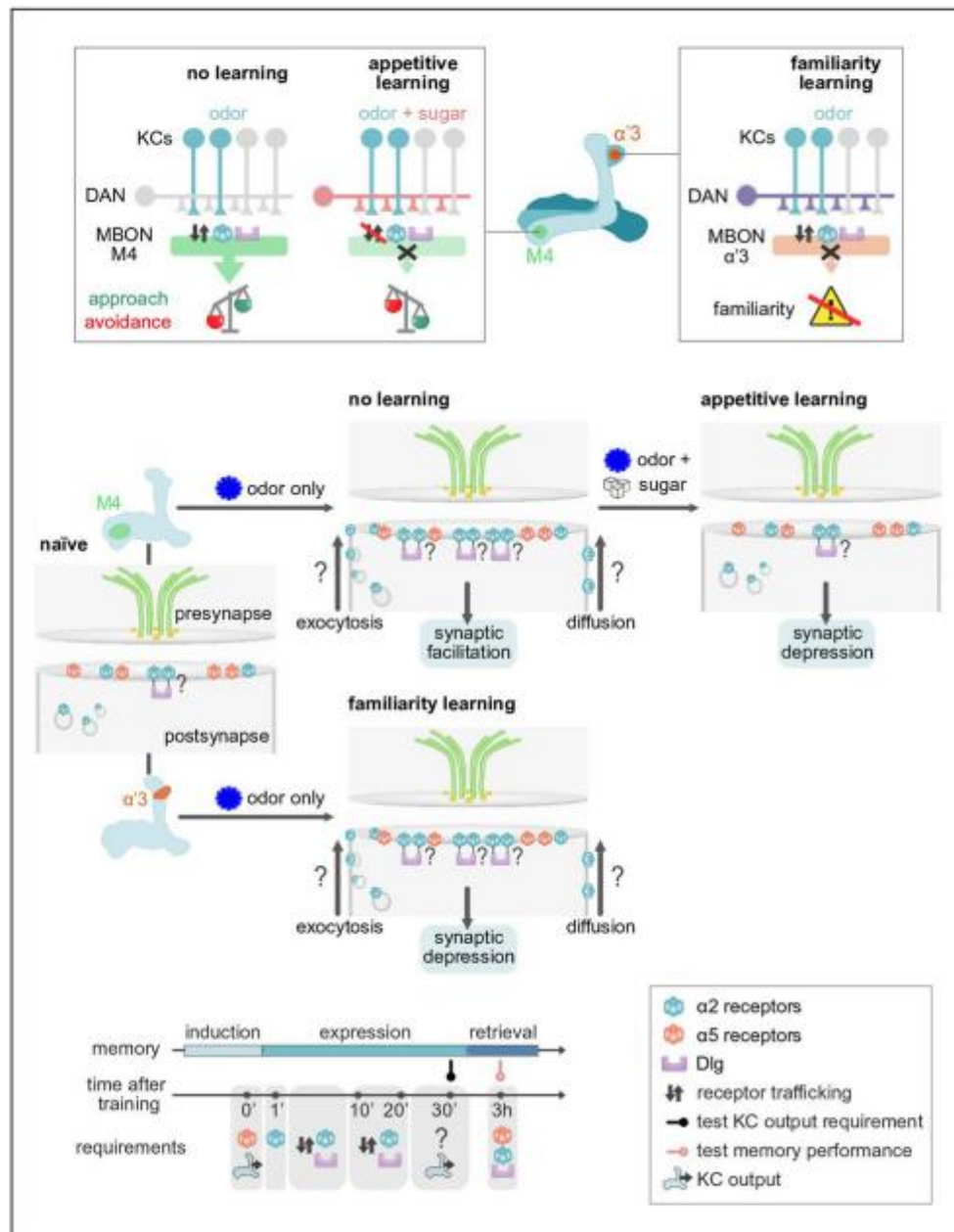
Figure 9. Model of postsynaptic plasticity sequence across compartments. Top panels (circuit and behavior level): Mushroom body (MB) compartments investigated. Odors elicit high responses in M4 neurons inducing α2 receptor dynamics. High activity in M4 tilts the balance toward odor avoidance. Learning (or concurrent odor exposure with dopamine application) reduces receptor exchange. This results in reduced postsynaptic responses and tilts the balance toward approach behavior. Suppressed dynamics through learning could be reminiscent of a 'dark current' mechanism as found in

Figure 9 continued on next page

Figure 9 continued

the mammalian visual system (please see Discussion). At the level of the α'3 compartment repeated odor exposure triggers increased α2 receptor dynamics. In this compartment, the increased dynamics result in reduced odor-evoked activity in the MB output neurons (MBONs) resulting in familiarity learning (less behavioral responsiveness to familiar compared to novel odors). Middle panels (synaptic level): Our data are consistent with a model in which α5 subunit containing receptors (red) mediate the early phase of postsynaptic memory storage, potentially by leading to elevated calcium flux (not addressed in this study) at individual postsynaptic densities (see Discussion and *Figure 10* showing separated PSDs (postsynaptic densities) and analyses concerning input specificity). Concurrent events see changed dynamics of the α2 receptor (blue). Changed dynamics likely reflect changed exocytosis of intracellular receptor populations or lateral diffusion across membranes. Nicotinic receptor subunits hereby potentially interact with adaptor proteins to bind to discs large (Dlg). Importantly, we identify elevated α2 subunit dynamics in the context of associative (M4; Kenyon cells [KC] and dopaminergic neuron [DAN] activation needed for memory formation) and non-associative (α'3 MBONs; odor activates both KCs and DANs) memory expression. Increased α2 subunit dynamics in both cases are triggered by odor application. At the level of M4, suppressed dynamics, would correspond to postsynaptic depression, while at the level of α'3 MBONs increased dynamics could result in postsynaptic depression. Therefore, different learning rules might govern the incorporation, exchange, or stabilization of receptors in or out of synapses. Please see Discussion for further details. Bottom panel: Proposed time line of molecular correlates and experimental read-outs of memory induction and expression (please see Discussion for details).

MBONs do not appear to exhibit prominent spines on their dendrites (*Takemura et al., 2017*) (but see section below: Are cholinergic and glutamatergic synapses interchangeable?). Therefore, increased dendritic activation could lead to a change in membrane resistance and result in synaptic interference.

It should also be noted that M4, which shows depression (*Figure 5*), and M6 have common but also distinct physiological roles, for instance, during aversive memory extinction (*Felsenberg et al., 2018*). Besides that, different temporal requirements for M4 and M6 memory expression have been reported (*Bouzaiane et al., 2015*). It is therefore possible that physiological changes in the context of appetitive learning lead to different plasticity profiles in M4 and M6 neurons, respectively, or that initial potentiation over time can be reverted to depression. As noted above, MBON drive is bidirectionally modifiable and has the propensity to both potentiate and depress (*Owald et al., 2015*; *Bouzaiane et al., 2015*; *Lewis et al., 2015*; *Handler et al., 2019*). It remains unclear, whether the applied protocols would elicit plasticity (and if so depression or facilitation) at the M4 dendrites, which is difficult to assess with our experimental design. In summary, the observed ex vivo plasticity trace (*Figure 3*) should solely be viewed as a proof of principle that postsynaptic (MBON) plasticity can take place without presynaptic (KC) contribution per se.

Local acetylcholine application to the MB can also activate calcium transients in dopaminergic presynaptic terminals (*Cervantes-Sandoval et al., 2017*). Therefore, our protocol could in principle include some dopaminergic contributions already at the pre-training level. However, control experiments using the paired training protocol in the absence of CsChrimson expression in DANs, do not show any signs of plasticity (*Figure 3* and *Figure 3—figure supplement 1*). Moreover, it has been previously demonstrated that, to actually release dopamine from the presynaptic terminal, a coincident signal via carbon monoxide is required (*Ueno et al., 2017*; *Ueno et al., 2020*). Therefore, an unwanted activation of DANs in our experiments is unlikely.

Previous studies have shown that loss of DopR (dDA1) causes aversive and appetitive memory impairments (*Kim et al., 2007*; *Qin et al., 2012*). Intriguingly, specifically re-expressing DopR in KCs rescued loss of both types of memory (*Kim et al., 2007*). However, while the reported memory impairments in *dopR*-deficient animals were strong for aversive memories, they were only partial for appetitive memories, indicating that appetitive memory traces could be mediated via other dopamine receptors at the MBON level. Future experiments will need to investigate which dopamine receptors are required at the level of the MBONs as well as the in vivo time course of dopaminergic signaling.

Nicotinic receptors could follow defined temporal sequences to mediate memory expression

Lasting plasticity traces as observed here (*Figure 3*) appear to fit the core criteria for long-term potentiation of vertebrate glutamatergic postsynapses (*Nicoll, 2017*; *Bliss and Lomo, 1973*). Plasticity can be divided into an 'induction' (*Nicoll, 2017*) period mediated via NMDARs and a subsequent 'expression' (*Nicoll, 2017*) period that requires altered AMPAR dynamics (*Nicoll, 2017*). Our findings here lead to a model, where the nicotinic α5 subunit is required for the induction of appetitive memories at *Drosophila* MBONs (*Figure 2* [affecting 'immediate' appetitive memory], *Figure 9*). We propose that α5 nAChR subunits (that can form homomeric channels *Lansdell et al., 2012*; *Eadaim et al., 2020*)

could take on a similar role to NMDARs. α5 would gate the potentiation or depression of synaptic strength influencing the incorporation or exchange of additional receptor subunits or complexes. In line with this, we show that knockdown of α5 subunits interferes with familiarity learning in the α'3 compartment of the MBs: flies no longer form familiarity memories, they react to a novel odor the same way as to a familiar one, 'as if they had learned that this new odor was familiar before' (*Figures 7 and 8*). Moreover, we do not observe α5 subunit dynamics (*Figure 7*), whereas knockdown of α5 leads to decreased levels of α2 subunits (*Figure 4*), and α2 dynamics are no longer observable when knocking down α5 in the MBONs of the α'3 compartment (*Figure 7*). Thus, we can draw first analogies to glutamatergic systems governing plasticity in vertebrates. Whether more core criteria are met for the comparison of invertebrate and vertebrate plasticity systems, further depends on whether the here observed receptor dynamics will actually translate to exo-/endocytosis of postsynaptic receptors or lateral diffusion of receptor subunits along the MBON dendrites (see *Figure 9*). Our established system should provide the means to investigate this further in the future.

We also find that later forms of appetitive memory expression require both the α2 and α1 receptor subunits (*Figure 2*). A recent study (*Ihara et al., 2020*) has demonstrated that, when expressed heterologously, these subunits can co-assemble to form heterodimers with β subunits, which, depending on the precise composition of these channels, can harbor different properties, potentially reminiscent to AMPAR (*Greger et al., 2017*). However, MB distribution profiles of α1 and α2 subunits do not match completely, for instance, at the level of the γ5 or α'2 compartments (*Figure 4*), indicating that they could also partake in different or independent receptor configurations.

In order to dissect distinct roles for receptor plasticity in memory induction and expression, we experimentally probed several time points during associative appetitive memory formation. First, we probed 30-min memory following KC block to invariantly interfere with the memory acquisition and not the retrieval stage (*Figure 1*). Second, we probed immediate and 3-hr memory performance following receptor knockdown to distinguish between memory induction and memory expression requirements (*Figure 2*). Third, we investigate the time course of receptor dynamics during memory expression following memory induction with a resolution of 5 to 10-min intervals after artificial training (*Figures 6 and 7*). The overarching picture indicates that, indeed, directly following training, memory induction requires α5. Subsequently, at the resolution of minutes, regulation of α2 levels contributes to memory expression. While we cannot resolve the temporal time course at the level of T-maze behavior (*Figure 2*) or FRAP experiments (*Figure 6*) below several minutes, our in vivo training data (*Figure 5*) suggests that α2 requirement already becomes apparent within 1 min after training.

We show that familiarity learning, a specific form of habituation encoded at a higher-order integration center, the MBs, can take place when knocking down α2 nAChR subunits in α'3 MBONs in principle (*Figure 8*), however, at clearly decreased efficacy and only after several trials. We speculate that the observation of memories still being expressed per se in this context could be explained by redundancies with α1 or other subunits (but see heterogeneous localization and enrichment in different MB compartments, *Figure 4*). Redundancies could also explain why we partially observe functional phenotypes after knockdown of individual subunits but only moderate structural changes. We would also like to point out that subunits we did not identify absolutely as required for memory expression (*Figure 2*) in this study could nonetheless partake in distinct phases of plasticity processes.

In the context of both familiarity learning and appetitive conditioning, odor exposure induces increased α2 subunit dynamics (*Figures 6 and 7*) accompanying postsynaptic depression (*Owald et al., 2015*; *Hattori et al., 2017*; *Figure 7*), while not or mildly affecting α5 subunits (for familiarity learning). Therefore, the same basic mechanisms, odor-induced α2 receptor dynamics, seem to express two opposed plastic outcomes in the context of associative and non-associative memories and contribute to different learning rules across MB compartments (*Hige et al., 2015*; *Aso and Rubin, 2016*). We speculate that α2 dynamics induced by odor in the M4/6 dendrites could be reminiscent of dark currents in the vertebrate visual system (*Hagins et al., 1970*), allowing for rapid adaptation with low levels of synaptic noise. Receptor exchange at the level of M4/6 dendrites would actually take place when no associations are formed and stalled when DANs (triggered by sugar) are simultaneously active with KCs (triggered by odor). Indeed, repeated OCT stimulation (*Figure 5—figure supplement 1*) led to a facilitation of calcium transients (potentially corresponding to an increase of receptor incorporation), while depression (in this case likely to be mediated by removal of receptors, but see above) is triggered by paired training (*Figure 5*). In contrast, at the level of the α'3 compartments, odor

activates both MBONs and DANs. Here, the plasticity rule would be reversed. Synaptic depression is accompanied by actively changing the receptor composite. We speculate that such plasticity could function reminiscent of mechanisms observed for climbing fiber-induced depression of parallel fiber to Purkinje cell synapses (*Ito, 2001*). However, whether increased dynamics can be translated to more incorporation or removal of α2-type receptors, or depending on the plasticity rule both, will require high-resolution imaging experiments in the future.

Are cholinergic and glutamatergic synapses interchangeable?

Our study fuels the question of how unique properties of individual neurotransmitter systems at synapses are. While dopamine signaling is remarkably conserved between invertebrates and vertebrates, cholinergic and glutamatergic systems appear, now more than before (with this study), somewhat interchangeable. While vertebrates (but also evolutionarily distant *Caenorhabditis elegans*), for instance, use acetylcholine at the neuromuscular junction and store memories predominantly at glutamatergic synapses, it is the other way around in *Drosophila* and other invertebrates, such as *Sepia* (*Barnstedt et al., 2016*; *Owald and Waddell, 2015*; *Shomrat et al., 2011*; *Ackermann et al., 2015*; *Owald and Sigrist, 2009*). Now we show that, at cholinergic synapses, α5 and α2 subunits, at least to a certain extent, behave in a potentially comparable way to NMDARs and AMPARs at glutamatergic synapses during postsynaptic plasticity which underlies memory storage. In this context, we offer several lines of evidence that invertebrates utilize postsynaptic plasticity during memory storage.

We therefore propose that, across phyla, postsynaptic plasticity, with the propensity to store memories and adapt network function plastically, can take place regardless of neurotransmitter identity.

One key difference between the dendritic arbors of the MBONs analyzed (e.g. *Figure 10a*) in this study compared to dendrites of glutamatergic neurons in vertebrates, is a lack of anatomical spines (*Figure 10b*). Without spines, how can input specificity be preserved at MBON postsynaptic densities? KC output to MBON input analysis of the recently published fly hemibrain connectome (*Scheffer et al., 2020*; neuprint.org; *Clements et al., 2020*) suggests that, at the ultrastructural level, MBON postsynaptic densities are separated spatially (*Figure 10b*). Compartmentalization could therefore be mediated by, for instance, biochemical separation of PSDs. Importantly, input-specific plasticity has been shown to be inducible in non-spiny neurons in vertebrates, with diffusion barriers established, e.g., through calcium buffers, between postsynaptic densities (*Goldberg et al., 2003*).

Interestingly, our MBON input analysis further revealed that postsynaptic plasticity mechanisms could actually add a layer to promote input specificity. Indeed, we find that single presynaptic KC release sites that innervate MBON dendrites can also target other MBONs and/or other postsynaptic targets simultaneously (*Figure 10c–g*). Plasticity confined to single postsynaptic densities innervated by a KC terminal could therefore change the weight of transmission for one target (e.g. MBONs involved in memory storage, such as M4 *Owald et al., 2015*), while not changing the weight of the connection to other targets (e.g. MBONs not involved in a specific action or other targets of non-MBON identity, *Figure 10h*). It should be noted that this architecture does not exclude presynaptic plasticity mechanisms (*Stahl et al., 2022*; for instance, following aversive conditioning). Indeed, we would speculate that synaptic connections can be subdivided into distinct compartments on both the pre- and the postsynaptic side, potentially through transsynaptic molecules (*Owald and Sigrist, 2009*; *Tang et al., 2016*), allowing for fine-tuned and target-dependent changes of parameters within either side of a synapse.

Together, we propose a model (*Figure 9*) in which α5 subunit containing receptors could mediate the early phase of postsynaptic memory storage, and we speculate this could lead to elevated postsynaptic calcium flux (not addressed in this study). Concurrent events see changed dynamics of the α2 receptor. Nicotinic receptor subunits hereby could interact with adaptor proteins to bind to Dlg, reminiscent to what is known for AMPAR (*Won et al., 2017*). Importantly, we identify elevated α2 subunit dynamics in the context of associative and non-associative memory expression. Increased α2 subunit dynamics in both cases are triggered by odor application. At the level of M4/6, suppressed dynamics would correspond to synaptic depression, while at the level of α'3 MBONs increased dynamics may result in postsynaptic depression. Therefore, different learning rules could govern the incorporation or exchange or mobilization of receptors in or out of synapses. The precise molecular and biophysical parameters underlying these plasticity rules are currently unknown and will need to be addressed in
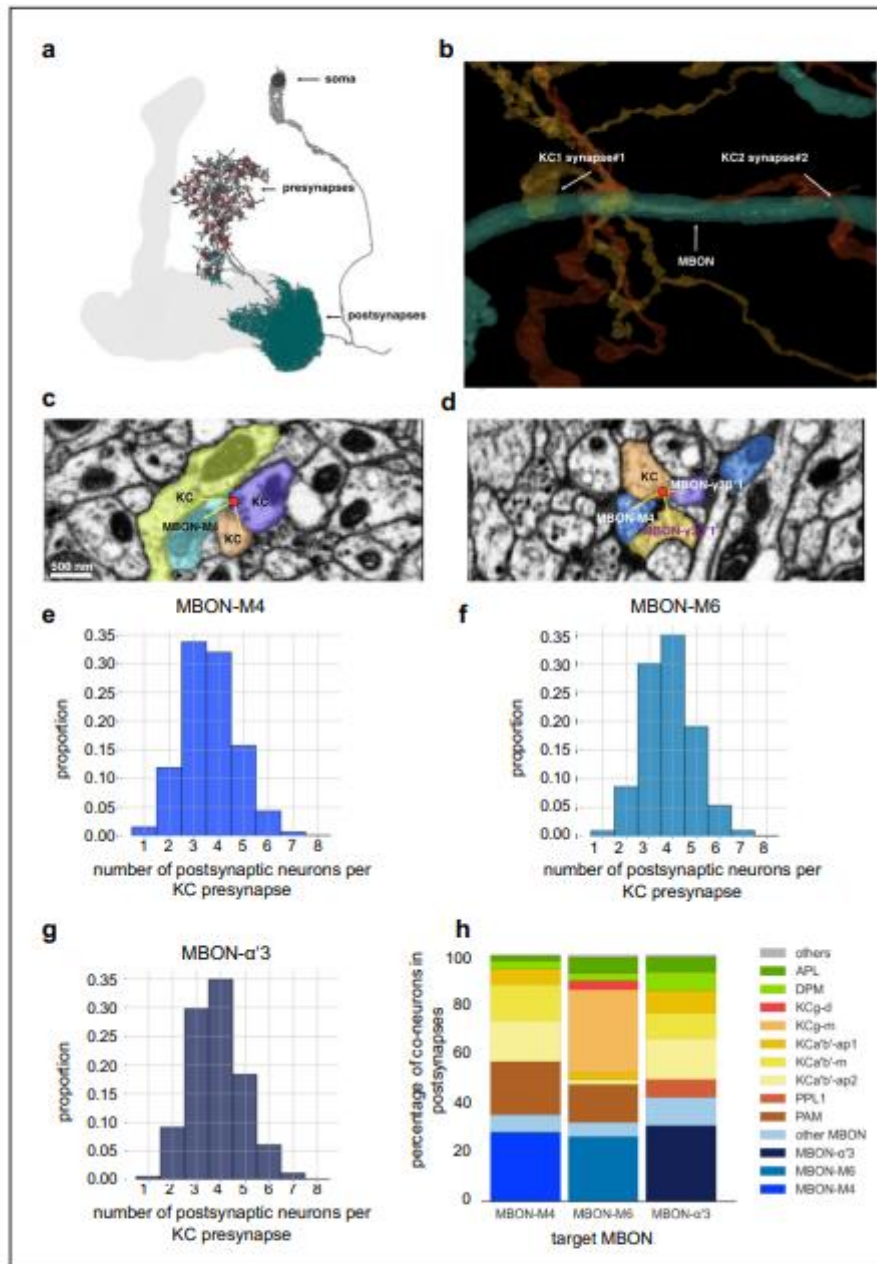
Figure 10. Mushroom body (MB) output connectomics (a) Example MB output neuron (MBON; here: M6) with pre- and postsynapses labeled. (b) Reconstructed example synapses from electron microscopic (EM) volume (neuprint.org): two different Kenyon cells (KCs) connect to the same MBON on the postsynaptic side. (c) EM image (neuprint.org) showing a KC presynapse simultaneously innervating two other KCs and the M4 MBON. Scale bar: 500 nm. (d) EM image (neuprint.org) showing a KC presynapse simultaneously innervating the M4 MBON and two sites of another MBON. (e) Analysis of

Figure 10 continued on next page

Figure 10 continued

number of postsynaptic partners for each KC presynapse identified providing input to M4. The histogram shows the distribution of KC synapses to M4 relative to how many postsynaptic partners the KC presynapses have. (**f**) Analysis of number of postsynaptic partners for each KC presynapse identified providing input to M6. The histogram shows the distribution of KC synapses to M6 relative to how many postsynaptic partners the KC presynapses have. (**g**) Analysis of number of postsynaptic partners for each KC presynapse identified providing input to α'3 MBONs (pooled). The histogram shows the distribution of KC synapses to α'3 MBONs relative to how many postsynaptic partners the KC presynapses have. (**h**) Percentage of types of neurons that share a KC presynapse with a given MBON.

the future. One option could include potential exchange of α2 subunits for a receptor complex with higher calcium permeability.

Our findings are consistent with the current MB skew model (*Owald and Waddell, 2015*), where the summed MBON output will determine an animal's choice. However, we add an additional layer, already at the MBON input site. Changes do not happen at the presynaptic compartment only but potentially at both synaptic compartments. Thus, the power to store (potentially conflicting) information separately at either the pre- or postsynaptic site, equips the system with additional flexibility. How precisely pre- to postsynaptic and post- to presynaptic signaling is regulated will need to be addressed in the future but will likely involve transsynaptic signaling routes (*Owald and Sigrist, 2009*; *Tang et al., 2016*). Importantly, the identified modes of postsynaptic plasticity will open avenues for investigations looking into pre- versus postsynaptic contributions during reversal learning, reconsolidation, and extinction learning (*Felsenberg et al., 2017*; *Lüscher and Malenka, 2011*).

Methods
Fly genetics
Flies were raised on standard food under standard laboratory conditions unless stated otherwise (25°C, 65%, 12-hr light-dark cycle; *Owald et al., 2015*; *Raccuglia et al., 2019*). Driver lines used were MB011B (Split-Gal4) (*Aso et al., 2014a*) (Split-Gal4), MB112C (*Aso et al., 2014a*) (Split-Gal4), MB461B (*Aso et al., 2014a*) (Split-Gal4), MB027B (*Aso et al., 2014a*) (Split-Gal4), R13F02-Gal4 (*Aso et al., 2014a*), OK107-Gal4 (*Barnstedt et al., 2016*), VT1211-GAL4 (*Owald et al., 2015*), and R58E02-LexA (*Handler et al., 2019*). We used the following UAS-nAChR^{RNAi} flies (*Barnstedt et al., 2016*; *Cervantes-Sandoval et al., 2017*): Bloomington stock numbers 28688, 27493, 27671, 31985, 25943, 27251, and 25835. Additionally, we used (*Bachmann et al., 2004*; *Soukup et al., 2013*) Dlg^{S97}-RNAi as well as UAS-Dlg^{GFP}, tubP-GAL80^{ts} (*Perisse et al., 2013*), UAS-Shi^{ts1} (*Perisse et al., 2013*), 247-dsRed (*Owald et al., 2015*), LexAop-CsChrimson, UAS-GCaMP6f (*Barnstedt et al., 2016*), and UAS-SynaptoPhluorin (*Lin et al., 2014a*). Note that complex genotypes did not always permit usage of MB011B for genetical access to M4/6 neurons throughout the manuscript. In that case, in order to reduce genetic complexity, we used VT1211-Gal4.

Behavior
T-maze memory
3–9 days old mixed-sex populations were trained and tested together as previously described (*Owald et al., 2015*). Odors used were 3-octanol (OCT, Aldrich) and 4-methylcyclohexanol (MCH, Aldrich) diluted in mineral oil (approximately 1:100 for aversive, 1:1000 for appetitive memory, absolute concentrations were minimally adjusted to prevent odor bias). For aversive protocols, flies were exposed to the CS+ for 1 min with 12 1.5 s long 120 V electric shocks (interstimulus interval: 3.5 s) followed by 45 s of air, 1 min of CS− exposure and another 30 s of air. Flies were given 2 min to choose between the CS+ and CS− in a T-Maze during retrieval in the dark. For appetitive conditioning, flies were starved for 20–24 hr before the experiment. Flies were exposed to the CS− for 2 min. After 30 s, flies were exposed to the CS+ paired with sugar for 2 min followed by another 30 s of air. Performance indices were calculated as described previously (*Owald et al., 2015*). Time of retrieval is stated in the figures. For Shi^{ts} experiments, flies were kept at 32°C 30 min prior to and during training and brought to room temperature directly afterward. Room temperature was approximately 23°C. For *Figure 2* and *Figure 2—figure supplement 1*, behavioral data sets from separate experiments were pooled. Note that 'screening hit' data displayed in *Figure 2a and b* and *Figure 2—figure supplement 1a, b* were replotted to allow for comparison of genotypes with the corresponding genetic controls in

Figure 2—figure supplement 2e-i. Gal80^{ts} flies were always raised at 18–20°C and were placed at 32°C 3–5 days before the experiment (*Figure 2*) or were kept at 18–20°C throughout (*Figure 2— figure supplement 2*).

Familiarity learning

Familiarity training was essentially performed as described before (*Hattori et al., 2017*) with slight adjustments. Flies were covered in yellow dust (*Hattori et al., 2017*) (Reactive Yellow 86, Fisher Scientific) and placed in a cylindrical custom designed chamber. To ensure a constant air stream, we placed the chamber between an air and a vacuum pump (800 ml/min). Air permeable cotton wool was used to close the open ends of the chamber. The air supply was either connected to pure mineral oil or MCH diluted in mineral oil at a concentration of 1:50. For switching between odor and mineral oil, a clamp was manually opened and closed. Video recording was performed at 26 frames per second. For recordings and analyses we used Python (v3.6) in Anaconda Jupyter Notebook environment.

Imaging

Confocal single-photon imaging and receptor quantification

Fixed explant brain imaging

Brains were dissected on ice, fixed in 4% paraformaldehyde (Sigma) for 20 min, and placed in PBST (phosphate-buffered saline, 0.1% Triton) for 30 min followed by washing with PBS for 20 min twice. Vectashield was used as mounting medium. Flies were 2–8-day-old females raised at room temperature.

Recording endogenous fluorescence

Imaging was performed using a confocal single-photon inverse microscope (Leica SP5/STED) equipped with a ×64 oil objective. Laser power and gain were adjusted between experiments, making normalization of the signals necessary. Values for the heatmap in *Figure 4* were normalized to the mean MB fluorescence value to ensure comparability. Voxel size was (height × width × depth) 123 nm × 123 nm × 500 nm. ROIs were drawn manually in ImageJ using the 247-dsRed channel for orientation (*Figure 4a*). Heat maps were created in Microsoft Excel. For quantifications following knockdown, the $\gamma5$ compartment was normalized to $\gamma4$ (($\gamma5 - \gamma4$)/ $\gamma4$), and the $\beta'2$ to the $\beta'1$ compartment (($\beta'2 - \beta'1$)/ $\beta'2$) of the same animal. Each 'n' corresponds to one hemisphere.

In vivo two-photon calcium imaging

To measure odor responses, female 3–6-day old flies expressing UAS-GCaMP6f alone or together with UAS-RNAi to $\alpha2$ or $\alpha5$ at the level of M4/6 were tethered under the multiphoton microscope (Femtonics), essentially as described before (*Owald et al., 2015; Böhme et al., 2019*). To measure M4/6 responses to odor presentation alone, five alternating 1 s OCT and MCH puffs were applied with 30 s in between each presentation. Fluorescent signals were recorded from dendrites in the $\beta'2$ MB compartment using MESc software (Femtonics) at a frame rate of roughly 30 Hz. ROIs incorporating the dendritic arbors were manually drawn. Data was processed using a Savitzky-Golay filter. Further analysis was performed using Matlab. For absolute training, we imaged from axonal arbors, and the following protocol was applied: after initial testing for odor responses, starved flies were exposed to 1-s odor puffs (MCH) twice with a 30 s gap between the applications. Corresponding odor responses were averaged. Paired training consisted of odor application (five consecutive 1-s odor puffs [MCH] with 6 s gap), while the fly fed on a sucrose droplet (saturated solution) for 30 s delivered by a custom-made feeding arm (*Lin et al., 2014b*). Unpaired training consisted of 30 s sucrose feeding followed by 30 s of odor applications as described above but with a delay of 45 s. The training was monitored with a video camera to verify accurate feeding of the fly. After a 1-min break, two odor puffs with a gap of 30 s were applied. Again, corresponding odor responses were averaged. Peak responses and areas under the curve (AUCs) were calculated using R and the first 3 s following odor onset were analyzed in order to cover entire responses. The AUCs pre- and post-training were normalized to the mean pre-training values of a group, respectively. The averaged test responses pre-training were compared to the average post-training responses (9–12 hemispheres were analyzed from 5 to 7 animals per genotype and condition) using a paired t-test or Wilcoxon matched-pairs signed rank test.

In vivo confocal single-photon imaging of receptor dynamics and calcium transients

3–4 days after enclosure, female flies were prepared as described above and imaged. Imaging was performed using a SP5 single-photon confocal microscope (Leica microsystems). Recording frame rate was 3 Hz. For bleaching high laser power was focused on the $\alpha'3$ compartments for 15–25 s. The baseline was recorded after bleaching, immediately before fixed inter-stimulus interval training (*Hattori et al., 2017*). OCT was presented 10 times for a second with a 6-s pause in between. Odor delivery (CON electronics) was controlled by the Leica acquisition software. After training, the same brain plane was recorded for 10 s with a pixel size of 200 nm in time intervals of 0, 5, 10, 15, 20, 30, and 60 min after training. For control experiments, air only was delivered to the chamber. Images of the same time interval recordings were averaged and processed in ImageJ. Gaussian blur ($\sigma=0.5$) was applied for smoothing, and ROIs were selected manually.

In vivo two-photon imaging of receptor dynamics

FRAP experiments were performed in vivo. 2–8-day-old flies were anesthetized on ice and mounted in a custom-made chamber. The head capsule was opened under room temperature sugar-free HL3-like saline, and legs were immobilized with wax. Sugar-free HL3-like saline containing 30 units of papain (Roche) was applied to the head capsule for 8 min to digest the brain's glial sheath and facilitate removal. Images were acquired using a multiphoton microscope (Nikon) with a ×25 water-immersion objective, controlled by Nikon NIS Elements software. Diluted odors (MCH or OCT in mineral oil 1:1000) were delivered on a clean air carrier stream using a six-channel delivery system (CON electronics). The flies were subjected to experimental conditions including either no odor (air), odor only, odor paired with local dopamine (10 mM) injection via a micropipette, or local dopamine injection only (see *Figure 6b* and *Figure 6—figure supplement 1b* for experimental protocol schematics). Photobleaching was accomplished using focused, high intensity laser exposure for ~1 min. Analysis of fluorescence recovery was performed using FIJI. ROIs were manually selected, and the percent recovery fluorescence was calculated by subtraction of the post-bleaching baseline fluorescence and division by the pre-bleaching baseline fluorescence. To fit the inverse exponential decay that is expected for FRAP data, we first inverted the percent fluorescence recovery values by subtracting them from 1 and then log-transformed the resulting values. These log-transformed values were used in a linear mixed effects model without intercept using the interaction between condition and time as fixed effect - to determine condition-specific differences of the recovery kinetics - and time as random effect (R package lme4). A linear mixed effect model was used to appropriately model repeated measures within animals. By inverting and log-transforming the fluorescence recovery values, this approach is equivalent to fitting an inverted exponential decay function. For plotting, all values including regression coefficients were back-transformed to the original scale. Significance of recovery of individual conditions was assessed using the regression coefficients of the condition-time interaction of the linear mixed model. Differences of recovery between pairs of conditions were tested using pairwise comparisons of estimated marginal means of the linear mixed model (R package emmeans). Correction for multiple pairwise comparisons was performed using Tukey's method.

Explant brain widefield imaging, neurotransmitter application, and optogenetics

Postsynaptic plasticity induction

Brains of 3–10-day-old mixed sex flies were dissected on ice. Flies expressed CsChrimson[tdTomato] under control of R58E02-LexA and UAS-GCaMP6f (and $\alpha2$ RNAi) under control of MB011B. The head capsule and sheath were removed in carbogenated solution (103 mM NaCl, 3 mM KCl, 5 mM N-Tris, 10 mM trehalose, 10 mM glucose, 7 mM sucrose, 26 mM NaHCO$_3$, 1 mM NaH$_2$PO$_4$, 1.5 mM CaCl$_2$, 4 mM MgCl$_2$, 295 mOsm, pH 7.3) with forceps. The brain was subsequently perfused with carbogenated solution containing TTX (2 µM; 20 ml/10 min flow speed) and imaged using an Olympus MX51WI wide field microscope with a ×40 Olympus LUMPLFLN objective and an Andor iXON Ultra camera controlled by Solis software. An Olympus U25ND25 light filter was placed in the beam path to minimize baseline CsChrimson activation. A custom designed glass microcapillary was loaded with uncarbongenated solution containing 0.1 mM acetylcholine and maneuvered to the M6 dendrites.

The injection pressure of a P25-1-900 picospritzer was calibrated between 3 and 8 psi (depending on initial calcium responses). Each local acetylcholine application spanned 15 ms with a 4 s inter-injection interval.

Three pulses of acetylcholine followed by a 2–3-min break were recorded after which the optogenetic response was assessed by applying 2 s red light pulses with an inter-red light-interval of 4 s. Three acetylcholine pulses were recorded followed by either five acetylcholine injections, five red light pulses, or both paired. For paired training, both stimuli began simultaneously and the acetylcholine injection lasted for 15 ms (and gave rise to a calcium transients typically lasting >1 s, please see example in Figure 3), while the paired red light pulse lasts for 2 s, allowing for maximal temporal overlap. This process was repeated 5×, with a 4-s break between trials. Following the training trial, three final acetylcholine test injections were applied after 1 min. For analysis, the first of the three acetylcholine injections was always discarded because of initial dilution of the capillary tip, and the remaining two peak intensities were averaged.

All peaks within an experiment were quantified relative to the fluorescence baseline that we calculated for pre- and post-training acetylcholine responses. Baselines were set independently for each pre- and post-training recording using the polynomial interpolation function in NOSA (neuro-optical signal analysis) (Oltmanns et al., 2020). For investigating α2 knockdown, only the paired condition was tested.

For controls not expressing CsChrimson, we used VT1211-Gal4 driving UAS-GCaMP6f, instead of MB011B, for technical reasons. This was combined with either expression of R58E02-LexA or LexAop-CsChrimson[tdTomato]. Only paired training was investigated in this context.

Excitability of KC axons

To test whether KC axons were excited by focal acetylcholine injections at the level of M4/6 dendrite innervation, either UAS-SynaptoPhluorin or UAS-GCaMP6f was expressed under the control of OK107-Gal4. Following the acetylcholine injection experiment, the capillary was exchanged with a capillary containing the same solution with additional 300–400 mM KCl, to evaluate tissue health (not shown for GCaMP6f imaging). To pick up potentially small changes, we increased the injection pressure to 8–14 Psi and the injection time to 150–225 ms (GCaMP6f, 8 s inter-injection interval and three consecutive injections) and 300–525 ms (SynaptoPhluorin, with an 8 s inter-injection interval and three consecutive injections).

Images were analyzed using NOSA (Raccuglia et al., 2019; Oltmanns et al., 2020) and GraphPad Prism.

Statistics

Statistical analyses were performed as stated in the previous method sections and figure legends. Data were always tested for normality using a Shapiro-Wilk test. If normally distributed, data were analyzed using ANOVA followed by post-hoc test or a (paired) t-test. If not normal, we used a Kruskal Wallis followed by post-hoc test, or a Wilcoxon matched-pairs signed rank test.

Tagged receptor subunits

All subunits were tagged using CRISPR technology and motifs previously described (Raghu et al., 2009). All EGFP-tagged AChR α subunits were generated by WellGenetics Inc (Taiwan) using

Table 1. Used EGFP positions and gRNA sequences of this study.

Subunit	EGFP position between AA	gRNA sequence
nAChRalpha1/CG5610	438D and 439L	ACAGATCGTCGTCGGCGCCC[GGG]
nAChRalpha2/CG6844	456G and 457L	CAGATTCAGCGGCTTGGTGG[GGG]
nAChRalpha4/CG12414	426M and 427D	AATAGCCGCCGTCCCCGATA[TGG]
AChRalpha5/CG32975	717G and 718S	CAGCACCCGAATGCCGGATG[CGG]
nAChRalpha6/CG4128	403T and 404A	TTACGCCGACGAGCCAATGG[CGG]
nAChRalpha7/CG32538	464G and 465S	GCAAGGGGATGACGGCAGCG[TGG]

CRISPR-based mutagenesis akin to Kondo and Ueda (*Kondo and Ueda, 2013*). Please see *Table 1* for position and sequence.

In brief, nAChR gRNA sequence was cloned into an U6 promoter plasmid. Cassette EGFP-PBacDsRed containing EGFP and 3xP3-DsRed and two nAChR α-homology arms were cloned into pUC57-Kan as donor template for repair.

nAChR alpha-targeting gRNAs and hs-Cas9 were supplied in DNA plasmids together with donor plasmid for microinjection into embryos of the w1118 strain. F1 flies carrying the 3xP3-DsRed selection marker were further validated by genomic PCR and sequencing. The 3XP3-DsRed marker was excised by Piggy Bac transposase leaving an exogenous 2aa linker of Valine and Lysine (GTTAAA) after excision.

Connectome analysis

In *Figure 10*, we analyzed the partial connectome of the female adult fly brain (hemibrain v1.2.1; *Scheffer et al., 2020*), using the neuprint-python package (https://github.com/connectome-neuprint/neuprint-python; *Berg et al., 2022*). To investigate the synaptic relationship between KC presynapses and MBON postsynaptic sites, we first identified KCs with the status 'Traced' in the connectome.

Second, for each MBON of interest, we identified the relevant KCs connected to it (which is a subset of the count in the previous step). Third, for each KC identified, we selected each presynaptic terminal (x, y, and z locations of synapses) connected to the MBON of interest, and for each of these presynapses, we identified all synaptic partners residing on the postsynaptic side. Fourth, for the MBON of interest, we counted the number of postsynaptic connections per individual presynapses (that also contain the specific MBON, *Figure 10e–g*). Finally, we identified the composition of all neurons identified as co-postsynaptic partners of KC to MBON synapses.

Acknowledgements

Additional information

Funding

eLife Research article

Author contributions

Carlotta Pribbenow, Conceptualization, Data curation, Formal analysis, Investigation, Writing – original draft, Writing – review and editing; Yi-chun Chen, Isabella Balles, Tania Fernández-d V Alquicira, Carolin Rauch, Sridhar R Jagannathan, Data curation, Formal analysis, Investigation, Writing – review and editing; M-Marcel Heim, Eric Reynolds, Data curation, Formal analysis, Investigation, Visualization, Writing – review and editing; Desiree Laber, Data curation, Investigation, Writing – review and editing; Silas Reubold, Data curation, Investigation, Visualization, Methodology, Writing – review and editing; Raquel Suárez-Grimalt, Jörg Rösner, Investigation, Methodology, Writing – review and editing; Lisa Scheunemann, Investigation, Writing – review and editing; Tanja Matkovic, Investigation; Gregor Lichtner, Formal analysis, Investigation, Visualization, Writing – review and editing; David Owald, Conceptualization, Resources, Supervision, Funding acquisition, Validation, Investigation, Visualization, Writing – original draft, Project administration, Writing – review and editing

Author ORCIDs

Carlotta Pribbenow http://orcid.org/0000-0002-1893-6435
Yi-chun Chen http://orcid.org/0000-0002-9187-930X
M-Marcel Heim http://orcid.org/0000-0002-8079-4204
Silas Reubold http://orcid.org/0000-0002-3308-3733
Eric Reynolds http://orcid.org/0000-0001-8597-6173
Tania Fernández-d V Alquicira http://orcid.org/0000-0003-2462-1664
Raquel Suárez-Grimalt http://orcid.org/0000-0002-5374-7963
Lisa Scheunemann http://orcid.org/0000-0002-6013-388X
Gregor Lichtner http://orcid.org/0000-0002-5890-1958
Sridhar R Jagannathan http://orcid.org/0000-0002-2078-1145
David Owald http://orcid.org/0000-0001-7747-7884

Decision letter and Author response

Decision letter https://doi.org/10.7554/eLife.80445.sa1
Author response https://doi.org/10.7554/eLife.80445.sa2

Additional files

Supplementary files
- MDAR checklist
- Supplementary file 1. Supplementary statistics.
- Source data 1. Source data.

Data availability

All data generated or analysed during this study are included in the manuscript and supporting files. The code used in this study is available on GitHub, (copy archived at swh:1:rev:0550ee981ec5b6e-b7e76e9062e3c9c8dead42306; *Jagannathan, 2022*). Materials can be requested from the corresponding author.

References

Ackermann F, Waites CL, Garner CC. 2015. Presynaptic active zones in invertebrates and vertebrates. *EMBO Reports* **16**:923–938. DOI: https://doi.org/10.15252/embr.201540434, PMID: 26160654

Aso Y, Hattori D, Yu Y, Johnston RM, Iyer NA, Ngo TTB, Dionne H, Abbott LF, Axel R, Tanimoto H, Rubin GM. 2014a. The neuronal architecture of the mushroom body provides a logic for associative learning. *eLife* **3**:e04577. DOI: https://doi.org/10.7554/eLife.04577, PMID: 25535793

Aso Y, Sitaraman D, Ichinose T, Kaun KR, Vogt K, Belliart-Guérin G, Plaçais PY, Robie AA, Yamagata N, Schnaitmann C, Rowell WJ, Johnston RM, Ngo TTB, Chen N, Korff W, Nitabach MN, Heberlein U, Preat T,

Neuroscience

Branson KM, Tanimoto H, et al. 2014b. Mushroom body output neurons encode valence and guide memory-based action selection in Drosophila. eLife 3:e04580. DOI: https://doi.org/10.7554/eLife.04580, PMID: 25535794

Aso Y, Rubin GM. 2016. Dopaminergic neurons write and update memories with cell-type-specific rules. eLife 5:e16135. DOI: https://doi.org/10.7554/eLife.16135, PMID: 27441388

Aso Y, Ray RP, Long X, Bushey D, Cichewicz K, Ngo TT, Sharp B, Christoforou C, Hu A, Lemire AL, Tillberg P, Hirsh J, Litwin-Kumar A, Rubin GM. 2019. Nitric oxide acts as a cotransmitter in a subset of dopaminergic neurons to diversify memory dynamics. eLife 8:e49257. DOI: https://doi.org/10.7554/eLife.49257, PMID: 31724947

Bachmann A, Timmer M, Sierralta J, Pietrini G, Gundelfinger ED, Knust E, Thomas U. 2004. Cell type-specific recruitment of Drosophila lin-7 to distinct MAGUK-based protein complexes defines novel roles for sdt and dlg-S97. Journal of Cell Science 117:1899–1909. DOI: https://doi.org/10.1242/jcs.01029, PMID: 15039455

Barnstedt O, Owald D, Felsenberg J, Brain R, Moszynski J-P, Talbot CB, Perrat PN, Waddell S. 2016. Memory-relevant mushroom body output synapses are cholinergic. Neuron 89:1237–1247. DOI: https://doi.org/10.1016/j.neuron.2016.02.015, PMID: 26948892

Berg S, Schlegel P, Svirskas R. 2022. Neuprint-python. GitHub. https://github.com/connectome-neuprint/neuprint-python

Bilz F, Geurten BRH, Hancock CE, Widmann A, Fiala A. 2020. Visualization of a distributed synaptic memory code in the Drosophila brain. Neuron 106:963–976. DOI: https://doi.org/10.1016/j.neuron.2020.03.010, PMID: 32268119

Bliss TV, Lomo T. 1973. Long-Lasting potentiation of synaptic transmission in the dentate area of the anaesthetized rabbit following stimulation of the perforant path. The Journal of Physiology 232:331–356. DOI: https://doi.org/10.1113/jphysiol.1973.sp010273, PMID: 4727084

Böhme MA, McCarthy AW, Grasskamp AT, Beuschel CB, Goel P, Jusyte M, Laber D, Huang S, Rey U, Petzoldt AG, Lehmann M, Göttfert F, Haghighi P, Hell SW, Owald D, Dickman D, Sigrist SJ, Walter AM. 2019. Rapid active zone remodeling consolidates presynaptic potentiation. Nature Communications 10:1085. DOI: https://doi.org/10.1038/s41467-019-08977-6, PMID: 30842428

Boto T, Louis T, Jindachomthong K, Jalink K, Tomchik SM. 2014. Dopaminergic modulation of cAMP drives nonlinear plasticity across the Drosophila mushroom body lobes. Current Biology 24:822–831. DOI: https://doi.org/10.1016/j.cub.2014.03.021, PMID: 24684937

Bouzaiane E, Trannoy S, Scheunemann L, Plaçais PY, Preat T. 2015. Two independent mushroom body output circuits retrieve the six discrete components of Drosophila aversive memory. Cell Reports 11:1280–1292. DOI: https://doi.org/10.1016/j.celrep.2015.04.044, PMID: 25981036

Cervantes-Sandoval I, Phan A, Chakraborty M, Davis RL. 2017. Reciprocal synapses between mushroom body and dopamine neurons form a positive feedback loop required for learning. eLife 6:e23789. DOI: https://doi.org/10.7554/eLife.23789, PMID: 28489528

Clements J, Dolafi T, Umayam L, Neubarth NL, Berg S, Scheffer LK, Plaza SM. 2020. neuPrint: Analysis Tools for EM Connectomics. bioRxiv. DOI: https://doi.org/10.1101/2020.01.16.909465

Cohn R, Morantte I, Ruta V. 2015. Coordinated and compartmentalized neuromodulation shapes sensory processing in Drosophila. Cell 163:1742–1755. DOI: https://doi.org/10.1016/j.cell.2015.11.019, PMID: 26687359

Crittenden JR, Skoulakis EM, Han KA, Kalderon D, Davis RL. 1998. Tripartite mushroom body architecture revealed by antigenic markers. Learning & Memory 5:38–51 PMID: 10454371.

Dent JA. 2010. The evolution of pentameric ligand-gated ion channels. Advances in Experimental Medicine and Biology 683:11–23. DOI: https://doi.org/10.1007/978-1-4419-6445-8_2, PMID: 20737785

Dubnau J, Grady L, Kitamoto T, Tully T. 2001. Disruption of neurotransmission in Drosophila mushroom body blocks retrieval but not acquisition of memory. Nature 411:476–480. DOI: https://doi.org/10.1038/35078077, PMID: 11373680

Eadaim A, Hahm ET, Justice ED, Tsunoda S. 2020. Cholinergic synaptic homeostasis is tuned by an NFAT-mediated α7 nachr-kv4/shal coupled regulatory system. Cell Reports 32:108119. DOI: https://doi.org/10.1016/j.celrep.2020.108119, PMID: 32905767

Ehmann N, Owald D, Kittel RJ. 2018. Drosophila active zones: from molecules to behaviour. Neuroscience Research 127:14–24. DOI: https://doi.org/10.1016/j.neures.2017.11.015, PMID: 29258853

Eichler K, Li F, Litwin-Kumar A, Park Y, Andrade I, Schneider-Mizell CM, Saumweber T, Huser A, Eschbach C, Gerber B, Fetter RD, Truman JW, Priebe CE, Abbott LF, Thum AS, Zlatic M, Cardona A. 2017. The complete connectome of a learning and memory centre in an insect brain. Nature 548:175–182. DOI: https://doi.org/10.1038/nature23455, PMID: 28796202

Felsenberg J., Barnstedt O, Cognigni P, Lin S, Waddell S. 2017. Re-Evaluation of learned information in Drosophila. Nature 544:240–244. DOI: https://doi.org/10.1038/nature21716, PMID: 28379939

Felsenberg J, Jacob PF, Walker T, Barnstedt O, Edmondson-Stait AJ, Pleijzier MW, Otto N, Schlegel P, Sharifi N, Perisse E, Smith CS, Lauritzen JS, Costa M, Jefferis G, Bock DD, Waddell S. 2018. Integration of parallel opposing memories underlies memory extinction. Cell 175:709–722. DOI: https://doi.org/10.1016/j.cell.2018.08.021, PMID: 30245010

Glanzman DL. 2010. Common mechanisms of synaptic plasticity in vertebrates and invertebrates. Current Biology 20:R31–R36. DOI: https://doi.org/10.1016/j.cub.2009.10.023, PMID: 20152143

Goldberg JH, Tamas G, Aronov D, Yuste R. 2003. Calcium microdomains in aspiny dendrites. Neuron 40:807–821. DOI: https://doi.org/10.1016/s0896-6273(03)00714-1, PMID: 14622584

Greger IH, Watson JF, Cull-Candy SG. 2017. Structural and functional architecture of AMPA-type glutamate receptors and their auxiliary proteins. Neuron 94:713–730. DOI: https://doi.org/10.1016/j.neuron.2017.04.009, PMID: 28521126

Hagins WA, Penn RD, Yoshikami S. 1970. Dark current and photocurrent in retinal rods. Biophysical Journal 10:380–412. DOI: https://doi.org/10.1016/S0006-3495(70)86308-1, PMID: 5439318

Hancock CE, Rostami V, Rachad EY, Deimel SH, Nawrot MP, Fiala A. 2022. Visualization of Learning-induced synaptic plasticity in output neurons of the Drosophila mushroom body γ-lobe. Scientific Reports 12:10421. DOI: https://doi.org/10.1038/s41598-022-14413-5, PMID: 35729203

Handler A, Graham TGW, Cohn R, Morantte I, Siliciano AF, Zeng J, Li Y, Ruta V. 2019. Distinct dopamine receptor pathways underlie the temporal sensitivity of associative learning. Cell 178:60–75. DOI: https://doi.org/10.1016/j.cell.2019.05.040, PMID: 31230716

Hattori D, Aso Y, Swartz KJ, Rubin GM, Abbott LF, Axel R. 2017. Representations of novelty and familiarity in a mushroom body compartment. Cell 169:956–969. DOI: https://doi.org/10.1016/j.cell.2017.04.028, PMID: 28502772

Hige T, Aso Y, Modi MN, Rubin GM, Turner GC. 2015. Heterosynaptic plasticity underlies aversive olfactory learning in Drosophila. Neuron 88:985–998. DOI: https://doi.org/10.1016/j.neuron.2015.11.003, PMID: 26637800

Honegger KS, Campbell RAA, Turner GC. 2011. Cellular-resolution population imaging reveals robust sparse coding in the Drosophila mushroom body. The Journal of Neuroscience 31:11772–11785. DOI: https://doi.org/10.1523/JNEUROSCI.1099-11.2011, PMID: 21849538

Ichinose T, Aso Y, Yamagata N, Abe A, Rubin GM, Tanimoto H. 2015. Reward signal in a recurrent circuit drives appetitive long-term memory formation. eLife 4:e10719. DOI: https://doi.org/10.7554/eLife.10719, PMID: 26573957

Ichinose T, Kanno M, Wu H, Yamagata N, Sun H, Abe A, Tanimoto H. 2021. Mushroom body output differentiates memory processes and distinct memory-guided behaviors. Current Biology 31:1294–1302. DOI: https://doi.org/10.1016/j.cub.2020.12.032, PMID: 33476556

Ihara M, Furutani S, Shigetou S, Shimada S, Niki K, Komori Y, Kamiya M, Koizumi W, Magara L, Hikida M, Noguchi A, Okuhara D, Yoshinari Y, Kondo S, Tanimoto H, Niwa R, Sattelle DB, Matsuda K. 2020. Cofactor-enabled functional expression of fruit fly, honeybee, and bumblebee nicotinic receptors reveals picomolar neonicotinoid actions. PNAS 117:16283–16291. DOI: https://doi.org/10.1073/pnas.2003667117, PMID: 32611810

Ito M. 2001. Cerebellar long-term depression: characterization, signal transduction, and functional roles. Physiological Reviews 81:1143–1195. DOI: https://doi.org/10.1152/physrev.2001.81.3.1143, PMID: 11427694

Jagannathan S. 2022. Postsynapticplasticity. swh:1:rev:0550ee981ec5b6eb7e76e9062e3c9c8dead42306. Software Heritage. https://archive.softwareheritage.org/swh:1:dir:6e3eb90d9f713e67ab67fd52ac62d455dc7e803b;origin=https://github.com/owaldlab/2022_postsynapticplasticity;visit=swh:1:snp:704e43b1d1e66683eba9496f91aec488c4399d98;anchor=swh:1:rev:0550ee981ec5b6eb7e76e9062e3c9c8dead42306

Kandel ER, Dudai Y, Mayford MR. 2014. The molecular and systems biology of memory. Cell 157:163–186. DOI: https://doi.org/10.1016/j.cell.2014.03.001, PMID: 24679534

Kim YC, Lee HG, Han KA. 2007. D1 dopamine receptor dda1 is required in the mushroom body neurons for aversive and appetitive learning in Drosophila. The Journal of Neuroscience 27:7640–7647. DOI: https://doi.org/10.1523/JNEUROSCI.1167-07.2007, PMID: 17634358

Kondo S, Ueda R. 2013. Highly improved gene targeting by germline-specific Cas9 expression in Drosophila. Genetics 195:715–721. DOI: https://doi.org/10.1534/genetics.113.156737, PMID: 24002648

Korte M, Schmitz D. 2016. Cellular and system biology of memory: timing, molecules, and beyond. Physiological Reviews 96:647–693. DOI: https://doi.org/10.1152/physrev.00010.2015, PMID: 26960344

Krashes MJ, Keene AC, Leung B, Armstrong JD, Waddell S. 2007. Sequential use of mushroom body neuron subsets during Drosophila odor memory processing. Neuron 53:103–115. DOI: https://doi.org/10.1016/j.neuron.2006.11.021, PMID: 17196534

Lansdell SJ, Collins T, Goodchild J, Millar NS. 2012. The Drosophila nicotinic acetylcholine receptor subunits Dα5 and Dα7 form functional homomeric and heteromeric ion channels. BMC Neuroscience 13:73. DOI: https://doi.org/10.1186/1471-2202-13-73, PMID: 22727315

Lewis LPC, Siju KP, Aso Y, Friedrich AB, Bulteel AJB, Rubin GM, Grunwald Kadow IC. 2015. A higher brain circuit for immediate integration of conflicting sensory information in Drosophila. Current Biology 25:2203–2214. DOI: https://doi.org/10.1016/j.cub.2015.07.015, PMID: 26299514

Lin AC, Bygrave AM, de Calignon A, Lee T, Miesenböck G. 2014a. Sparse, decorrelated odor coding in the mushroom body enhances learned odor discrimination. Nature Neuroscience 17:559–568. DOI: https://doi.org/10.1038/nn.3660, PMID: 24561998

Lin S, Owald D, Chandra V, Talbot C, Huetteroth W, Waddell S. 2014b. Neural correlates of water reward in thirsty Drosophila. Nature Neuroscience 17:1536–1542. DOI: https://doi.org/10.1038/nn.3827, PMID: 25262493

Lüscher C, Malenka RC. 2011. Drug-Evoked synaptic plasticity in addiction: from molecular changes to circuit remodeling. Neuron 69:650–663. DOI: https://doi.org/10.1016/j.neuron.2011.01.017, PMID: 21338877

McGuire SE, Le PT, Davis RL. 2001. The role of Drosophila mushroom body signaling in olfactory memory. Science 293:1330–1333. DOI: https://doi.org/10.1126/science.1062622, PMID: 11397912

Nicoll RA. 2017. A brief history of long-term potentiation. Neuron 93:281–290. DOI: https://doi.org/10.1016/j.neuron.2016.12.015, PMID: 28103477

Oltmanns S, Abben FS, Ender A, Aimon S, Kovacs R, Sigrist SJ, Storace DA, Geiger JRP, Raccuglia D. 2020. NOSA, an analytical toolbox for multicellular optical electrophysiology. Frontiers in Neuroscience 14:712. DOI: https://doi.org/10.3389/fnins.2020.00712, PMID: 32765213

Owald D, Sigrist SJ. 2009. Assembling the presynaptic active zone. Current Opinion in Neurobiology 19:311–318. DOI: https://doi.org/10.1016/j.conb.2009.03.003, PMID: 19395253

Owald D, Felsenberg J, Talbot CB, Das G, Perisse E, Huetteroth W, Waddell S. 2015. Activity of defined mushroom body output neurons underlies learned olfactory behavior in Drosophila. Neuron 86:417–427. DOI: https://doi.org/10.1016/j.neuron.2015.03.025, PMID: 25864636

Owald D, Waddell S. 2015. Olfactory learning skews mushroom body output pathways to steer behavioral choice in Drosophila. Current Opinion in Neurobiology 35:178–184. DOI: https://doi.org/10.1016/j.conb.2015.10.002, PMID: 26496148

Pai TP, Chen CC, Lin HH, Chin AL, Lai JSY, Lee PT, Tully T, Chiang AS. 2013. Drosophila orb protein in two mushroom body output neurons is necessary for long-term memory formation. PNAS 110:7898–7903. DOI: https://doi.org/10.1073/pnas.1216336110, PMID: 23610406

Perisse E, Yin Y, Lin AC, Lin S, Huetteroth W, Waddell S. 2013. Different kenyon cell populations drive learned approach and avoidance in Drosophila. Neuron 79:945–956. DOI: https://doi.org/10.1016/j.neuron.2013.07.045, PMID: 24012007

Perisse E, Owald D, Barnstedt O, Talbot CB, Huetteroth W, Waddell S. 2016. Aversive learning and appetitive motivation toggle feed-forward inhibition in the Drosophila mushroom body. Neuron 90:1086–1099. DOI: https://doi.org/10.1016/j.neuron.2016.04.034, PMID: 27210550

Plaçais PY, Trannoy S, Friedrich AB, Tanimoto H, Preat T. 2013. Two pairs of mushroom body efferent neurons are required for appetitive long-term memory retrieval in Drosophila. Cell Reports 5:769–780. DOI: https://doi.org/10.1016/j.celrep.2013.09.032, PMID: 24209748

Qin H, Cressy M, Li W, Coravos JS, Izzi SA, Dubnau J. 2012. Gamma neurons mediate dopaminergic input during aversive olfactory memory formation in Drosophila. Current Biology 22:608–614. DOI: https://doi.org/10.1016/j.cub.2012.02.014, PMID: 22425153

Raccuglia D, Huang S, Ender A, Heim MM, Laber D, Suárez-Grimalt R, Liotta A, Sigrist SJ, Geiger JRP, Owald D. 2019. Network-specific synchronization of electrical slow-wave oscillations regulates sleep drive in Drosophila. Current Biology 29:3611–3621. DOI: https://doi.org/10.1016/j.cub.2019.08.070, PMID: 31630955

Raghu SV, Joesch M, Sigrist SJ, Borst A, Reiff DF. 2009. Synaptic organization of lobula plate tangential cells in Drosophila: Dalpha7 cholinergic receptors. Journal of Neurogenetics 23:200–209. DOI: https://doi.org/10.1080/01677060802471684, PMID: 19306209

Scheffer LK, Xu CS, Januszewski M, Lu Z, Takemura S-Y, Hayworth KJ, Huang GB, Shinomiya K, Maitlin-Shepard J, Berg S, Clements J, Hubbard PM, Katz WT, Umayam L, Zhao T, Ackerman D, Blakely T, Bogovic J, Dolafi T, Kainmueller D, et al. 2020. A connectome and analysis of the adult Drosophila central brain. eLife 9:e57443. DOI: https://doi.org/10.7554/eLife.57443, PMID: 32880371

Schwaerzel M, Heisenberg M, Zars T. 2002. Extinction antagonizes olfactory memory at the subcellular level. Neuron 35:951–960. DOI: https://doi.org/10.1016/s0896-6273(02)00832-2, PMID: 12372288

Séjourné J, Plaçais P-Y, Aso Y, Siwanowicz I, Trannoy S, Thoma V, Tedjakumala SR, Rubin GM, Tchénio P, Ito K, Isabel G, Tanimoto H, Preat T. 2011. Mushroom body efferent neurons responsible for aversive olfactory memory retrieval in Drosophila. Nature Neuroscience 14:903–910. DOI: https://doi.org/10.1038/nn.2846, PMID: 21685917

Shomrat T, Graindorge N, Bellanger C, Fiorito G, Loewenstein Y, Hochner B. 2011. Alternative sites of synaptic plasticity in two homologous " fan-out fan-in " learning and memory networks. Current Biology 21:1773–1782. DOI: https://doi.org/10.1016/j.cub.2011.09.011, PMID: 22018541

Soukup SF, Pocha SM, Yuan M, Knust E. 2013. DLin-7 is required in postsynaptic lamina neurons to prevent light-induced photoreceptor degeneration in Drosophila. Current Biology 23:1349–1354. DOI: https://doi.org/10.1016/j.cub.2013.05.060, PMID: 23850283

Stahl A, Noyes NC, Boto T, Botero V, Broyles CN, Jing M, Zeng J, King LB, Li Y, Davis RL, Tomchik SM. 2022. Associative learning drives longitudinally graded presynaptic plasticity of neurotransmitter release along axonal compartments. eLife 11:e76712. DOI: https://doi.org/10.7554/eLife.76712, PMID: 35285796

Stuart GJ, Spruston N. 2015. Dendritic integration: 60 years of progress. Nature Neuroscience 18:1713–1721. DOI: https://doi.org/10.1038/nn.4157, PMID: 26605882

Takemura SY, Aso Y, Hige T, Wong A, Lu Z, Xu CS, Rivlin PK, Hess H, Zhao T, Parag T, Berg S, Huang G, Katz W, Olbris DJ, Plaza S, Umayam L, Aniceto R, Chang LA, Lauchie S, Ogundeyi O, et al. 2017. A connectome of A learning and memory center in the adult Drosophila brain. eLife 6:e26975. DOI: https://doi.org/10.7554/eLife.26975, PMID: 28718765

Tang A-H, Chen H, Li TP, Metzbower SR, MacGillavry HD, Blanpied TA. 2016. A trans-synaptic nanocolumn aligns neurotransmitter release to receptors. Nature 536:210–214. DOI: https://doi.org/10.1038/nature19058, PMID: 27462810

Thompson AJ, Lester HA, Lummis SCR. 2010. The structural basis of function in Cys-loop receptors. Quarterly Reviews of Biophysics 43:449–499. DOI: https://doi.org/10.1017/S0033583510000168, PMID: 20849671

Trannoy S, Redt-Clouet C, Dura JM, Preat T. 2011. Parallel processing of appetitive short- and long-term memories in Drosophila. Current Biology 21:1647–1653. DOI: https://doi.org/10.1016/j.cub.2011.08.032, PMID: 21962716

Tully T, Preat T, Boynton SC, Del Vecchio M. 1994. Genetic dissection of consolidated memory in *Drosophila*. *Cell* **79**:35–47. DOI: https://doi.org/10.1016/0092-8674(94)90398-0, PMID: 7923375

Ueno K, Suzuki E, Naganos S, Ofusa K, Horiuchi J, Saitoe M. 2017. Coincident postsynaptic activity gates presynaptic dopamine release to induce plasticity in *Drosophila* mushroom bodies. *eLife* **6**:e.21076. DOI: https://doi.org/10.7554/eLife.21076, PMID: 28117664

Ueno K, Morstein J, Ofusa K, Naganos S, Suzuki-Sawano E, Minegishi S, Rezgui SP, Kitagishi H, Michel BW, Chang CJ, Horiuchi J, Saitoe M. 2020. Carbon monoxide, a retrograde messenger generated in postsynaptic mushroom body neurons, evokes noncanonical dopamine release. *The Journal of Neuroscience* **40**:3533–3548. DOI: https://doi.org/10.1523/JNEUROSCI.2378-19.2020, PMID: 32253360

Widmer YF, Fritsch C, Jungo MM, Almeida S, Egger B, Sprecher SG. 2018. Multiple neurons encode crebb dependent appetitive long-term memory in the mushroom body circuit. *eLife* **7**:e39196. DOI: https://doi.org/10.7554/eLife.39196, PMID: 30346271

Won S, Levy JM, Nicoll RA, Roche KW. 2017. Maguks: multifaceted synaptic organizers. *Current Opinion in Neurobiology* **43**:94–101. DOI: https://doi.org/10.1016/j.conb.2017.01.006, PMID: 28236779

Wu J-K, Tai C-Y, Feng K-L, Chen S-L, Chen C-C, Chiang A-S. 2017. Long-Term memory requires sequential protein synthesis in three subsets of mushroom body output neurons in *Drosophila*. *Scientific Reports* **7**:7112. DOI: https://doi.org/10.1038/s41598-017-07600-2, PMID: 28769066

Yamazaki D, Hiroi M, Abe T, Shimizu K, Minami-Ohtsubo M, Maeyama Y, Horiuchi J, Tabata T. 2018. Two parallel pathways assign opposing odor valences during *Drosophila* memory formation. *Cell Reports* **22**:2346–2358. DOI: https://doi.org/10.1016/j.celrep.2018.02.012, PMID: 29490271

Zhao X, Lenek D, Dag U, Dickson BJ, Keleman K. 2018. Persistent activity in a recurrent circuit underlies courtship memory in *Drosophila*. *eLife* **7**:e31425. DOI: https://doi.org/10.7554/eLife.31425, PMID: 29322941

Lebenslauf

Mein Lebenslauf wird aus datenschutzrechtlichen Gründen in der elektronischen Version meiner Arbeit nicht veröffentlicht

Lebenslauf

Mein Lebenslauf wird aus datenschutzrechtlichen Gründen in der elektronischen Version meiner Arbeit nicht veröffentlicht

Komplette Publikationsliste

Pribbenow C, Häring E. Gesundheitsgefährdung durch falsche Lagerung? Mikrobiologische Untersuchung von Champignons, die unterschiedlich gelagert wurden. Junge Wissenschaft. Ausgabe: 103, 2014.

Pribbenow C, Chen YC, Heim MM, et al. Postsynaptic plasticity of cholinergic synapses underlies the induction and expression of appetitive and familiarity memories in Drosophila. *eLife.* 2022; 11:e80445. doi:10.7554/eLife.80445

Pribbenow C, Owald D. Skewing information flow through pre- and postsynaptic plasticity in the mushroom bodies of Drosophila. Learn Mem. 2024; 14;31(5):a053919. doi: 10.1101/lm.053919.124.

Danksagung